Schweizerische Eidgenossenschaft
Confédération suisse
Confederazione Svizzera
Confederaziun svizra

Federal Department of the Environment, Transport, Energy and Communications DETEC

Swiss Federal Office of Energy SFOE
Energy Research and Cleantech

SWEET Call 1-2021: DeCarbCH

Deliverable report

Deliverable n°	5.1.1.
Deliverable name	Simulation model of several energy concepts for typical industrial profiles set up and database of solutions established (database and simulation tool)
Authors The authors bear the entire responsibility for the content of this report and the conclusions drawn therefrom.	Frédéric Bless, OST-IES, **frederic.bless@ost.ch** Sidharth Paranjape, OST-IES **sidharth.paranjape@ost.ch** Cordin Arpagaus, OST-IES, **cordin.arpagaus@ost.ch** Stefan Bertsch, OST-IES, **stefan.bertsch@ost.ch**
Delivery date	03.2023

Table of contents

sweet swiss energy research for the energy transition

Summary

Heat pumps models have been developed for different heat pumping cycles to better compare them and find the most suited solution for a given application. These models have been already used in several case studies in 2022 (case studies paid directly by industry) to assess optimal heat pump integration in a process. Using these case studies the models could be improved. Some of the studies have led to publications in conference proceeding where the name of the companies have been anonymised[1]. Furthermore, a model comparing solar thermal and high-temperature heat pump in term of levelized cost of heat was developed and published[2]. From these case studies, several heating and cooling systems data were analysed from different Swiss companies. Heat pumps allow increasing energy efficiency and reducing cooling load while at the same time electrifying heat production. Although this double advantage has been recognized for a long time, heat pumps are not spreading quickly in the industry. Analysis of case studies presented in deliverable 5.3.1. (At least two system-level case studies on evolving technologies significantly reducing carbon emissions started) have been possible by using simulation models to compare different heat pump cycles (i.e., standard cycle, combined cycle, transcritical cycle, solar and heat pump). This allows to get more accurate estimates of potential efficiencies, operating range, etc. than a pinch tool that uses constant temperatures for heat input and heat rejection for heat pumps, without a physical model. It also allows estimating the cost efficiency of such a system better, as shown in deliverable 5.3.1. In addition, a tool was designed to quickly analyse techno economical parameters for industrial heat pumps using a simple and user-friendly excel file.

1 Introduction

The Coefficient of Performance (COP) is the main parameter to describe the efficiency of a vapor compression heat pump. The Carnot COP, which represents the maximum attainable COP for an ideal thermodynamically reversible cycle, is calculated by dividing the temperature of the heat sink (process heat demand) by the temperature lift between the sink and the source. A first estimate for realistic COP is obtained by multiplying the Carnot COP by the 2nd Law efficiency. For example, a 2nd Law efficiency of 0.45 is reasonable for several industrial HTHPs, as shown by (Arpagaus, 2018, 2020; Arpagaus et al., 2018).

In deliverable 5.3.1, a polynomial fit was used to estimate the COP of the heat pump systems. We wrote: “A more detailed thermodynamic heat pump model could consider the influence of refrigerant (e.g., HFOs, NH_3, CO_2, R600), compressor efficiency (e.g., screw, piston, turbo compressors), cycle optimizations (e.g., multistage, economizer, MVR combination), temperature glide, capacity, etc. However, this is outside the scope of this study but could eventually lead to a more integrated techno-economic calculation tool.”

This deliverable now presents such thermodynamic heat pump models, which can lead to not only a better COP of the heat pump and an optimized integration, but also a better estimation of concrete systems available in the current market.

[1] Payá, J., Cazorla-Marín, A., Hassan, A.H., Arpagaus, C.: Techno-economic evaluation of different technologies to produce steam at 150 °C in the Spanish industry, 12th CNIT, XII National and y III International Conference on Engineering Thermodynamics, June 29 - July 1, 2022, Madrid, Spain

Arpagaus, C., Bless, F., Bertsch, S.: Techno-economic analysis of steam generating heat pumps for integration into distillation processes, 15th IIR-Gustav Lorentzen conference on Natural Refrigerants, June 13-15, 2022, Trondheim, Norway, **http://dx.doi.org/10.18462/iir.gl2022.0029**

Ayou, D.S., Arpagaus, C., Bertsch, S.S., Coronas, A.: Large-temperature-lift heat pumps for simultaneous heating and cooling applications in the dairy industry, 15th IIR-Gustav Lorentzen conference on Natural Refrigerants, June 13-15, 2022, Trondheim, Norway, **http://dx.doi.org/10.18462/iir.gl2022.0074**

Arpagaus, C., Bless, F., Bertsch, S.S.: Techno-Economic Analysis of Steam-Generating Heat Pumps in Distillation Processes. 3rd High-Temperature Heat Pump Symposium, 29-30 March, 2022, Copenhagen, Denmark, **https://hthp-symposium.org**

[2] Saini, P., Ghasemi, M., Arpagaus, C., Bless, F., Bertsch, S., Zhang, X.: Techno-economic comparative analysis of solar thermal collectors and high-temperature heat pumps for industrial steam generation, Energy Conversion and Management, Volume 277, 1 February 2023, 116623, https://doi.org/10.1016/j.enconman.2022.116623

2 Deliverable content: model descriptions

Models for heat pump closed-cycle, transcritical, open-loop, and combined cycles are explained. Furthermore, a model estimating the best cost-effective ratio of thermal solar vs. industrial heat pump power is also described.

All the models are static. Dynamic models are far more challenging to develop and calibrate to a real system. For most applications steady-state models are sufficient to design and dimension the heat pump. They are widely spread in research for this purpose.

2.1 Heat pump and solar panel with thermal storage comparison

A simulation model was developed with Puneet Saini and Mohammad Ghasemi from the Department of Energy and Construction Engineering, Dalarna University, Falun S-79188 (Sweden), comparing the techno-economic aspects of high-temperature heat pumps and parabolic-trough collectors producing steam at 140° (3.6 bar(a)), for various industrial boundary conditions.

The analysis of this simulation was published in the Energy Conversion and Management journal [Saini2023]. The physical model is similar to the one presented in deliverable 5.3.1. to calculate the heat pump payback time but also included a concentrated solar system model. The focus is on steam generation, commonly used in many process heating industries. The characteristics of commercial high-temperature heat pumps and parabolic-trough collector products are used as input to the simulation model to obtain energetic results. Finally, results are generalized using solar fraction as an indicator to distinguish the economic advantage of each technology. Solar fraction is the amount of heat produced by solar over the total heat demand. High solar fraction needs larger thermal storage and is more expensive.

The results show that the levelized cost of heat (LCOH) increases with solar fraction; a solar fraction limit exists when producing heat from solar thermal gets expensive compared to the high-temperature heat pump. This limit is higher for high direct normal irradiation (DNI) regions and lower for low DNI regions. The limit increases with higher electricity prices and heat pump CAPEX for the high-temperature heat pump. In low CAPEX and electricity cost situations for a high-temperature heat pump, a threshold DNI of 764 kWh/m^2 is needed for parabolic-trough collectors to produce heat at a cheaper rate. In the high CAPEX scenario, this threshold DNI changes to 1′200 kWh/m2, and the average solar fraction limit varies from 25 % to 55 %. In high DNI locations (1′500 to 2′000 kWh/m2), 15 % to 30 % for medium DNI (1′001 to 1′499 kWh/m2), and 0 % to 10 % for low DNI locations (0 to 999 kWh/m2). For more details, we refer to the article [Saini2023]

2.2 Closed-loop cycle heat pump model

The closed-loop cycle heat pump model simulates the steady state of a heat pump where both the evaporating and condensing temperatures are below the critical temperature of the refrigerant. Therefore, the refrigerant condenses in the heat sink heat exchanger and evaporates in the heat source heat exchanger. This section describes the input needed to run the simulation and gives the output of the model.

Input
Heat source temperature profile
Heat sink temperature profile
Refrigerant
Various internal process parameters of the heat pump, which are suggested in the program

The model uses thermodynamic relations and assumptions to simulate the states of the heat pump for the corresponding refrigerant. The main assumptions are:

- no pressure nor heat loss in the heat pump pipes,

- isenthalpic expansion, and
- a fixed Pinch value in every heat exchangers (standard 5 K) .

Once each state has been simulated in the model using a solver such as EES (Engineering Equation Solver) the following outputs can be produced.

Output
COP (Coefficient of Performance)
Carnot COP
2nd Law efficiency
Volumetric heating capacity to determine cost of equipment
Internal Heat Pump Parameters (high & low pressures, pressure ratio, refrigerant mass flow, condensation & evaporation temperatures, temperature at the compressor outlet) to judge if a cycle with these conditions is feasible in production

The Carnot COP is calculated by dividing the temperature of the heat sink (process heat demand) by the temperature lift between the sink and the source. The COP of the heat pump is calculated by using the ratio of the enthalpy heat capacity in the heat sink and the enthalpy capacity of the compressor. The 2nd Law efficiency is the ratio between the COP real and the ideal Carnot efficiency. Typical industrial 2nd law efficiency is around 45% for systems with small temperature glides (typ. < 10 K) at heat input and heat rejection.

2.3 Transcritical heat pump model

Transcritical heat pumps deliver heat at a temperature higher than the critical refrigerant temperature. Thus, the refrigerant does not condense in the heat sink but is cooled down with a temperature glide (sensible cooling). The heat exchanger is therefore called a gas cooler and not a condenser.

The transcritical heat pump model is similar to the closed-loop heat pump model. It uses the same assumption and needs almost the same input:

Input
Heat source temperature profile
Heat sink temperature profile
Refrigerant
Various internal process parameters of the heat pump, which are suggested in the program

The calculations are performed similarly with the exception that the refrigerant temperature at the outlet of the gas cooler is given using the heat sink inlet temperature and the Pinch value.

The **output** of the transcritical model is the same as the ones of the closed-loop model. However, the COPs are calculated a bit differently as the gas cooler no longer has a constant temperature as described in [Jensen2018]. The equation used for ideal efficiency is the Lorentzen COP and is the ratio of the entropic mean temperature of the heat sink relative to the difference between the entropic mean temperatures of the heat sink and heat source. The second law of efficiency is hence the Lorentzen efficiency which is defined as the ratio between the actual heat pump COP and the Lorenz COP. The details are well described in [Jensen2018].

2.4 Open-loop cycle heat pump model

The open-loop cycle uses water as the refrigerant and has only one heat exchanger to evaporate the water. The steam is compressed to the desired steam pressure multiple times in series if necessary.

The heat sink temperature and the Pinch point need to be given to determine the evaporating temperature.

Input
Desired steam pressure
Heat source temperature profile
Various internal process parameters of the heat pump, which are suggested in the program

A maximal steam compressor ratio is allowed in the model (typically 3). If the pressure ratio between the steam evaporating pressure and the desired pressure is higher, a new compression step is added until each compressor has a pressure ratio below the given limit. If multiple compressors are used, intercooling using water injection reduces the temperature on each compressor outlet to the saturated temperature for the given pressure in order to reduce excessive temperatures.

Output
COP: Coefficient Of Performance
Carnot COP
Second law of efficiency
Volumetric heating capacity to determine cost of equipment
Internal Heat Pump Parameters (high & low pressures, pressure ratio, refrigerant mass flow, condensation & evaporation temperatures, temperature at the compressor outlet) to judge if a cycle with these conditions is feasible in production

The Carnot COP is calculated using the heat source temperature and the steam final saturated temperature. The heat pump COP is estimated using the enthalpy capacity of the steam (difference between the final and initial states) over the sum of the enthalpy capacities of the compression steps.

2.5 Combined-loop cycle heat pump model

The closed-loop and the open-loop models can be combined. The heat source of the open-loop model will be the heat sink of the closed-loop model. To match each model's dimension, the open-loop model's heat source capacity needs to correspond to the heat sink capacity. The COP is calculated using the enthalpy capacity of the steam (difference between the final and initial states) over the sum of the enthalpy capacities of the compression steps, including the refrigerant's close-loop cycle compression.

2.6 Simple techno-economical calculation tool using Excel

The model derived in principle for deliverable 5.3.1 to estimate the different payback and discount payback times has been implemented in an easy-to-use Excel file. The file is usable in three languages (English, French, and German) and guides the user through the input necessary to calculate the financial estimation.

3 Conclusions

A simulation to compare steam-generating heat pump and parabolic-trough collectors to produce steam at 3.6 bar (140°C) has been made in collaboration with the Department of Energy and Construction Engineering of the Dalarna University in Sweden. Results have been published [Saini2023], and the partnership should continue in order not only to compare both technologies but also to optimise the

combination of them and to implement it in a plant. Furthermore, different heat pump models were developed and then tested on 15+ case studies, while several publications have been published using these models [Längauer2021], [ArpagausHTHPS2022], and [ArpagausIIRGL2022].

Furthermore, an easy-to-use Excel file has been created to help industry to quickly estimate an industrial heat pump's payback and discounted payback time. The calculations used in this file were described in the previous deliverable 5.3.1.

4 References

Jensen, J. K., Ommen, T., Reinholdt, L., Markussen, W. B., & Elmegaard, B. Heat pump COP, part 2: Generalized COP estimation of heat pump processes. *13th IIR-Gustav Lorentzen Conference on Natural Refrigerants* (Vol. 2, pp. 1136-1145). **2018**, International Institute of Refrigeration. **https://doi.org/10.18462/iir.gl.2018.1386**

Saini, P., Ghasemi, M., Arpagaus, C., Bless, F., Bertsch, S., & Zhang, X. Techno-economic comparative analysis of solar thermal collectors and high-temperature heat pumps for industrial steam generation. *Energy Conversion and Management*, *277*, 116623, **2023**.

Längauer, A.; Adler, B; Arpagaus, C.; Bless, F.; Bertsch, S.: Vergleich der Rotationswärmepumpe mit konventionellen Kompressionswärmepumpen in industriellen Prozessen, *DKV Tagung*, 17.-19. November, **2021**, Dresden.

Arpagaus, C., Bless, F., Bertsch, S.S.: Techno-Economic Analysis of Steam-Generating Heat Pumps in Distillation Processes. *3rd **H**igh-**T**emperature **H**eat **P**ump **S**ymposium*, 29-30 March, **2022**, Copenhagen, Denmark, **https://hthp-symposium.org**

Arpagaus, C., Bless, F., Bertsch, S.: Techno-economic analysis of steam generating heat pumps for integration into distillation processes, *15th **IIR**-**G**ustav **L**orentzen conference on Natural Refrigerants*, June 13-15, **2022**, Trondheim, Norway, **http://dx.doi.org/10.18462/iir.gl2022.0029**

Arpagaus, C., Bless, Paranjape S., F., Bertsch, S.: Integration of High-Temperature Heat Pumps in Swiss Food Processes, *ICR2023, 26th International Congress of Refrigeration,* August 21st-25th, **2023,** Paris, France **(submitted)**

Appendix

EES Models can send directly for the people interested by contacting the authors.

Excel heat pump financial tool (print screens of entry mask):

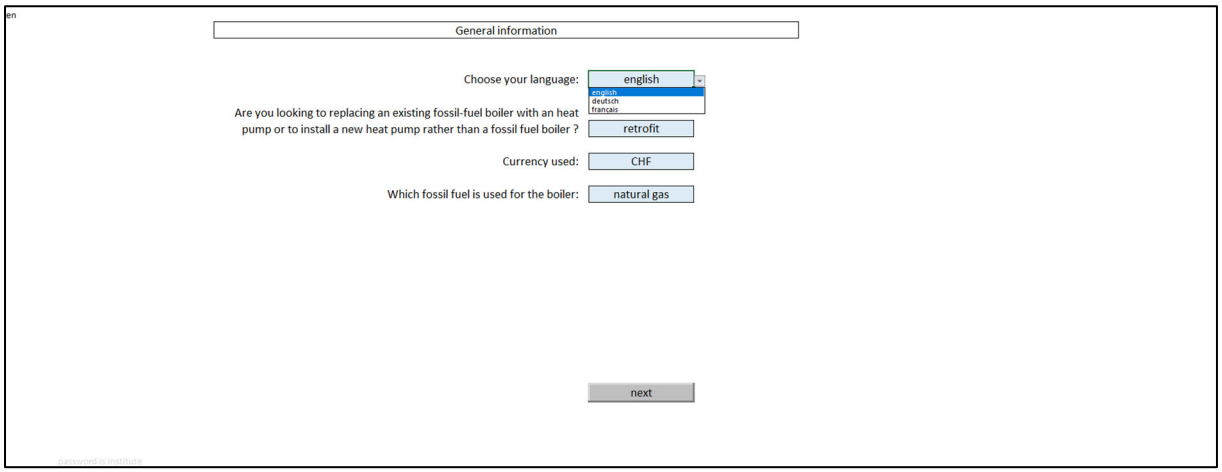

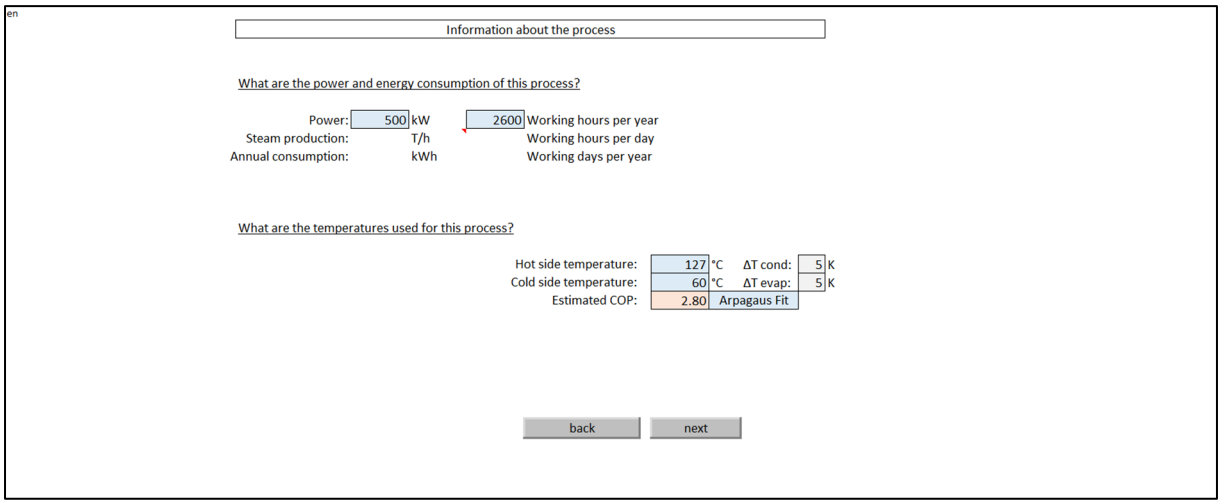

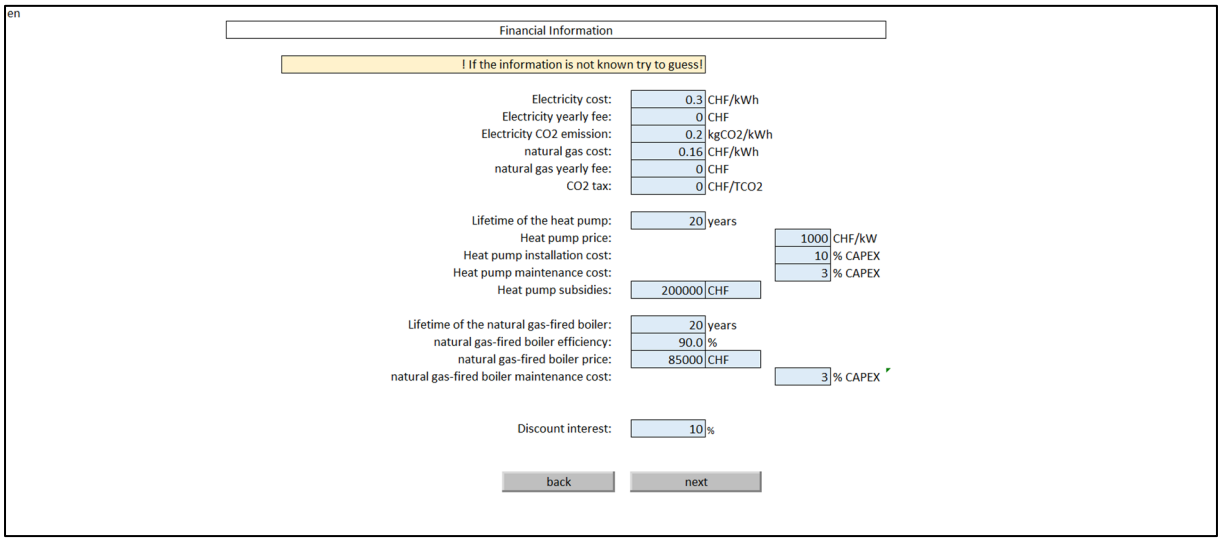

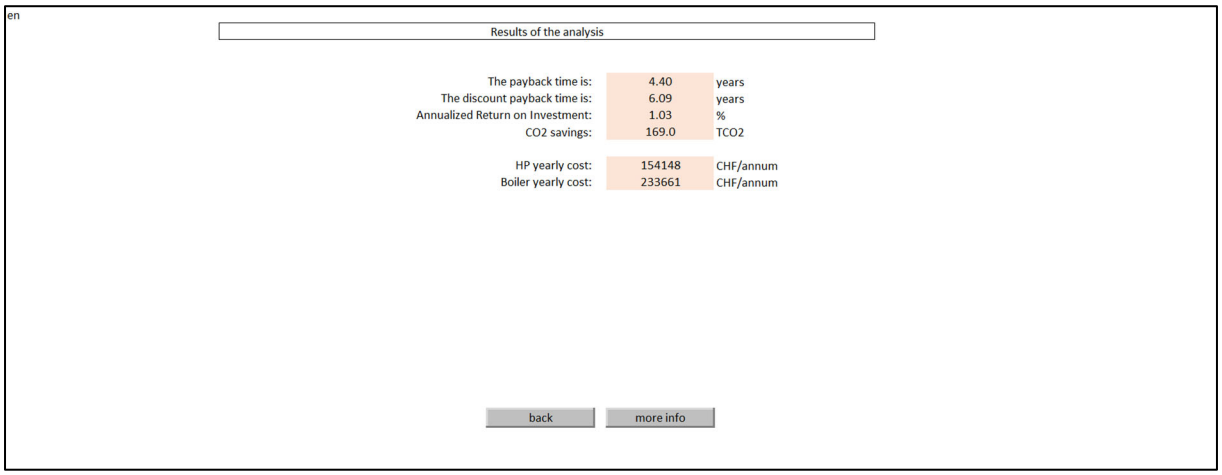

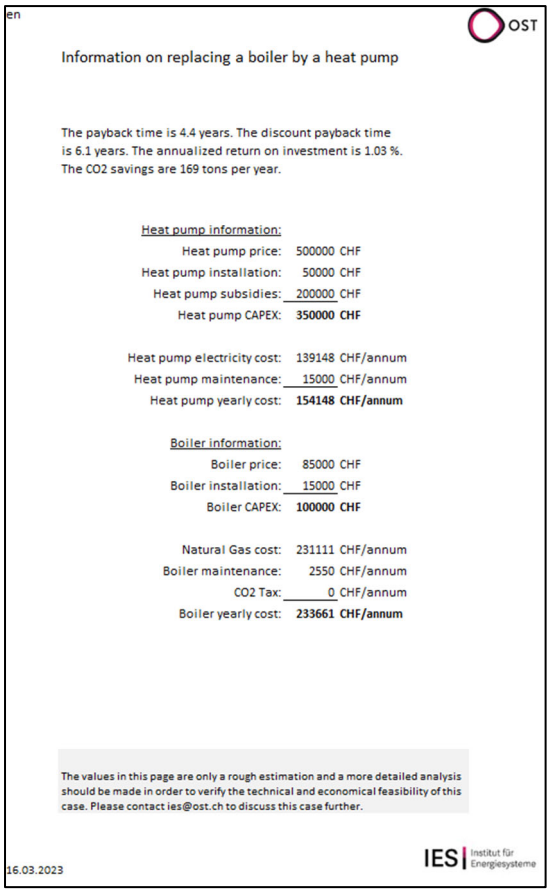

The following publications have already been published, or have been submitted already (the latter ones are watermarked). More publications on similar topics are in planning.

Energy Conversion and Management 277 (2023) 116623

Contents lists available at ScienceDirect

Energy Conversion and Management

journal homepage: www.elsevier.com/locate/enconman

Techno-economic comparative analysis of solar thermal collectors and high-temperature heat pumps for industrial steam generation

Puneet Saini [a,b,c,*], Mohammad Ghasemi [a], Cordin Arpagaus [d], Frédéric Bless [d], Stefan Bertsch [d], Xingxing Zhang [a]

[a] Department of Energy and Construction Engineering, Dalarna University, Falun S-79188, Sweden
[b] Department of Civil and Industrial Engineering, Uppsala University, Uppsala S-75236, Sweden
[c] Absolicon Solar Collectors AB, Fiskaregatan 11, Härnösand S-87133d, Sweden
[d] Eastern Switzerland University of Applied Sciences, Institute for Energy Systems, Werdenbergstrasse 4, CH-9471 Buchs, Switzerland

ARTICLE INFO

Keywords:
High-temperature heat pump
Parabolic trough collector
Solar fraction
Techno-economic analysis

ABSTRACT

Industrial heat production is responsible for around 20% of total greenhouse gas emissions in Europe. To achieve the climate change goals defined in the Paris Climate Agreement, the EU commission has shifted its focus on sustainable means to generate heating. Moreover, global dependencies are leading to a re-organization of natural gas supplies. Therefore, there is a need for less vulnerable and less price-volatile solutions for heating. This paper focuses on two decarbonization technologies for industrial process heat supply: a) electricity-driven steam-generating high-temperature heat pumps (HTHP), a technology that is more efficient than fossil fuel boilers in generating steam, and b) solar parabolic trough collector (PTC), which can produce heat economically and at a minimal carbon footprint compared to other technologies. The main aim of this paper is to evaluate the levelized cost of heat (LCOH) of these technologies to fulfill a comparative techno-economic analysis. A maximum PTC collector's solar fraction limit (SF_{limit}) is defined to indicate when the LCOH for these two technologies is equal. This allows for distinguishing between the economic stronghold of each technology. The evaluation is carried out through the annual energy simulations using TRNSYS and Excel spreadsheets for HTHPs, while TRNSED and OCTAVE are used for the solar thermal part. Boundary conditions for European geographical constraints have been applied to establish use cases for the analysis. The result shows that the design of a PTC system with optimal SF can reach cost parity with HTHP for most of the analyzed locations. The developed methodology serves as a valuable guide to quickly determine a preferred lower carbon heat solution, thus easing the decision-making for industries.

1. Introduction

"Heat is half" of the global primary energy consumption [1]. The generation of heat from various fuel sources results in nearly 40 % of the global CO_2 emissions. Decarbonizing the heating supply is the "elephant in the room" and needs significant attention from policymakers to promote the right technological solution to facilitate the rapid replacement of gas, coal, and other fossil fuels.

Heat is consumed in buildings for space heating, domestic hot water, and industries to generate steam or hot water. The major focus regarding technical solutions for clean heating is often on electrification using electrical heaters or heat pumps (HPs). Residential heating demand can be decarbonized using commercial HPs, and their significance is further emphasized in Repower EU, which aims to deploy 60 million HPs by 2030, a projected 4-fold increase from current numbers [2].

It is important to note that industrial process heating demand constitutes 66 % of the EU's overall heating demand [3]. In addition, the concepts of positive energy district (PED) and climate-neutral city are promising nowadays, but they have not yet included industrial heating demand within their boundaries. With the ongoing challenges in gas

Abbreviations: CAPEX, Capital expenses; COP, Coefficient of performance; DNI, Direct Normal Irradiation; EIR, Electricity inflation rate; HP, Heat pump; HTHP, High-temperature heat pump; IEA, International Energy Agency; KPI, Key performance indicator; LCOH, Levelized cost of heat; LPR, Load profile; OPEX, Operation expenses; PTC, Parabolic trough collector; PED, Positive energy districts.; ST, Solar thermal; SHIP, Solar heat for the industrial process.

* Corresponding author at: Department of Energy and Construction Engineering, Dalarna University, Falun S-79188, Sweden.
E-mail addresses: pks@du.se, puneet@absolicon.com (P. Saini).

https://doi.org/10.1016/j.enconman.2022.116623
Received 21 August 2022; Received in revised form 9 November 2022; Accepted 21 December 2022
Available online 31 December 2022

supply, natural gas prices have increased exponentially in the past few years, thus creating an energy-tense situation in the EU [4]. This implies that a less price-volatile and reliable supply of fuels for industrial process heat should be prioritized. The process heat required in most industries is in the medium temperature range (i.e., 80 to 250 °C). Several technologies in the market can achieve this temperature with low carbon emissions, such as solar thermal (ST) collectors, high-temperature heat pumps (HTHP), and boilers utilizing green fuels such as waste biomass or biogas, or renewable electricity.

Industries typically use fossil fuel boilers to generate steam, which is used as a heat transfer fluid to carry out several processes. Retrofitting any new technology in an existing boiler system requires a detailed understanding of system boundary conditions. Economic feasibility is a crucial decisive criterion for industries to evaluate any technology. From market experience, it is realized that large multinationals can facilitate the capital expenditure (CAPEX) for an efficiency improvement process (such as the implementation of ST, HTHP) only if the payback is less than 5 years.

An indicative pre-feasibility assessment using economic key performance indicators (KPIs) can facilitate industries toward quick decision-making for a go/no-go decision concerning a detailed evaluation of any technology. Therefore, this paper is themed around doing a comparative techno-economic analysis for heat generation using typical boundary conditions encountered in industries. The focus is on two technologies to generate steam, i.e. (a) steam-generating HTHPs and (b) Parabolic trough collector (PTC), which is a type of concentrating ST collector. The sections provide a literature review and the current development status of using these technologies for industrial applications.

1.1. High-temperature heat pumps

1.1.1. HP use in industries

HTHPs can be a good alternative solution in industries where waste heat is available such as in drying, sterilization, papermaking, distillation, or food preparation processes [5]. HPs can upgrade low-temperature waste heat into suitable high-temperature levels. Moreover, multi-temperature HPs, which can utilize multi-temperature heat sources in different hydraulic configurations, are also an appropriate solution to increase the overall system efficiency [6]. However, HTHP use is often restricted by the temperature need of an industrial plant. If the steam temperature required is within the range (e.g., low-pressure steam), an HTHP can be used as a one-to-one replacement technology for an existing boiler system. However, the redundancy of heat supply is often necessary for industries by installing a boiler parallel to the heat pump as a backup or covering peak loads. Several industrial sectors, such as food, beverage, dairy, and mining, need temperatures suitable for existing steam heat pumps. Even if the steam temperature required is higher than the HTHP supply range, it is possible to find a process that operates at lower temperatures and runs them exclusively using HPs. Another option is combining the HTHP system with mechanical vapor recompression to increase steam pressure [7].

A heat pump requires a heat source and electricity inputs for operation. Therefore, replacing existing steam boilers with HTHP increases the plant's electricity consumption. In some cases, this may require an increase in the electrical grid capacity, thus resulting in an additional cost for users. As the coefficient of performance (COP) for HPs is more than the efficiency of fossil fuel boilers, implementing HP would result in CO_2 savings in most cases. However, if the grid electricity is highly carbon intensive (such as if produced by coal), and if the existing boiler uses low carbon fuel (such as waste biomass), then a detailed CO_2 savings analysis becomes imperative to make sure that an HP solution results in positive CO_2 replacement. Hybridization of HTHPs with other backup sources (e.g., green boiler, solar thermal, thermal storage) is the way forward for industries while assuring the system's reliability. In developing countries, grid reliability is low, so hybridization becomes more critical to ensure process operation.

Process heat demand mostly occurs above 80 °C, which coincides with the starting sink temperature range of HTHPs. HTHP applications between 100 and 160 °C are mostly found in food and tobacco, chemical, and paper industries for drying, pasteurization, sterilization, evaporation, and distillation [8]. The next sub-section provides an overview of different heat pump products.

1.1.2. Research overview and commercial suppliers

Despite promising advantages, there are still some barriers to the widespread deployment of industrial HTHPs, such as a lack of awareness and confidence in industries, integration challenges, and a lack of skilled personnel for upkeep [9]. However, a significant research effort is being made to overcome these barriers.

Today, there are more than 300 good practices of industrial HPs applications in processes such as drying, washing, evaporation, distillation, and cooling [10]. Currently, there are 20 projects realized for heat pumps with steam generations above 100 °C. The recently concluded HTHP symposium in the Year 2022 has attracted several researchers and industrial partners to come forward to collaborate [11]. Research projects and case studies create a huge knowledge base to promote this technology's rapid deployment. IEA HPT has conducted several Annex projects dedicated to industrial HPs, such as Annex 21, 35, and 48 [12]. The second phase of IEA Annex 48 on industrial HPs focuses on overcoming the existing hindrances for larger market penetration of industrial HPs. The ongoing Annex 58 (2021 to 2023) is specifically dedicated to HTHP with supply temperatures over 100 °C and aims to support understanding of the technology's potential among various stakeholders, such as manufacturers, end-users, consultants, energy planners, and policymakers [13].

A major development focus is new environmentally friendly refrigerants with low global warming potential while achieving high heat sink temperatures [14]. Increasing numbers of manufacturers can offer steam heat pumps suitable for industries. These companies provide heat sink temperatures mostly between 90 °C and 200 °C, with few suppliers providing products exceeding 200 °C using steam as an energy carrier [15]. The heating capacities vary from about 20 kW to 20 MW based on cycle design (single- or two-stage), refrigerant type, compressor types, internal heat exchangers, etc. The COP values range from 1.5 to 5 at temperature lifts of 130 to 40 K, respectively. IEA HPT Annex 58 project has identified at least 25 manufacturers providing steam-generating heat pumps. The technology readiness level of the recalled products ranges from 4 to 7 to a maximum temperature of up to 280 °C. The specific investment cost of the heat pumps ranges from 200 to 2′000 €/kW_{th}. The large variation can be attributed to various technological alternatives and installation boundaries. The average lifetime of an HTHP is between 10 and 35 years and correlates with its thermal capacity, with a lifetime of up to 30 years for capacities more than 5 MW [13].

1.1.3. Integration approaches for HTHP

1.1.3.1. Heat pump integration with boilers. Understanding an existing industrial system is imperative for the retrofit design of any thermal solution. In an industrial setting, a boiler is typically used to generate steam, hot water, or hot oil to heat various processes. When designing such conventional systems, the knowledge of the expected peak load alone from industries is sufficient in many cases. The peak load then helps determine the size of the heat generation equipment, such as a boiler. Depending on the type of industry, the heat load can vary daily, weekly, or monthly. Planning of HTHP in an industrial system can be released in several steps, starting from measuring the existing system data, and identifying the potential for waste heat recovery [16]. This can be done using pinch analysis by generating composite curves of various heating and cooling streams. Using this approach, an optimal integration point can be found for HTHP, given the techno-economic

constraints. For example, HTHP can be used as a parallel operation with a boiler to generate steam to feed into the main steam header. Another possibility is to use HP only for a specific process, therefore isolating that process from the boiler [17].

1.1.3.2. Heat pump integration with various processes. The process integration of HTHP often benefits lower temperature lifts, thus better COP, than when HTHP is used for central steam generation. One such use of HTHP is for drying applications. Drying is an energy-intensive process with significant potential for waste heat recovery from outgoing moisture content in exhaust gases. Heat losses in drying process plants in Europe amount to about 11.3 EJ [18]. The European goal is to develop HTHPs technically and economically feasible for heat recovery in industrial drying and dehydration processes to utilize them at higher temperatures up to 160 °C. When HP technology is deployed to 50 % of all European drying processes, it is expected to reduce 3 % to 7 % of CO_2 emissions [19].

Several EU projects have been funded to achieve this goal. Among others, the "Dryficiency" project, which intended to develop two HTHP systems expected to save energy and reduce emissions. These systems focused on drying and dehydration processes up to 160 °C. As a result, energy savings of up to 80 % were expected, and emissions reductions by 75 % compared to the existing system. As a result, two vapor compression HPs have been introduced and utilized in real production plants in industrial drying processes in three European manufacturing companies in the food and brick industries [20].

The project "FRIENDSHIP" intends to study HTHPs, heat storage systems, and solar technologies and how they can be combined to optimize the system for the intended process. The systems created from this project are expected to provide heating and cooling, ranging from 300 °C to −40 °C [21]. The goal is to understand how much emissions can be reduced using the mentioned technologies. Within the project "SuPrHeat", three HTHP systems are developed using different heat transfer fluids. These heat pumps will supply heat at temperatures up to 200 °C. Water, hydrocarbons, and CO_2 will be used in the developed heat pumps, which will be integrated into existing facilities [22].

1.1.3.3. Heat pump integration in district heating. Besides industrial applications, HTHPs are an important bridge technology to decarbonize heat in the district heating sector [23]. Large-scale HPs in district heating plants can deliver supply temperatures between 85 °C and 120 °C. In addition, renewable electricity from solar PV and wind turbines can be used to run the HPs and other system auxiliaries. The political incentives in Denmark support Danish research to develop more efficient HPs to reach 0 % CO_2 emissions by 2050. Industrial HP installations comprise 77 projects with a total capacity of around 120 MW, of which 66 cases use HPs in district heating. HPs with a combination of solar thermal collectors and large pit storage is an effective combination to achieve a nearly 100 % renewable heating system [24].

1.2. Solar thermal for industrial applications

1.2.1. Solar thermal for industries

Solar energy is often mistakenly synonymous with solar PV, which produces electricity using photovoltaic cells. However, another market segment of solar energy is known as solar thermal (ST)/solar heating solutions. ST is distinct from solar PV from technology and the final energy-form perspective. ST has a decade-long, worldwide implementation history and is the 3rd largest renewable energy source with a total installed capacity of 522 GW_{th}. The cumulative collector area installed up to 2021 is 746 million m^2 (equivalent to 75 000 soccer fields) [25]. Studies have shown that solar thermal technologies need up to 4 times less land area for the same final thermal output than solar PV [2627]. In addition, there has been a significant decrease in the capital cost and LCOH for solar thermal plants in the past few years [28].

There are several types of solar thermal collectors available in the market. The selection of a collector type depends on the required temperature levels, the process medium, and the local annual irradiation characteristics. For temperatures above 150 °C, usually tracking concentrating collectors can be applied. Within the temperature range between 100 °C and 150 °C, both collector types (concentrating and non-concentrating) can be technically suitable and need project-specific evaluation. The technology selection for a specific site and application is typically based on the lowest heat generation costs during the service life.

Solar heat for the industrial process (SHIP) is a sub-sector in the market, where the collectors are often used to generate steam for the industries. The SHIP market has gained significant attention in the past few years. In 2021, a total of 78 SHIP plants were installed worldwide with a collector area of 52′000 m^2. Up to 2021, the total installed SHIP projects approached 1000, with a cumulative collector area of 1.23 million m^2 [25]. The growth rate for SHIP plants is expected to be significant, given the high heating costs that industries are facing due to the restricted gas availability.

There are many solar thermal collector types that can medium temperature range needed for many industries. Concentrating technologies are primarily used for steam generation applications. Linear fresnel collectors such as those provided by [2930] are light weight and can reach temperatures up to 300 °C. The optical losses are higher in Fresnel collectors due to the flat mirrors, which do not represent a true parabola. However, a significant advantage lies in a fixed receiver (usually glass covered) which eliminates the need for moving joints carrying working fluid. Large parabolic dish collectors with dual axis are realised in a few projects in India and Australia [31 32]. Dual axis tracking leads to a point focus concentrator, and thus possibilities to reach high temperatures. Despite this, the commercial applications of such collectors is limited to only few projects.

In stationary collectors, a vacuum flat plat collector can generate low-pressure steam [33]. Even though the concentration ratio for such a collector is 1 Sun (or slightly higher for non-imaging collectors), lower heat losses due to vacuum lead to higher fluid temperatures in collectors. However, due to no tracking system in such collectors, the stagnation conditions are difficult to manage compare to tracking technologies.

Out of different solar thermal technologies, PTC is widely used and holds the top spot for total capacity installed worldwide SHW. PTC collectors consist of a parabolic shape reflector with a high reflectivity surface. The sun ray's incident on the surface with an incidence angle is longitudinal, and the collector tracks the sun in a transversal plane. These rays are concentrated on a receiver, which absorbs this heat, and then heats the working fluid. There are many construction variants of PTC available commercially. The large aperture PTC collectors with glass reflector and vacuumed receivers are used in many CSP plant. The advantage lies in a high concentration ratio and lower heat losses, which helps reach the high fluid temperature required for power generation. For industrial-scale PTC collectors, several design aspects need to account for, such as modularity, low weight for roof top installation, lower cleaning cost, etc. Fig. 1 exemplifies the industrial PTC type with key components [34]. The collector has no vacuum in receiver tubes, unlike in large PTC, instead the whole PTC is covered with a glass cover to avoid soiling.

Mexico has the highest number of SHIP plants installed, with a capacity weighted LCOH of 36 €/MWh, competitive with fossil fuels such as liquefied petroleum gas (LPG), fuel oil, and diesel, suggesting the potential for further market growth. In Europe, from the year 2014 to 2019, the total installed cost of SHIP projects has decreased by 40 %, reaching a value of around 550 €/m^2 aperture area. In addition, the economy of scale and policy support can further help to reduce heating costs [28].

1.2.2. Solar thermal integration with industrial processes

While designing the system for users, the dynamics of the solar

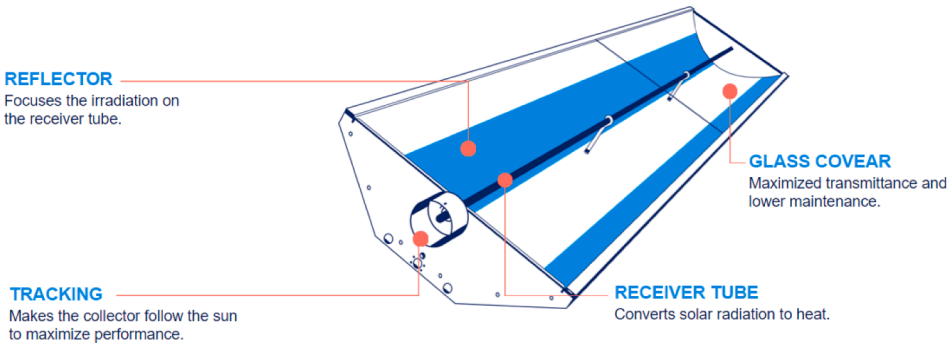

Fig. 1. A view of glass-covered small-scale parabolic trough collector with its key components.

thermal collector, heat load profile, and storage system are important [35]. Fig. 2 shows a typical boiler system in industries, where red concentring circles with number marks the integration points for ST collectors. The integration points before the boiler are from 1 to 3 i.e. make-up water, condensate heating, and feed water heating. Most low-temperature collectors are used to pre-heat the boiler feed water or make-up water temperature, as the temperature levels are appropriate for such collectors. If an economizer already exists in the boiler, the solar feed water heating often decrease the economiser's effectiveness, making feed water heating a less attractive integration point.

If integrated for steam generation (points 4 and 5), collectors can displace the fuel energy in the boiler to provide the latent heat. Therefore, integration after the boiler for steam generation allows for a higher solar fraction (SF) than integration before the boiler. There is also a possibility for process integration (number 6), where solar collector system is used to meet heat demand for a specific process with or without thermal storage. Process integration in some cases allows to have lower operating temperature in the collector resulting in high efficiency. Task 49 of IEA SHC provides detailed guidelines regarding design principles and integration recommendations for ST collectors [36].

1.2.3. *Hybridization of solar thermal with heat pumps*

Terrestrial irradiation has daily and seasonal variations. For a typical solar PV system, the grid acts as a large battery that balances the production and demand with minimal waste of electricity. However, the solar heating systems are often retrofitted with individual/stand-alone boilers to continue the operation for non-sunny hours.

As most industries have constant heating demand throughout the day (and year). ST System design with a low SF allows the solar production to always be less than the user's heat demand, thus increasing the system's utilization. Therefore, SHIP systems are typically designed with low solar fraction and backup systems. However, if an ST is designed without thermal storage, the fraction of the overall heat demand met with solar collectors be limited.

To achieve high solar fraction, steam storage is often a limiting component restricting the cost feasibility of the system. Due to its very low density, steam storage is not economical. It is usually stored as sensible heat in solid media or liquid using oil or pressurized hot water. It is observed that for a given constant load profile, the economic feasibility of the solar thermal installation decreases after a threshold solar fraction due to the need for high thermal storage capacity. As the specific heat cost of a pressurized thermal storage is higher than that of a solar thermal collector, thus large tank volumes in the system result in a relatively high cost of heating. This situation puts a financial limit on the maximum solar fraction achievable.

As industries are looking for nearly 100 % renewable heating systems, solar thermal has the opportunity to collaborate with other technological alternatives to compensate for the solar irradiation lack or fluctuation during the night and day. Fig. 3 exemplifies such a system concept to reach high renewable heating fractions using a concept involving several technologies, such as thermal storage and a heat pump driven by green electricity. The existing boiler use can be minimised if the system components are sized optimally.

Previous studies have shown that hybridizing the heat pump with solar thermal collector results in the lowest levelized cost of heating

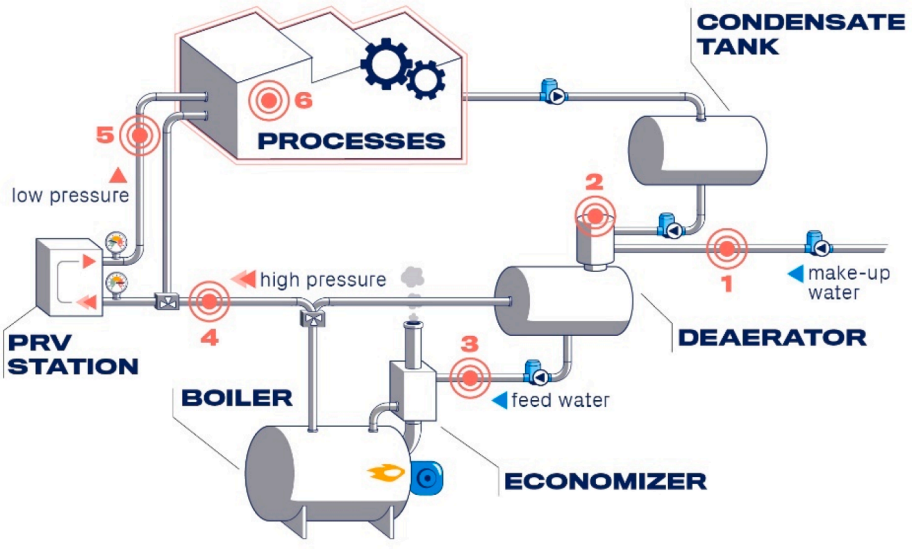

Fig. 2. Schematic of a typical industrial boiler-based energy system (red concentring circles represents the possible integration points for ST collectors).

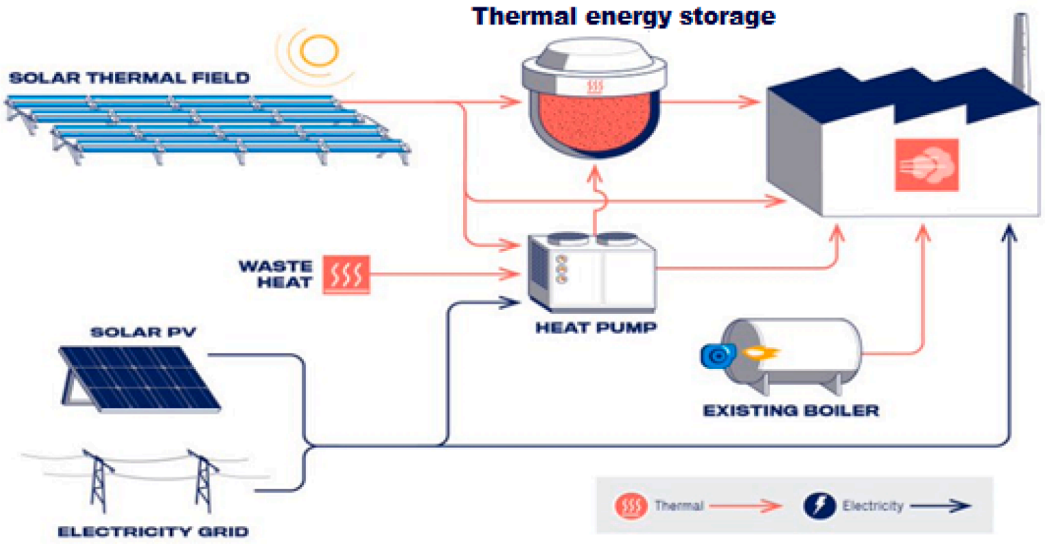

Fig. 3. Example of a hybrid system of PTC and HTHP to achieve high renewable heating fractions in industries.

(LCOH) compared when these technologies are used individually. Therefore, more research is needed to understand the techno-economic boundaries of solar thermal and HTHP in stand-alone and hybrid modes. This paper takes a step by looking into a comparative analysis of these two technologies. The current study is a base to investigate the combined hybrid systems in future applications.

2. Objectives

The central objective of this paper is a comparative analysis of both HTHP and PTC systems for steam applications using industrial boundary conditions. Previous studies have performed a general feasibility analysis for solar thermal technologies or heat pumps. However, only a few have investigated comparing these technologies on a large spatial scale with techno-economic boundaries. Moreover, there is a lack of studies comparing HTHP for steam generation with PTC-based collectors. Therefore, Platzer (2021) [37] proposed a unified cost indicator method to compare different technological scenarios for process heating in industries. The indicator includes the system's energy, economic and environmental performance, enabling decision-makers to evaluate several scenarios under the same base conditions.

The most relevant work to the current paper is by Meyers et al. (2018) [38], where the authors have developed a techno-economic comparison methodology using maximum turn-key solar investment as an indicator. This methodology can be used as a criterion to quickly compare and select between solar thermal and heat pumps based on boundary conditions.

However, the study did not consider the effect of SF on LCOH. This variation is critical to consider while comparing technologies, especially with high-temperature solar thermal, due to the lack of steam storage technologies. The LCOH of the ST system increases exponentially after a threshold SF due to the diminishing added value of heat storage. Therefore, when comparing other technologies with ST, the SF is a critical criterion to define and is not considered in previous studies. The current paper has overcome the limitations by using comprehensive variables as a comparison basis for both HTHP and ST. The paper also considers updated analysis from a techno-economic perspective capturing the recent development in PTC and HTHP while considering the effects of improved efficiency and cost reductions.

3. Research methodology

This study aims to assess the energy and economic performances of Industrial PTC and HTHP in the context of European climates. Fig. 4 shows the flow chart of the methodology used for analysis. First, the evaluation is carried out through annual energy simulations performed with dynamic simulation software. After this, a systematic approach is followed to provide the reader with the information needed to understand the results. Fig. 4 shows the workflow used during this study.

The analysis is carried out for 3 different load profiles with constant peak demand to capture a broad range of industrial load conditions. The geographical focus for simulations is limited to Europe. However, the results obtained are parametrized to direct normal irradiation (DNI) and can be used to assess the performance for any given location.

In Step 1, simulations for HTHP are conducted using TRNSYS for given load profiles to calculate the COP and thermal output [39]. The outputs are based on a performance map obtained from an HTHP supplier (ref) for a broad range of operating conditions.

In Step 2, dynamic simulations for PTC collectors are done. The product chosen for this study is restricted to a PTC manufactured by a Swedish company named Absolicon solar collector AB [34]. The product is designed for industrial applications and fits this study well.

Simulation of the PTC system is done in two sub-steps. The component performance is analyzed using TRNSED, and the system performance is simulated using the developed model in OCTAVE. Storage sizing optimization obtains each location's SF vs LCOH curve. The LCOH calculations for ST and HTHP are done using a developed model in Excel.

Finally, in Step 3, based on the results obtained, the LCOH of both technologies is compared to provide boundary conditions to identify the strong economic hold of each technology. An indicator SF_{limit} is introduced to distinguish the economic advantage and to generalize the results.

The next section defines the critical boundary conditions and assumptions made for the simulations.

4. System boundaries and model

4.1. Load profiles and heating demand

The heat demand in the industries depends on the process characteristics and varies, which is difficult to capture by one study. However, the selection of load profiles to represent a significant share of industries is the focus of this paper. Three different load demand profiles are considered for the analysis. The peak heat demand is fixed at 500 kW_{th} (steam flow of 0.8 tonnes per hour), typical of many process industries.

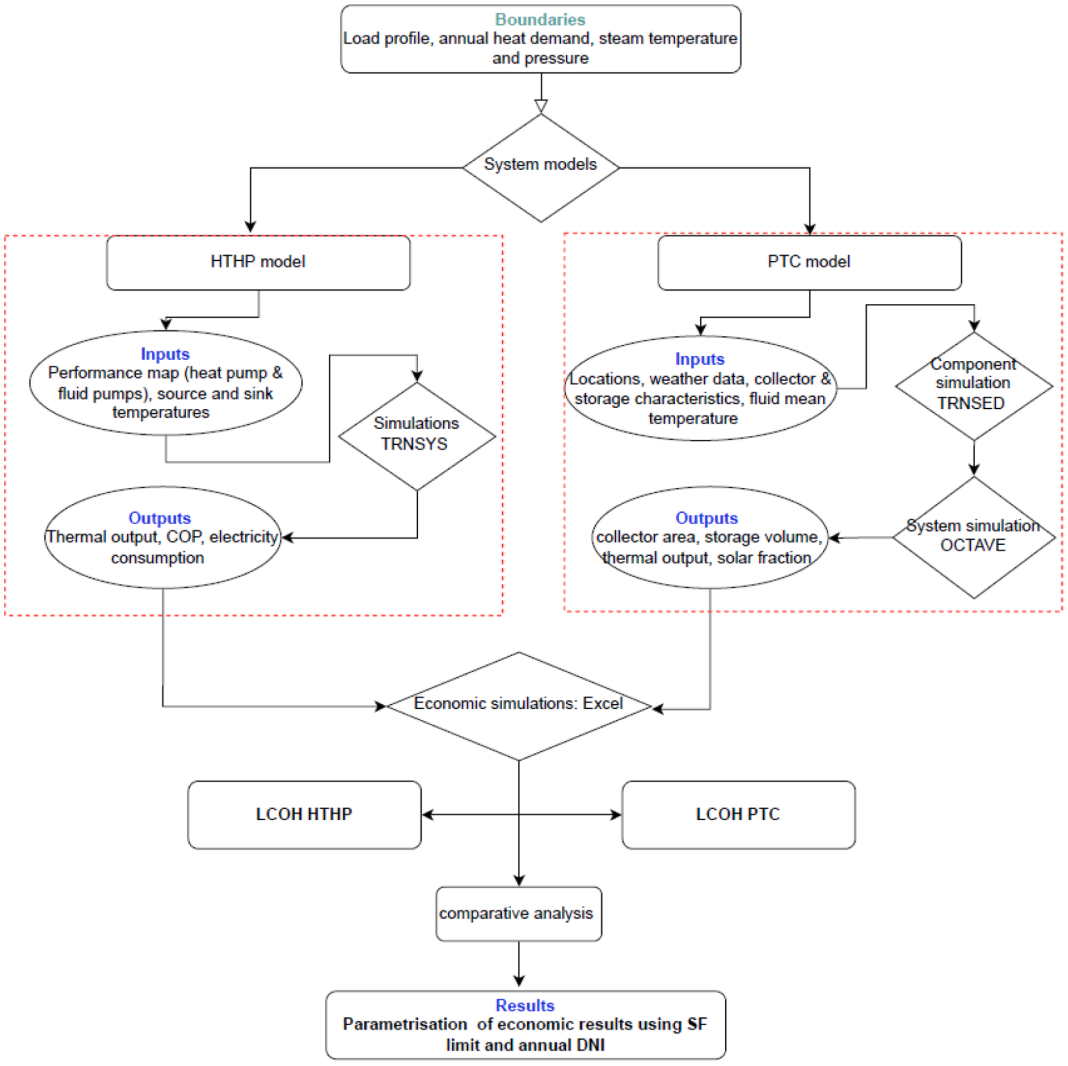

Fig. 4. Flow chart for the methodology used for this study.

As ST and HTHP are subjected to the same load constraints, the comparative results are not affected by the selection of peak load value. The steam demand is assumed at a constant temperature of 140 °C (saturation pressure 3.7 bar_a). The steam temperature range is commonly used in many food processing industries and fits well with temperature constraints for both medium-scale PTC and HTHP products.

The 3 chosen load profiles are explained as follows:

- **Continuous demand**: Uniform demand throughout the year with 8760 annual operational hours, which results in annual heat demand of 4380 MWh/year. Such load profiles are prevalent in many large production factories, such as the pharmaceutical sector.
- **Weekday demand**: Uniform demand throughout the weekdays of the year (no operation during the weekend). The annual heat demand for this case is 3132 GWh/year, corresponding to real cases in industrial load. An example of this load variation can be found in the food and beverage sector.
- **Daytime demand**: Uniform demand only during the day (10 h per day starting 8:00 to 18:00 for whole week), resulting in an annual heat load of 1825 GWh/year. This load profile is typical for a small/medium production facility.

A summary of the considered load profile cases for simulations is shown in Table 1.

Weekly variation for considered load profiles is shown in Fig. 5. The presented week pattern is repeated for a whole year to obtain the annual heat demand.

Table 1
Summary of the load profiles considered for simulations.

Load profile	Nos of operational days per year	Operational days per week	Operational hours per day	Peak Power [kW]	Annual heating load [GWh]	Time
1	365	7	24	500	4.38	24*7*365
2	261	5	24	500	3.13	24*5
3	365	7	10	500	1.82	8:00 to 18:00 each day

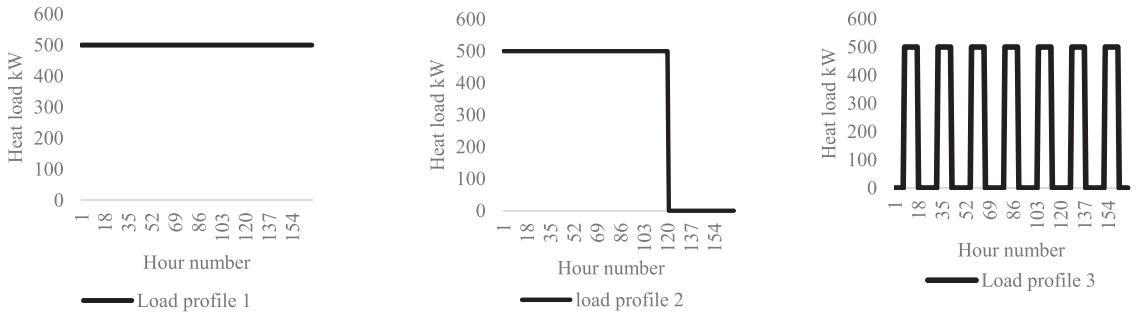

Fig. 5. Weekly variation of different load profiles considered for the analysis.

4.2. HTHP boundaries

4.2.1. HTHP integration

After industrial boundary conditions, the next step is to design an HTHP system and evaluate the techno-economic conditions. HTHP can be integrated at several points, for example, central steam generation for the whole plant or a specific process. This integration type will decide the inlet temperature of the fluid stream at the sink of HTHP to further convert into steam. Steam generated by the HTHP will be fed to the steam line. Therefore, the sink inlet fluid can be tapped feedwater or deaerator of the existing boiler system. The feedwater pump used for the boiler can be utilized to obtain the required flow in the HTHP. If integrated with the boiler steam header, HTHP must generate steam at slight overpressure to ensure that steam from HTHP is preferred over boiler steam.

The HTHP is designed for peak heating capacity in this study. Therefore, it is considered the sole heat source for the energy system without any backup boiler. On the source side, the available wastewater stream is considered at the inlet, which transfers heat to the HP refrigerant and exits at a lower temperature depending on the temperature glide. On the sink side, the feed water stream enters the inlet and receives heat from HP to convert to steam, which is fed to the process line. A commercial HTHP (Kobelco model SGH 165) capable of generating steam at a maximum temperature of 165 °C is used to meet the steam requirement [40].

4.2.2. HTHP model

The HTHP used for this study can produce steam up to maximum temperature and pressure of 165 °C and 0.8 MPa-gauge, respectively. The applied refrigerant in this HP is a mixture of R134a and R245fa. The heat pump utilizes a semi-hermetic inverter twin screw compressor. The rated COP of the modeled HTHP is 2.5, specified at source and sink temperatures of 70 °C and 165 °C, respectively. A performance map based on data from the commercial HTHP [40] is used to calculate the electricity consumption. The performance map consists of the COP of the HTHP for various temperature lifts, as shown in Fig. 6. The temperature lift represents the difference between the fluid temperature at the heat source inlet and the heat sink outlet. The heat pump has a variable speed capacity to operate at the part load conditions. The electrical consumption derived from the annual simulations is then used to calculate the LCOH.

The design temperatures for the HP model are shown in Fig. 7. The source for the HP evaporator is considered a wastewater stream with a fixed temperature of 40 °C, available throughout the year. A temperature glide of 6 K is considered on the evaporator. The resulting temperature lift of the HTHP is 100 °C, corresponding to steam temperature of 140 °C. The feedwater temperature entering the HTHP arrives at 110 °C, resulting in a 30 K temperature difference on the heat sink side. The flow rate in the source and sink are varied to obtain the designed temperature glide and thermal capacity, respectively. The heat pump is designed for peak heating demand of 500 kW; the specifications are shown in Table 2.

Other than the electricity consumption of the HTHP, there are water pumps on the source and sink side, which also consume electricity and is

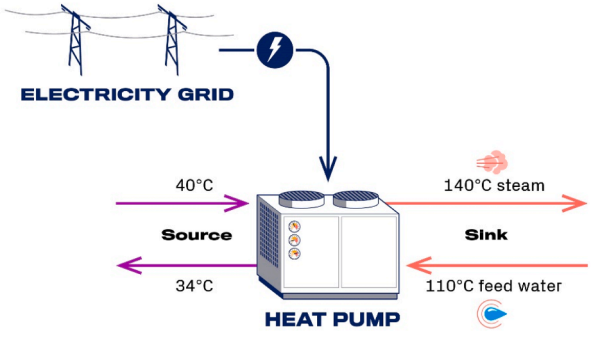

Fig. 7. Various fluid stream temperatures of the HTHP system considered for this study.

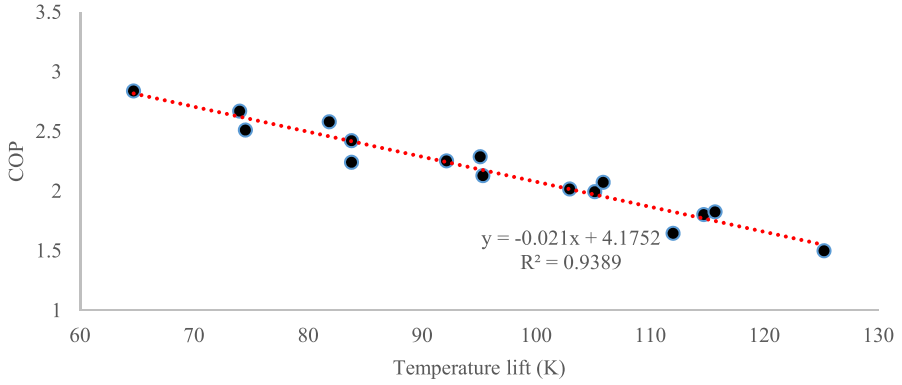

Fig. 6. Variation of HP COP with temperature lift.

Table 2
Specifications of HP considered in this study [40].

Parameter	Value
Compressor type	Semi-Hermetic Inverter Twin Screw
Refrigerant	Mixture of HFC134a & HFC245fa
Dimensions (W × H × L) [mm]	4′400 × 3′180 × 2′810
Weight [kg]	7′090
Heating capacity[t/h] @0.6MPaG, source 70 °C	0.839 @20 °C supply
Power [kW] @0.6MPaG, source 70 °C	253.9
Heating COP@0.6MPaG, source 70 °C	2.5

important in LCOH calculations. The pumps are sized to provide the desired flow rate in the network. Pressure drop calculations are done to estimate the total head in the network using Serghide's method [41]. The pump is designed for the total pressure drop of the network is 1 bar, assuming 20 % safety factor while accounting for bends and joints, etc. Based on the flow and pressure drop, a commercial pump is selected from the manufacturer catalog. The products are used to derive the pump curves (flow vs head and efficiency vs head) to simulate the working points of a given scenario and thus used for electricity consumption to calculate LCOH.

4.2.3. Economic inputs for HTHP

For the heat pump LCOH, it is necessary to include various costs. The analysis is done for 3 different capital expenditures (CAPEX) of 500, 1′000, and 1′500 Euro/kW_{th} values derived from data based on implemented HTHP case studies [13]. The operational costs for HTHP consider the electricity to run the heat pump compressor and fluid pumps. The O&M costs for HTHP are usually higher than those for boilers and are set to 5 % of the CAPEX value. The relevant parameters for HTHP thermo-economic modeling are shown in Table 3. The LCOH of both HTHP and PTC systems are compared for a time horizon of 15 years. The period is chosen to reflect the suitable timeline various multinational companies consider for energy-related investments. Three different electricity prices are chosen for analysis considering the range of industrial electricity tariffs in the EU.

For sensitivity analysis of LCOH, a total of 27 cases are analyzed, accounting for 3 different values of three variables (i.e., CAPEX, electricity price, and load profiles). The values of these variables are shown in Table 4.

4.3. ST simulations

4.3.1. PTC product description

The ST product considered for analysis is a PTC collector manufactured by the Swedish company Absolicon solar AB. The product T160 is a concentrating parabolic trough collector that focuses direct solar irradiance onto an absorber tube that runs along the focal line of the concentrator and contains a working fluid that gets heated when solar radiation is concentrated on it. The collector works on single-axis tracking using the astronomical watch, which tracks the solar collectors, so they always face the sun. The product can generate steam and hot water from 60 °C to 160 °C, and is therefore suitable for many industrial sectors (e.g., dairy, brewery, chemical, etc.). The collector can be categorized as a small PTC type and is certified by solar Keymark. The optical efficiency of the collector is 76.6 % based on aperture area. The key technical specifications of the collector are shown in Table 5.

The main components of a collector consist of:

- Reflector, which reflects the incoming radiation onto the receiver.
- The receiver tube absorbs reflected radiation and converts it into heat; this heat is then dissipated by the agent fluid that is pumped through the receiver tube
- The protective glass avoids heat losses and protects the collector from dust, snow etc.

Table 3
Assumptions regarded in HTHP simulations.

Parameter	Abbreviation	Value	Units	
System degradation rate	SD	0.5	%	
Specific capital expenditure	CAPEX	500/1′000/1′500	Euro/kW_{th}	
O&M cost	$EX_{o\&M}$	5	%	of CAPEX
HP lifetime		15	Years	
LCOH analysis period		15	Years	

Table 4
Different scenarios for the variables used in HTHP LCOH calculations.

Description	Abbreviation	Case 1	Case 2	Case 3
HP CAPEX [Euro/kW_{th}]	CAP	500	1′000	1′500
Electricity Price [Euro/MWh]	ELP	70	100	150
Load Profile [h/year]	LPR	8′760	6′264	3′650

4.3.2. Collector integration in the system

The overall system is divided into 2 circuits, as shown in Fig. 8. The pressurized water stays in a closed loop called the solar loop, or primary loop. Pressurized water is warmed up by circulating in the solar collectors and is later cooled down through the heat exchanger, which has its secondary side connected with a steam separator. The steam separator is a vessel that contains a mixture of steam and hot water. When the required pressure is reached in the vessel, the steam will be sent to the customer's main steam line.

The generated steam is separated from the remaining saturated liquid in the steam separator, and it has priority over the boilers-generated steam due to small overpressure. Its title is maintained high by the small overheating. The saturated liquid separated from the steam in the steam separator is mixed with the incoming water from the deaerator and recirculated to the steam heat exchanger. The separation of steam and water (that occurs by gravity) creates inside the steam separator two regions (one of steam and one of liquid at nearly the same temperature), the volumes of which can fluctuate and absorb small power surges or reductions.

The system arrangement considers PTC collector fields with a storage system to generate steam at 140 °C with feedwater temperature at 110 °C, same as considered for HTHP. Whenever solar production exceeds the demand, heat is diverted to thermal storage. When the steam is directly used in the process, the forward temperature from solar field is 145C, to have slight overpressure in the circuit compare to boiler steam pressure. The storage system is considered a pressurized tank using

Table 5
Key technical specifications of T160 PTC collector.

Item	Description
Collector type	Glass-covered PTC with one-axis tracking
Recommended heat transfer fluid	Water. Propylene Glycol (max 40 %)
Volume of heat transfer fluid in receiver tube[Liter]	2.2
Operational temperature [°C]	60 to 160
Stagnation temperature [°C]	460
Maximum operating pressure[bar]	16
Receiver	Stainless steel, optically selective coating
Glass	4 mm hardened glass, anti-reflective coating
Reflector	Polymer-embedded silver on steel sheet
Weight [kg]	148

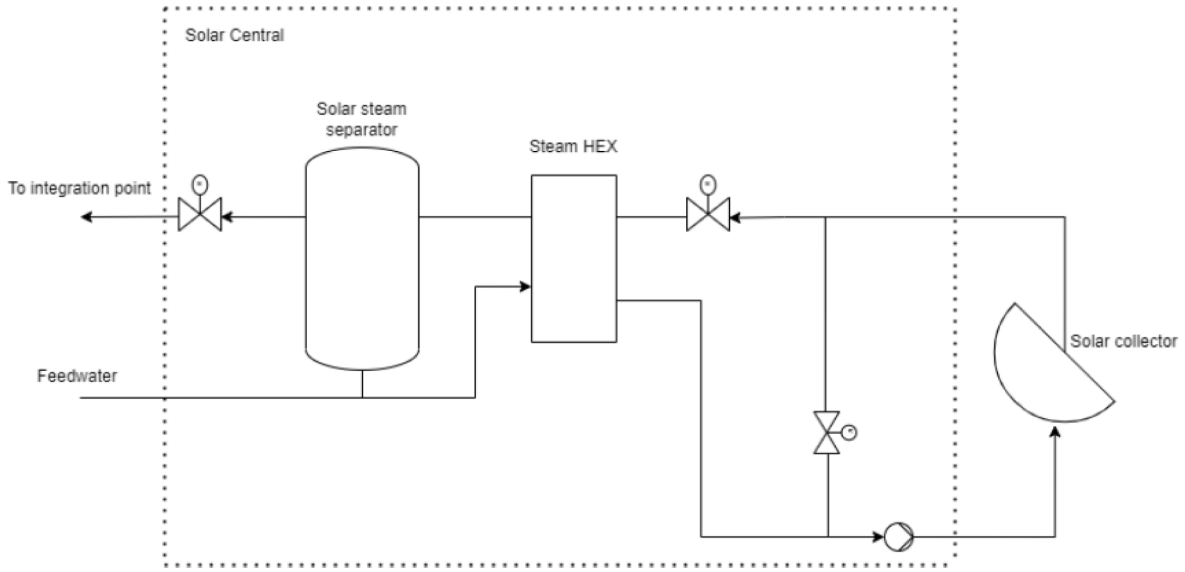

Fig. 8. A concept process and instrumentation diagram for PTC field integration in an existing boiler system for steam generation.

water as a storage media. When the storge is fully charged, the water Is heated to a maximum temperature of 170 °C. After discharging, the tank is cooled down, corresponding to the bottom temperature in the steam separator (approximately 150 °C). This results in an effective temperature difference of 20 °C In the thermal storage between charging and discharging.

4.3.3. Modelling of PTC system

A dynamic simulation of the collector performance was carried out for a statistically normal year based on climate data from Meteonorm using time step of 15 min. Simulations are based on the Solar Keymark ISO 9806 collector parameters of the Absolicon T160.

The simulation approach for PTC is based on 2 steps. In the first step, the collector is modelled without interacting with the heating load. This can be considered as if the collector operates under infinite load, and thus all the heat generated by the collector is fully utilized. The simulations are done using TRNSED, which is an add-on to TRNSYS. The collector performance parameters based on the aperture area used in the TRNSED are shown in Table 6.

The output of the component analysis results in an hourly profile of collector output with other variables. The output is used in the system model for defined industrial boundaries. System simulations are done using the OCTAVE tool, on an hourly time-step basis for a year. The tool simulates the collector interaction with the load. Several iterations are performed to obtain the collector area and storage volume for a range of solar fractions for specific loss factors. The loss factor represents the maximum quantity of heat allowed to spill from the collector at any time step and is fixed at 20 % of the collector production. The loss factor is chosen based on previous experience. Based on the simulations, a curve representing the collector area and storage volume needed for a range of solar fractions is obtained. The range of SF is restricted from 1 % to 91 %. It is possible to run simulations for SF approaching 100 %. However, this is avoided so to reduce the computational effort.

Moreover, it is uncommon to design a solar thermal system for such high SF due to the excessive tank volume required, which negates the installation's economic gains. The power consumption of the PTC system due to tracking and fluid pumps is also derived from simulation results. The collector area and tank volumes required for various solar fractions are then used to calculate the LCOH of the system, as explained in the next section.

4.3.4. Economic boundaries & geographical inputs

The data for PTC economic analysis includes the capital and O&M cost. The economic input values are based on data collected from the PTC manufacturer as shown in Table 7.

The simulation for PTC is done for various locations in Europe, as shown in Fig. 9. If the country's direct normal irradiance (DNI) is spatially uniform, then one city from each country is used for simulations. However, some of European countries (for e.g France, Italy and Germany), have a significant variation of DNI. Therefore, multiple cities within the same country are selected for better representation. The LCOH results of PTC for each country would be compared with the LCOH of HTHP to determine the solar fraction threshold below which ST is more economically attractive than HTHP. The annual DNI for simulated location varies from 642 kWh/m^2 (for London) upto 1848 kWh/m^2 (for Seville, Spain). The average DNI for all simulated location is 1098 kWh/m^2.

Table 6
Input Performance characteristics of T160 collector used for model [34].

Parameter	Value
Optical efficiency [%]	76.6
a_1 [W/m^{2}K]	0.368
a_2 [W/m^{2}K^2]	0.00322
K_d [-]	0.120
β, tilt [°]	Single-axis tracking E-W
γ, azimuth [°]*	0

Table 7
Assumptions regarded in PTC T160 simulations.

Item	Symbol	Value	Unit	Remarks
Capital expenditure	CAPEX	250, 350, 450	Euro/m^2	Represents the installed cost of CAPEX
O&M cost	$EX_{O\&M}$	0.1	%	
Solar collector lifetime		25	Years	
LCOH evaluation period		15	Years	
System degradation rate	SD	0.1	%	

Fig. 9. Map representing the various locations used for PTC simulations.

5. Key performance indicators

5.1. Levelized cost of heating

LCOH is a comparative indicator representing the cost of heating from any system considering capital, operation, and maintenance costs during the system's lifetime [42]. If the LCOH of a new solution is lower than the LCOH of the existing system, it implies that the new system implementation will have positive returns. It is a suitable performance indicator to compare various heat generation technologies.

LCOH is calculated based on Equation (1).

$$LCOH = \frac{CAPEX + Price_{el} \cdot \sum_{n=1}^{N} \left(\frac{W_{Sys}}{(1+DR)^n} \right) + \sum_{n=1}^{N} \left(\frac{EX_{O\&M}}{(1+DR)^n} \right)}{\sum_{n=1}^{N} \left(\frac{Q_{Yield}(1-SD)^n}{(1+DR)^n} \right)} \quad (1)$$

where:

$CAPEX$ = Capital cost of technology used (including installation and commissioning) (€].

W_{Sys} = Annual power consumption of technologies (Electricity for fluid pumps, heat pump, and collector tracking system) (kWh).

$EX_{O\&M}$ = operation and maintenance cost per year (€/year].

$Price_{el}$ = Current unit price of grid electricity (€/MWh).

DR = Discount rate (%).

SD = degradation rate (%] of each technology.

N = Project lifetime (years).

Q_{Yield} = Heat yield of the system (kWh/year).

5.2. SF_{limit}

To compare the cost of heating between HTHP and ST based on location-specific characteristics such as annual DNI, a new comparative indicator SF_{limit} is defined for the analysis. The SF_{limit} refers to the point on the SF-LCOH curve of a PTC when the LCOH of HTHP for the analyzed condition becomes equal to the LCOH of ST. Therefore, if a PTC system is designed for an SF which exceeds the SF_{limit}, then the LCOH of PTC at the designed SF will be higher than HTHP. In other words, below the SF limit value, the LCOH of the ST system will always remain below the HTHP LCOH. Therefore, a higher value of SF_{limit} would represent better cost feasibility and favorable conditions for PTC installation.

6. Results

6.1. HTHP simulation results

Table 8 shows the results for LCOH calculations for HTHP for 27 simulated scenarios representing load profiles, investment cost, and electricity price variation. For any specific load profile, the CAP1-ELP1 represents the LCOH of HTHP assuming CAPEX 1 (500 €/kW_{th}), and Electricity prices 1 (70 €/MWh_e), as shown previously in Table 4.

The results show that the LCOH of HTHP varies from 45 to 130 €/MWh for the simulated scenarios. The minimum LCOH (45 €/MWh) is obtained for the lowest CAPEX and ELP values in LPR1, when the HTHP is utilised throughout the year. For the same CAP and ELP combination, LCOH increases while moving from LPR1 to LPR3 due to decreasing operational hours. Furthermore, for the same CAP value and any load profile, the LCOH increase with a higher electricity process (when

Table 8
HTHP LCOH [€/MWh] for simulated scenarios.

Case	HP CAPEX EUR/kW	Electricity price EUR/MWh	LCOH of HTHP (Euros/MWh) Load profile 1 LPR.1 8′760 h/a	Load profile 2 LPR.2 6′264 h/a	Load profile 3 LPR.3 3′650 h/a
CAP.1-ELP.1	500	70	45	49	58
CAP.1-ELP.2	500	100	59	63	73
CAP.1-ELP.3	500	150	84	88	98
CAP.2-ELP.1	1′000	70	51	58	75
CAP.2-ELP.2	1′000	100	66	73	89
CAP.2-ELP.3	1′000	150	91	98	114
CAP.3-ELP.1	1′500	70	58	67	91
CAP.3-ELP.2	1′500	100	73	82	106
CAP.3-ELP.3	1′500	150	98	107	130

moving from ELP 1 to ELP 3) (see Table 9).

6.2. PTC simulation results

The results from PTC simulations suggest that LCOH has a higher variation than HTHP. The reason can be attributed to a wide range of solar irradiation variations across simulated European locations. Furthermore, the LCOH also varies with solar fraction for any specific location.

The range of LCOH obtained from PTC varies is huge depening on the solar fraction. The minimum LCOH obtained is The lowest LCOH is obtained for high DNI regions (for example, cities in Spain, Portugal and Southern Italy), and at a lower solar fraction. Fig. 10 shows the variation of LCOH for PTC collectors at 3 different solar fractions (5 %, 25 %, and 50 %) and for LPR1 (8′760 h/a) using all simulated locations. A decreasing trend of LCOH with increasing DNI is due to high collector output. Furthermore, for the same DNI, the LCOH increases with an increase in solar fraction due to lower utilization of heat.

It is also important to consider that LCOH depends not only on the absolute annual DNI value but also on the temporal variation. The high temporal variation makes it difficult to achieve large SF due to the large tank volume needed, thus increasing the LCOH. This can be seen by comparing the 2 data points in Fig. 10 at 50 % SF (compared data points are marked black border). These 2 locations have nearly the same

Table 9
Summary of SF limit (%) of ABSOLICON PTC (T-160) and HTHP in different European countries for LPR.1. Empty values indicate that LCOH of ST is higher than LCOH of HTHP.

	PTC CAPEX (EUR/m^2)	350								
	HP CAPEX (EUR/kWth)	500 EUR/kW			1′000 EUR/kW			1′500 EUR/kW		
	Electricity cost (EUR/kWh)	70	100	150	70	100	150	70	100	150
	Case Number	CAP.1 ELP.1	CAP.1 ELP.2	CAP.1 ELP.3	CAP.2 ELP.1	CAP.2 ELP.2	CAP.2 ELP.3	CAP.3 ELP.1	CAP.3 ELP.2	CAP.3 ELP.3
Location	DNI (kWh/m^2)	Solar fraction limit (%)								
UK-London	642									
Czech-Prague	708									
Germany-Bonn	716									
Ireland-Dublin	730									
Poland-Warsaw	764									7
Netherlands-Groningen	779									
Slovenia-Ljubljana	780						7			8
France-Paris	790						6			8
Austria-Vienna	818						8			9
Belgium-Ostend	858			7			8			10
Denmark-Copenhagen	899						7			8
Bulgaria-Sofia	909			12			16		10	17
Estonia- Toravere	947						8			9
Hungary-Budapest	955			13			17		9	19
Finland-Helsinki	971			8			11			13
Germany-Munich	983			12			15		8	17
Spain-Santander	1008			14			22		12	25
Slovakia-Bratislava	1010			17		9	22		12	25
Italy-Milan	1011			19		12	24		13	27
Sweden-Norrkoping	1071			11			14			16
Sweden- Borlänge	1075			10			13			14
Bern, Switzerland	1180			8			21			26
Romania-Bucharest	1187		14	27	9	17	31	13	22	34
Greece-Athena	1277	15	28		21	38		28	43	
France-Montpellier	1393	14	24	42	16	31	44	23	36	47
France-Nice	1438	15	27	42	18	33	44	26	37	46
Croatia-Klis	1503	17	27	41	21	32	43	26	37	45
Italy-Rome	1528	21	38	53	29	46	55	37	49	56
Italy-Trapani	1564	28	46	56	37	52	58	45	54	59
Portugal-Porto	1601	22	34	47	27	40	49	33	43	51
Portugal-Lisbon	1660	30	48	57	39	52	58	47	55	59
Spain-Madrid	1713	30	42	52	35	46	55	41	50	57
Spain-Seville	1848	39	52	61	45	55	63	50	58	64

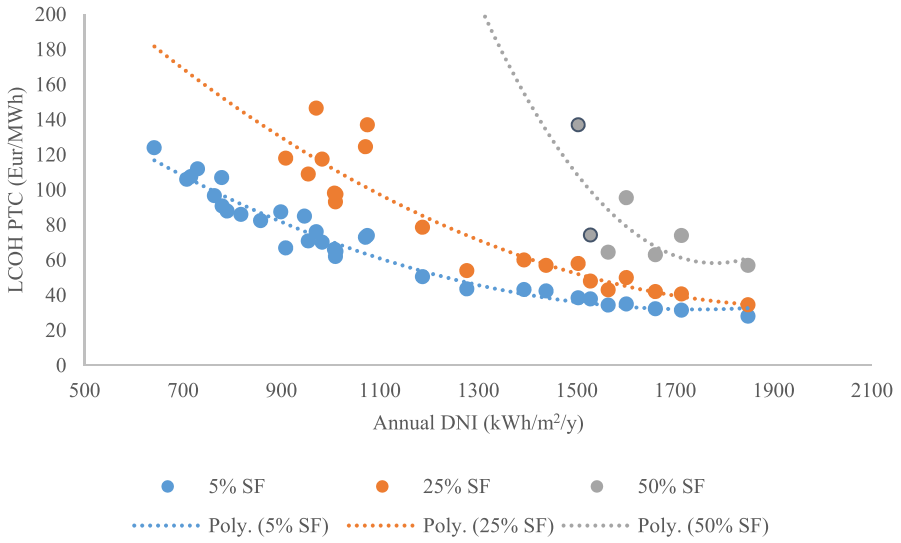

Fig. 10. Variation of LCOH with SF for all locations at 3 different solar fractions and load profile 1 (8760 h/a) and PTC CAPEX of 350 €/m2.

annual DNI value of around 1500 kWh/m^2. However, the LCOH for one location is much higher (147 €/MWh) than the other (75 €/MWh).

The range of PTC LCOH for all 3 load profiles is shown in Fig. 11. Results indicate that load profile 3 has the lowest LCOH at a high solar fraction (50 %), due to high coincidence in solar irradiation and load demand. LPR2 has the highest LCOH at any SF. This is due to the lack of heating load during the weekend in LPR2, which results in high storage volume or heat spillage from the collectors.

While comparing the LCOH of PTC or any ST product with other technologies, it is important to specify the SF at which the comparison is made.

The simulation results are used to generate SF-LCOH curve as exemplified in Fig. 12 for a location in Seville-Spain for Load profile 2 (LPR2) at PTC CAPEX of 350 €/m^2. As seen, LCOH will have a minimum constant value up to a certain SF, till all the collector heat is utilized by the system resulting in no excess heat and no storage tank. In the curve below, the minimum LCOH obtained is 46 €/MWh from SF of 1 % to 25 %.

However, after a threshold solar fraction, the thermal production of the collector exceeds the load demand, bringing the need for thermal storage. The introduction of thermal storage adds additional cost to the system, increasing the LCOH from 45 €/MWh at 25 % SF to 67 €/MWh at 46 % SF. After this point on the curve, the LCOH increases exponentially as the thermal storage size required is very high with an increase in SF.

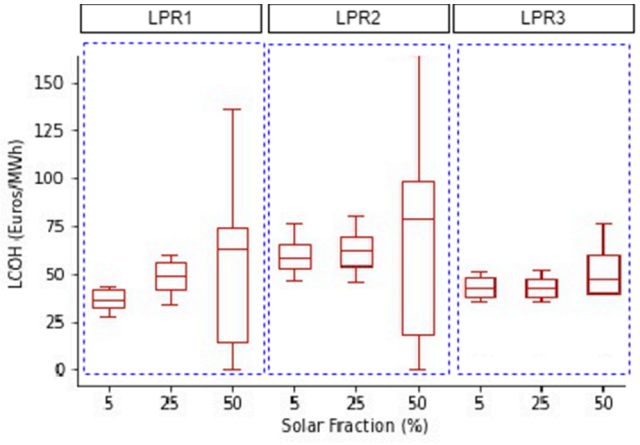

Fig. 11. Range of PTC LCOH for 3 load profiles and 3 different solar fractions for all simulated locations at ptc CAPEX of 350 €/m^2.

Increasing collector areas/tank volumes would diminish the returns for utilized heat, increasing the LCOH. This trend can be observed after SF of 46 %.

The curve shown in Fig. 12 is obtained for all the simulated locations and 3 different load profiles. It is then compared with HTHP's LCOH to obtain the corresponding SF limit.

Fig. 13 illustrates the LCOH comparison for both technologies for the Spain-Seville location. The curves shows the variation of PTC LCOH with SF for 3 different load profiles. For sake of comparison, the two horizontal lines in the graphs represent the minimum and maximum LCOH of HTHP for all simulated cases. Due to the high DNI in Spain, the minimum LCOH of PTC is always lower than HTHP for all simulated cases. It has been shown that for such a location for LPR 1, even with low CAPEX and OPEX of HTHP (bottom horizontal line), the SF_{limit} is at 37 %. SF_{limit} increases up to 65 % if the highest value of CAPEX and OPEX for HTHP are considered (top horizontal line).

Also, the minimum LCOH of PTC is higher in LPR2 compared to LPR1. This is due to the lack of weekend operation in LPR2, which results in high tank volume, and heat that cannot be utilized in the system, thus resulting in higher LCOH. The minimum LCOH of HTHP in LPR3 is higher than in LPR1 and LPR2. The reason for the same is a lower number of operational hours while having the same CAPEX of HTHP, which results in high LCOH.

Comparative results are shown for a low DNI location (Czech-Prague) in Fig. 14. As can be seen, the PTC LCOH for Prague in LPR.1 (a) and LPR.2 (b) are even higher than the worst case of HTHP LCOH (CAP3-ELP3). This implies that for such a case and under the analysed boundaries, HTHP would be more cost-effective option for heat generation than PTC. However, there would be a change by considering LPR.3, where PTC has lower LCOH upto SF of 15 % compared to CAP3-ELP3 scenarios. The SF_{limit} for this case is at 15.6 %.

6.3. *Comparative analysis using SF_{limit}*

Based on the analysis in section 6.2, the values of SF_{limit} for all simulated cases is shown in Table 8. The countries where no value of SF_{limit} is defined (such as in UK-London) indicate that LCOH of ST is always higher than LCOH of HTHP in all simulated cases. These countries often have very low annual DNI, resulting in lower economic feasibility for PTC.

Using the above results, SF_{limit} is generalized to location-specific characteristics such as annual DNI value. For each load profile, a linear correlation of annual DNI and SF_{limit} is shown in Fig. 15 for LPR1

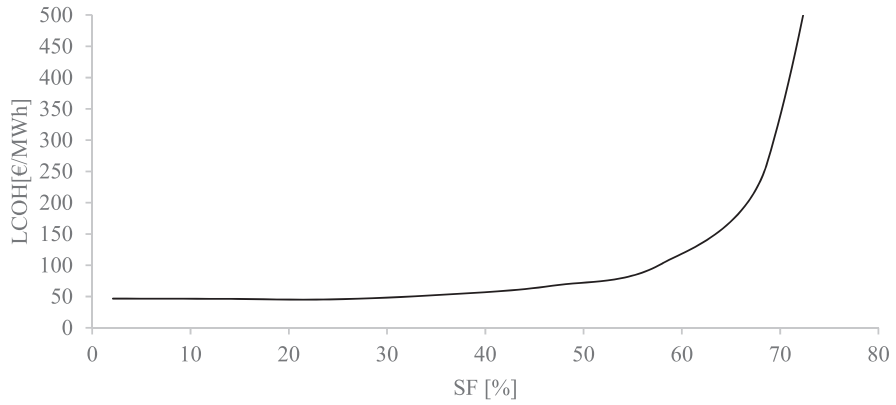

Fig. 12. Typical trend of LCOH versus SF (case of Seville-Spain (DNI: 1848 kWh/(m^2·year)) for LPR.2.

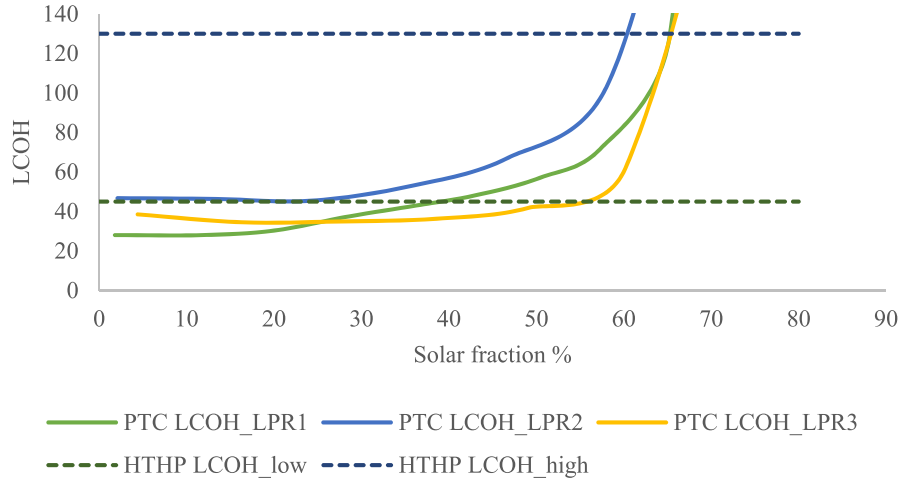

Fig. 13. LCOH comparison for HTHP (horizontal lines) and PTC (capex 350 €/m^2) for Spain-Seville (DNI: 1848 kWh/(m2·year)) (a) LPR.1, (b)LPR.2, (c)LPR.3.

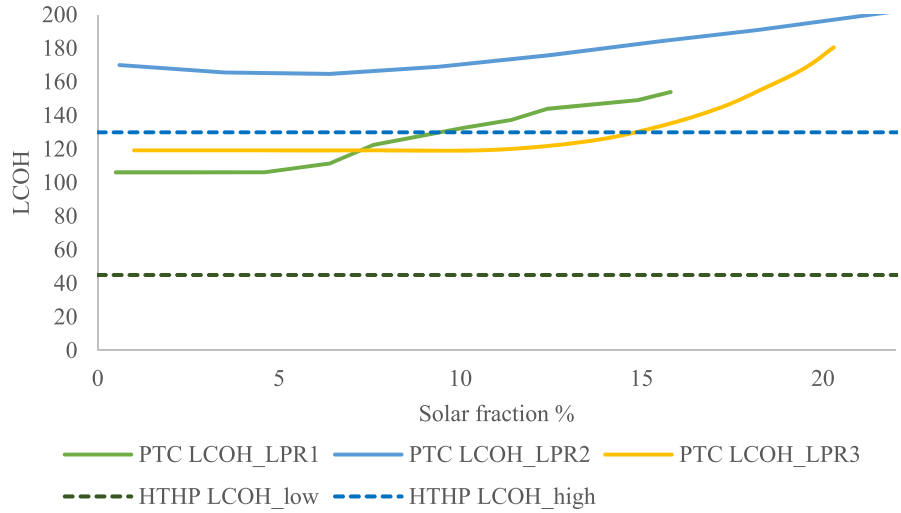

Fig. 14. LCOH and SF limit (comparing HTHP and PTC) for Czech- Prague (DNI: 708 [kWh/(m^2·year)]) (a)LPR.1, (b)LPR.2, (c)LPR.3.

at PTC CAPEX of 350 €/m^2. In this graph, the intersection of the DNI and HTHP curve provides SF_{limit} below which PTC is more competitive to HTHP.

In high DNI regions (1′500 to 2′000 kWh/m^2), the average SF_{limit} varies from 25 % to 55 %, indicating that ST technologies are a cheaper way of reducing the emission by at least 1/4th. In such regions, the demand up to 55 % can be met by solar thermal collectors at economical LCOH if the load profiles are favourable (LPR3). In medium DNI regions (1′001 to 1′499 kWh/m^2), SF_{limit} varies from 15 % to 30 %, lower than the high DNI regions. If the boundaries favor HTHP (low CAPEX, low electricity price, and high operational hours), the DNI at any location must be higher than 1200 kWh/m^2 for PTC to compete. In low DNI

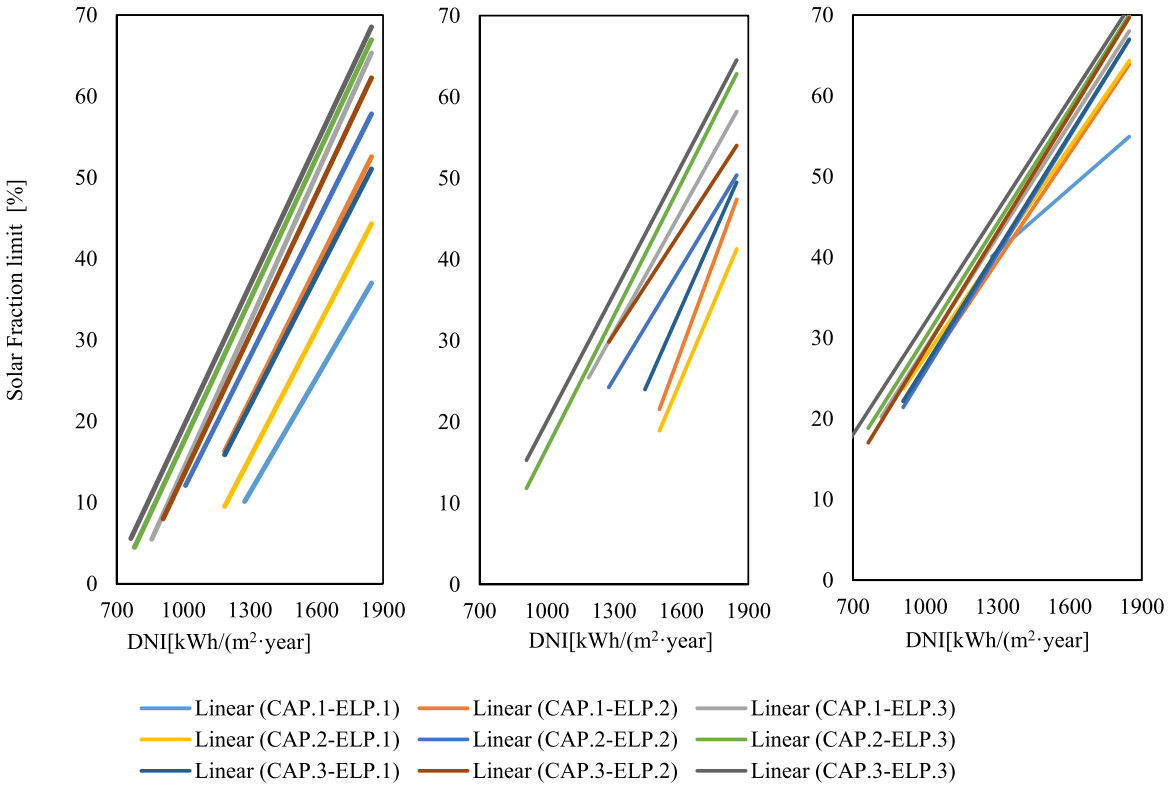

Fig. 15. Variation of SF_{limit} with DNI for LPR.1 (left), LPR.2 (middle), and LPR.3 (right) for PTC capex of 350 Euros/$m^{2.}$

regions (500 to 999 kWh/m^2), the maximum SF_{limit} obtained is 10 %. In such regions, HTHP is cheaper than PTC for low and medium CAPEX/el price value. However, if the electricity and CAPEX are high, PTC can compete with HTHP at a minimum DNI of 764 kWh/m^2.

Fig. 16 and Fig. 17 show the variation of DNI and SF_{limit} for PTC CAPEX of 250 €/m^2 and 450 €/$m^{2,}$ respectively.

Comparing the results for different load profiles, there is an increasing trend of SF_{limit} with increasing DNI when moving from LPR.1 to LPR.3, indicating better economic results for PTC. When the consumption and production have high coincidence, for example, in LPR.3, there is a small need for storage, which would result in lower LCOH for the PTC collector, and therefore higher value of the SF limit can be seen. For all load profiles, Higher SF_{limit} can be obtained for high DNI locations, due to high thermal output of the collectors. In LPR 3, a SF_{limit} can

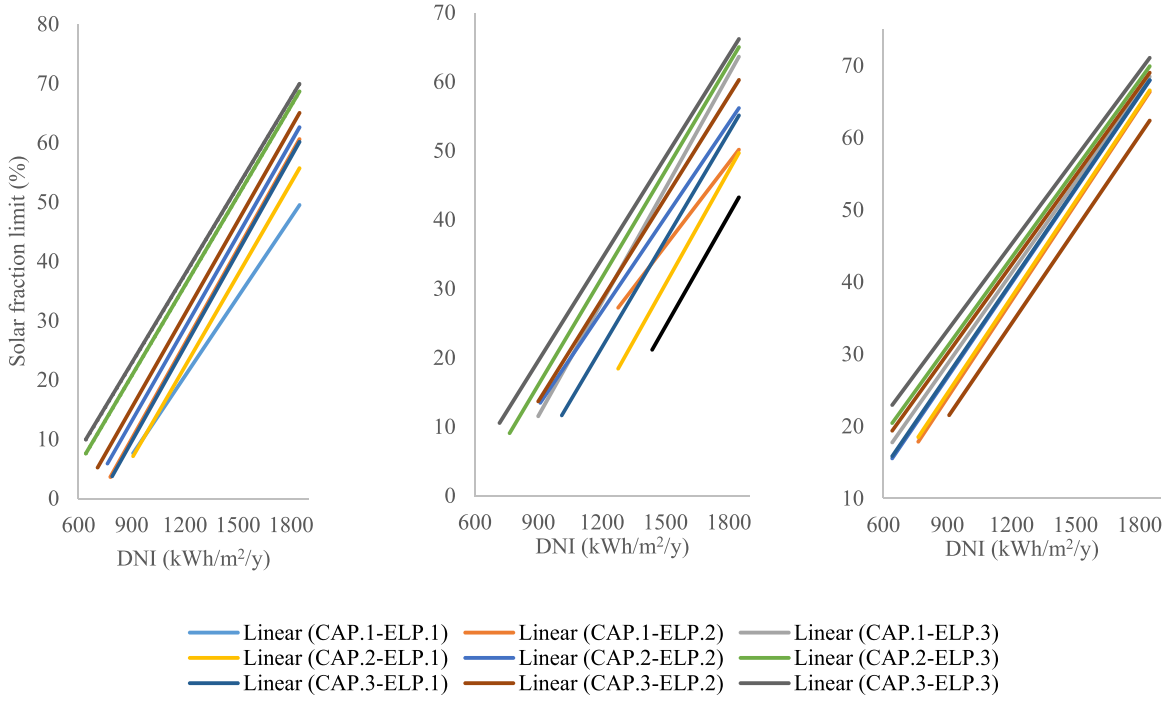

Fig. 16. Variation of SF_{limit} with DNI for LPR.1 (left), LPR.2 (middle), and LPR.3 (right) for PTC capex of 250 Euros/$m^{2.}$

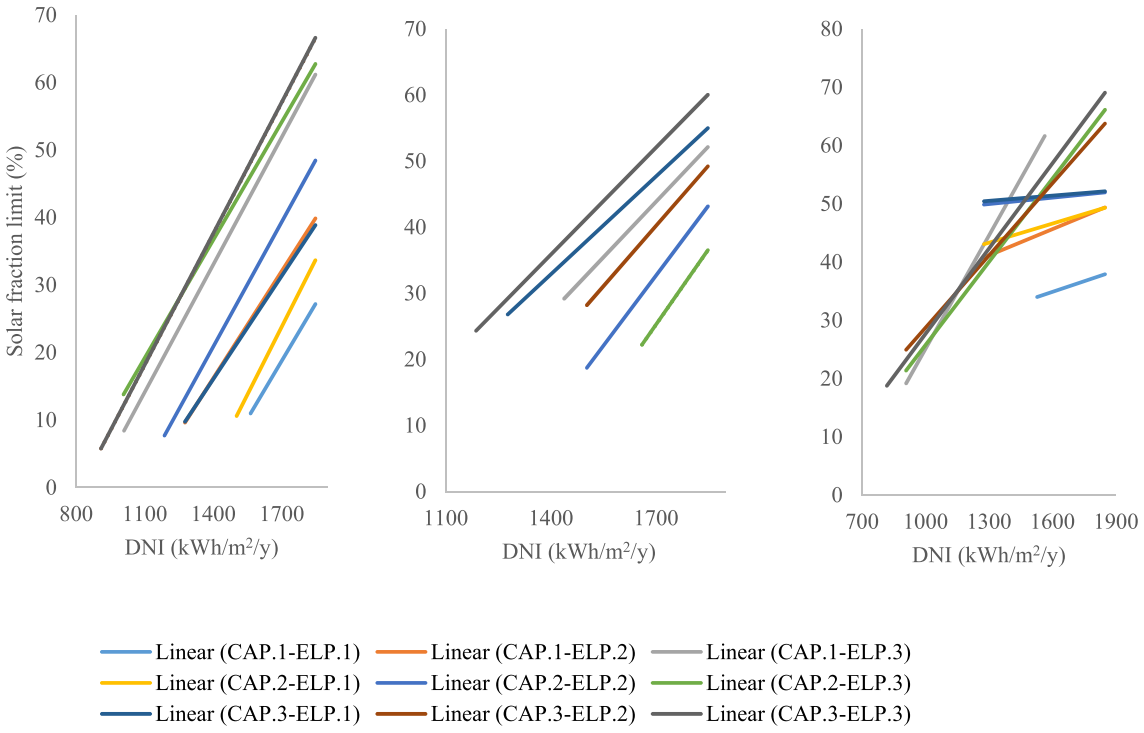

Fig. 17. Variation of SF_{limit} with DNI for LPR.1 (left), LPR.2 (middle), and LPR.3 (right) for PTC CAPEX of 450 Euros/m^2.

be obtained even for low DNI (764 kWh/m^2) due to a favourable match in DNI and load. The decrease in PTC CAPEX results in lower LCOH for any given solar fraction, eventually leading to high SF_{limit}. When the CAPEX of PTC is lower, and load profiles are favorable, a solar fraction limit of 32 % is obtained, even for the lowest DNI location. This indicates that cost decrease can result in PTC as the most economic heating source. On the contrary, if the PTC CAPEX is higher (450 €/m^2), HTHP is always competitive irrespective of DNI for CAP1-ELP1 scenarios. Such figures can be used to do a quick cost feasibility analysis for both ST and HTHP and can be a very useful tool for designers.

7. Discussions

The cost aspects of any technology for low-carbon process heat assessment are extremely case-sensitive. The developed methodology serves as a valuable guide to quickly determine a preferred lower carbon heat solution just by looking at the annual DNI of any location and finding the optimal SF_{limit} for that location. The analysis is comprehensive but restricted by the absolute values of the variables assumed. Several other aspects can change the techno-economic results in the near future. For example, the carbon tax can play a significant role in reducing the cost of heating. ST technologies consume significantly low electricity compared to HTHP technologies. If the CO_2 emission cost is accounted for, the results will favor ST technologies. Also, as the electricity grid will have more renewable penetrations, the HTHP will keep getting attractive from a cost and emission perspective.

The land usage for HTHP is much smaller compared to solar thermal collectors. This is a big advantage for HTHP, especially if the industries have limited ground or roof space for solar collector installations. HTHP, on the other hand, needs more developments for low-GWP refrigerants.

A way forward could be to use both technologies in conjunction where ST is designed up to the SF_{limit}, and HTHP is used to meet the rest of the load. A hybrid system of optimized solar thermal collectors with a small tank volume and HTHP can produce process heat at lower LCOH compared to the technologies used individually. Technology combination is imperative to reach clean and economical industrial heat ambitions. Such a hybrid system presented in Fig. 3 could have significant potential to decrease the cost and emission and will be of focus for future studies and publications. For new energy system planning, a bivalent system where only PTC and HTHP are used together, there is a possibility to reach 100 % renewable heating fraction if the electricity for HTHP is renewable. Such system an run without any need for boiler back ups. In case of reterofitting with existing boiler system, ST can be used as a starting point to cover part heat demand. Then HTHP can be introduced in the system designed for peak heat load demand to phase off the boiler completely.

In addition, to accelerate the decarbonization aims, the EU has set an ambition to build 100 positive energy districts and smart cities (climate-neutral cities) by the year 2025. However, the focus of current PEDs is mainly on residential and commercial buildings. The PED boundary unfortunately does not include industrial energy system at the moment. Nevertheless, there is a strong need to factuality the industrial decarbonisation and include industrial energy system in the PED development since it belongs to whole city energy infrastructure. If a city wants to achieve the climate-neutral goal, it must consider industrial segment. On the other hand, industry segment fits high synergies if it is considered in PED concept. For instance, the low temperature waste heat can be recovered from industries to meet space heating and DHW demand through 5th generation district heating network. In return, when PED produces extra energy, it can be exported to industries through above-addressed district heating via heat pumps to upgrade heat to the required temperature level. Therefore, to address the technologies for industrial heat is critical to fulfil the PED and climate-neutral city goals, such as HTHP and PTC, which can be the key technologies for a fully decarbonised urban energy system.

8. Conclusions

This paper compares the techno-economic aspects of HTHPs and PTC collectors for various industrial boundary conditions. The focus is on steam generation at 140 °C (3.6 bar_a), commonly used in many process heating industries. The characteristics of commercial HTHP and PTC products are used as input in the simulation model to obtain energetic results. For LCOH calculation, an excel model is used. Finally, results are

generalized using SF_{limit} as an indicator to distinguish the economic advantage of each technology.

The major conclusions of the study are as follows:

- The LCOH of HTHP for the analyzed boundary conditions ranges from 45 to 130 €MWh. There is a clear trend of increasing LCOH with higher electricity prices and specific CAPEX costs. As the HTHP was sized for a peak load capacity of 500 kW, the total CAPEX is the same for all 3 load profiles. However, the LCOH can be lowered by operating the HTHP for more hours. Therefore, the LCOH in scenario LPR1 is always lower than in LPR2 and LPR3 for the same cost of electricity prices.
- The least obtained LCOH comes from the PTC collector for high DNI regions and low solar fractions. If the meteorological conditions are suitable, PTC is a cheaper alternative to generate steam compared to HTHP. The LCOH range obtained from PTC simulations is 28 to 160 €/MWh up to 50 % SF. Lower values of LCOH can be observed for high DNI regions and vice versa. High DNI regions are, for example, Spain, Portugal, and Southern Italy. Furthermore, LCOH has an increasing variation with SF. The SF-LCOH curve is not dependent on the absolute DNI but on the distribution of the DNI on a temporal basis, which decides the storage volume needed to increase the SF.
- As the LCOH increases with SF, an SF_{limit} exists when producing heat from ST gets expensive compared to HTHP. This limit is higher for high DNI regions and lower for low DNI regions. The limit increases with higher ELP and CAP for the HP. In low CAPEX and electricity cost situations for an HTHP, a threshold DNI of 764 kWh/m^2 is needed for PTC to produce heat at a cheaper rate. In the high CAPEX scenario, this threshold DNI changes to 1′200 kWh/m^2, and the average SF limit varies from 25 % to 55 %. In high DNI locations (1′500 to 2′000 kWh/m^2), 15 % to 30 % for medium DNI (1′001 to 1′499 kWh/m^2), and 0 % to 10 % for low DNI locations (0 to 999 kWh/m^2).
- The decrease in PTC CAPEX results in lower LCOH for any given solar fraction, eventually leading to high SF_{limit}. When the CAPEX of PTC is lower and load profiles are favorable, a solar fraction limit of 32 % is obtained, even for the lowest DNI location. This situation indicates that cost decrease can result in PTC as the most economic heating source for low DNI locations.
- The industry segment fits high synergies if considered in the PED concept, while both HTHP and PTC can be the key technologies for a fully decarbonized urban energy system.

CRediT authorship contribution statement

Puneet Saini: Methodology. **Mohammad Ghasemi:** Writing – review & editing. **Cordin Arpagaus:** Supervision, Writing – review & editing. **Frédéric Bless:** Project administration, Supervision, Writing – review & editing. **Stefan Bertsch:** . **Xingxing Zhang:** Supervision, Writing – review & editing.

Declaration of Competing Interest

The authors declare that they have no known competing financial interests or personal relationships that could have appeared to influence the work reported in this paper.

Data availability

Data will be made available on request.

Acknowledgement

The authors would like to Absolicon solar collectors AB for their support to carry this study.

The Swiss authors gratefully acknowledge the financial support of the Swiss Federal Office of Energy SFOE as part of the SWEET (SWiss Energy research for the Energy Transition) project DeCarbCH (www.sweet-decarb.ch) and the projects Annex 58 HTHP-CH (Contract number SI/502336-01) and IntSGHP (Contract number SI/502292).

References

[1] "Heating – Analysis - IEA." https://www.iea.org/reports/heating (accessed Aug. 14, 2022).
[2] "Article - EHPA." https://www.ehpa.org/about/news/article/repowereu-heat-pump-strategy-required-to-help-sector-deliver/ (accessed Aug. 14, 2022).
[3] "Heating and cooling." https://energy.ec.europa.eu/topics/energy-efficiency/heating-and-cooling_en (accessed Aug. 14, 2022).
[4] Cebotari L. EU-Russia energy relations: problems and perspectives. Proc Int Conf Bus Excell Aug. 2022;16(1):1001–14. https://doi.org/10.2478/PICBE-2022-0093.
[5] Arpagaus C, Bless F, Uhlmann M, Schiffmann J, Bertsch SS. High temperature heat pumps: Market overview, state of the art, research status, refrigerants, and application potentials. Energy Jun. 2018;152:985–1010. https://doi.org/10.1016/J.ENERGY.2018.03.166.
[6] Arpagaus C, Bless F, Schiffmann J, Bertsch SS. Multi-temperature heat pumps: A literature review. Int J Refrig Sep. 2016;69:437–65. https://doi.org/10.1016/J.IJREFRIG.2016.05.014.
[7] Bless F, Arpagaus C, Bertsch SS, Schiffmann J. Theoretical analysis of steam generation methods - Energy, CO2 emission, and cost analysis. Energy Jun. 2017;129:114–21. https://doi.org/10.1016/J.ENERGY.2017.04.088.
[8] Bless CF, Arpagaus BS. Techno-economic analysis of steam generating heat pumps for integration into distillation processes. Accessed: Aug. 14, 2022. [Online]. Available: https://www.researchgate.net/publication/361800179_Techno-economic_analysis_of_steam_generating_heat_pumps_for_integration_into_distillation_processes.
[9] "White paper: Strengthening Industrial Heat Pump Innovation - Decarbonizing Industrial Heat." https://hthp-symposium.org/high-temperature-heat-pumps/white-paper-strengthening-industrial-heat-pump-innovation/ (accessed Aug. 14, 2022).
[10] "Home - Annex - 48." https://heatpumpingtechnologies.org/annex48/ (accessed Aug. 14, 2022).
[11] "HTHP Symposium 2022." https://hthp-symposium.org/hthp-symposium-2022/ (accessed Aug. 14, 2022).
[12] "Home - HPT - Heat Pumping Technologies." https://heatpumpingtechnologies.org/ (accessed Aug. 14, 2022).
[13] "Home - Annex 58." https://heatpumpingtechnologies.org/annex58/ (accessed Aug. 14, 2022).
[14] Kondou C, Koyama S. Thermodynamic assessment of high-temperature heat pumps using Low-GWP HFO refrigerants for heat recovery. Int J Refrig May 2015;53:126–41. https://doi.org/10.1016/J.IJREFRIG.2014.09.018.
[15] Zühlsdorf B, Bühler F, Bantle M, Elmegaard B. Analysis of technologies and potentials for heat pump-based process heat supply above 150 °C. Energy Convers Manag X Apr. 2019;2:100011. https://doi.org/10.1016/J.ECMX.2019.100011.
[16] Chen Q, Cleland DJ, Carson JK, Walmsley TG. Integration of desiccant wheels and high-temperature heat pumps with milk spray dryers. Appl Therm Eng Nov. 2022;216:119083. https://doi.org/10.1016/J.APPLTHERMALENG.2022.119083.
[17] Jiang J, Hu B, Wang RZ, Deng N, Cao F, Wang CC. A review and perspective on industry high-temperature heat pumps. Renew Sustain Energy Rev Jun. 2022;161:112106. https://doi.org/10.1016/J.RSER.2022.112106.
[18] Kosmadakis G. Estimating the potential of industrial (high-temperature) heat pumps for exploiting waste heat in EU industries. Appl Therm Eng Jun. 2019;156:287–98. https://doi.org/10.1016/J.APPLTHERMALENG.2019.04.082.
[19] Wilk V, Lauermann M, Helminger F. Decarbonization of industrial processes with heat pumps, doi: 10.18462/iir.icr.2019.0832.
[20] "Dryficiency project," 2022. https://dryficiency.eu/ (accessed Aug. 14, 2022).
[21] "Friendship." https://friendship-project.eu/ (accessed Aug. 14, 2022).
[22] "SuPrHeat." https://suprheat.dk/ (accessed Aug. 14, 2022).
[23] Barco-Burgos J, Bruno JC, Eicker U, Saldaña-Robles AL, Alcántar-Camarena V. Review on the integration of high-temperature heat pumps in district heating and cooling networks. Energy Jan. 2022;239:122378. https://doi.org/10.1016/J.ENERGY.2021.122378.
[24] Siddiqui S, Macadam J, Barrett M. The operation of district heating with heat pumps and thermal energy storage in a zero-emission scenario. Energy Rep Oct. 2021;7:176–83. https://doi.org/10.1016/J.EGYR.2021.08.157.
[25] Weiss W, Spörk-Dür M. Global Market Development and Trends 2021 solar heat worldwide 2022.
[26] Good C, Andresen I, Hestnes AG. Solar energy for net zero energy buildings – A comparison between solar thermal, PV and photovoltaic–thermal (PV/T) systems. Sol Energy Dec. 2015;122:986–96. https://doi.org/10.1016/J.SOLENER.2015.10.013.
[27] Meyers S, Schmitt B, Vajen K. Competitive Assessment between Solar Thermal and Photovoltaics for Industrial Process Heat Generation, 2016, doi: 10.18086/eurosun.2016.02.01.
[28] "IRENA report highlights falling solar heat project costs | Solarthermalworld." https://solarthermalworld.org/news/irena-report-highlights-falling-solar-heat-project-costs/ (accessed Aug. 14, 2022).
[29] "Industrial Solar | Startseite." https://www.industrial-solar.de/de/ (accessed Nov. 07, 2022).

[30] "Instalar calderas solares en industria como ingenieria y empresa instaladora." https://solatom.com/ (accessed Nov. 07, 2022).
[31] "Presenting the future of solar energy." http://www.quadsuntechnology.com/ (accessed Nov. 07, 2022).
[32] "bigdishsolar | About the world's largest paraboloidal dish solar concentrator." https://bigdishsolar.com/ (accessed Nov. 07, 2022).
[33] "TVP Solar." https://www.tvpsolar.com/ (accessed Nov. 07, 2022).
[34] "Absolicon - Production Line for T160 concentrating solar collector." https://www.absolicon.com/ (accessed Aug. 14, 2022).
[35] "IEA SHC || Task 64 || Solar Process Heat." https://task64.iea-shc.org/ (accessed Aug. 14, 2022).
[36] "IEA SHC || Task 49 || IEA SHC || Task 49." https://task49.iea-shc.org/ (accessed Aug. 14, 2022).
[37] W. J. Platzer, "Total Performance Assessment Method for Industrial Process Heat Systems," 2021, doi: 10.18086/swc.2021.01.04.
[38] Meyers S, Schmitt B, Vajen K. The future of low carbon industrial process heat: A comparison between solar thermal and heat pumps. Sol Energy Oct. 2018;173:893–904. https://doi.org/10.1016/J.SOLENER.2018.08.011.
[39] "TRNSYS : Transient System Simulation Tool." https://www.trnsys.com/ (accessed Aug. 14, 2022).
[40] "Standard Compressors/ KOBELCO COMPRESSORS CORPORATION | KOBELCO Kobe Steel,. Ltd." https://www.kobelco.co.jp/english/products/standard_compressors/ (accessed Aug. 14, 2022).
[41] Asker M, Emrah Turgut O, Turhan Coban M. A review of non iterative friction factor correlations for the calculation of pressure drop in pipes. Bitlis Eren Univ J Sci Technol 2014;4(1):1–8.
[42] Branker K, Pathak MJM, Pearce JM. A review of solar photovoltaic levelized cost of electricity. Renew Sustain Energy Rev Dec. 2011;15(9):4470–82. https://doi.org/10.1016/j.rser.2011.07.104.

DOI: 10.18462/iir.10.18462/iir.icr.2023.0367

Integration of High-Temperature Heat Pumps in Swiss Food Processes

Cordin ARPAGAUS*, Frédéric BLESS, Sidharth PARANJAPE, Stefan S. BERTSCH

OST Eastern Switzerland University of Applied Sciences, Institute for Energy Systems (IES), Werdenbergstrasse 4, CH-9471 Buchs

*corresponding author: cordin.arpagaus@ost.ch

ABSTRACT

High-temperature heat pumps (HTHP) with supply temperatures above 100 °C are becoming increasingly important in the industry. However, their adoption is slow due to a lack of knowledge on optimal integration, design, control and dynamic behavior, resulting in few practical implementation examples. This study aims to increase the integration of industrial HTHP in the Swiss food and beverage industry. First, an overview of heat demand, application potential, and suitable processes and temperatures is given. Then, based on available pinch analysis data and grand composite curves, two case studies of a spray drying and distillation application are analyzed to determine heat recovery potential and hot and cold utilities. Next, simplified process schematics are created with HTHP integration concepts. Finally, the overall efficiency, heat recovery, energy savings and CO_2 emissions reduction are quantified. The goal is to provide practical examples and a standardized approach for HTHP integration in the food and beverage industry.

Keywords: High-Temperature Heat Pump, Food Industry, Heat Recovery, Spray Drying, Distillation, Steam Generation

1. INTRODUCTION

High-temperature heat pumps (HTHP) with supply temperatures above 100 °C are a key technology for decarbonizing low-temperature process heat in industry. However, their market introduction is slow due to a lack of knowledge about optimal integration, design, control and dynamic behavior, resulting in few practical application examples. This study aims to examine case studies in the Swiss food industry and presents potential HTHP integration concepts in a standardized way.

First, a general overview of heat utilization in the Swiss food industry is given, and specific considerations are made for suitable processes with typical application temperatures. Then, some case studies of installed industrial heat pumps in the Swiss food and beverage sector are described.

Next, two case studies with a spray drying process of a multinational food manufacturer requiring 200 °C hot air and a schnaps distillation process requiring steam at about 118 °C and simultaneous cooling of the distillate are examined in more detail, and possible HTHP integration concepts are presented.

For this purpose, available energy and process data are analyzed and presented as Grand Composite Curves from the Pinch Analysis. This enables the identification of the heat recovery potential, hot and cold utilities, and the possible integration point of a HTHP. In addition, a planning methodology for the electrification of processes by heat pumps is presented.

Finally, simplified process schematics with suitable HTHP integration concepts are provided with quantified results on overall efficiency, heat recovery potential, energy savings and CO_2 emission reductions.

2. CURRENT STATE OF HEAT PUMPS IN SWITZERLAND AND APPLICATION POTENTIALS

2.1. Swiss heat pump sales and energy consumption

In 2022, heat pump sales in Switzerland increased to an all-time high of 41,209 units, representing a growth of 22.8% compared to 2021 (GKS, 2022). Especially in single- and multi-family houses, heat pumps are an established technology for space heating and hot water production. In the large heating capacity range above 100 kW, 232 heat pumps were sold (around 0.6% of all units). Figure 1 compares the sales statistics of heat pumps with oil/gas boilers and shows that the latter dominates in the larger heating capacity range, highlighting the need for decarbonization of the Swiss industry.

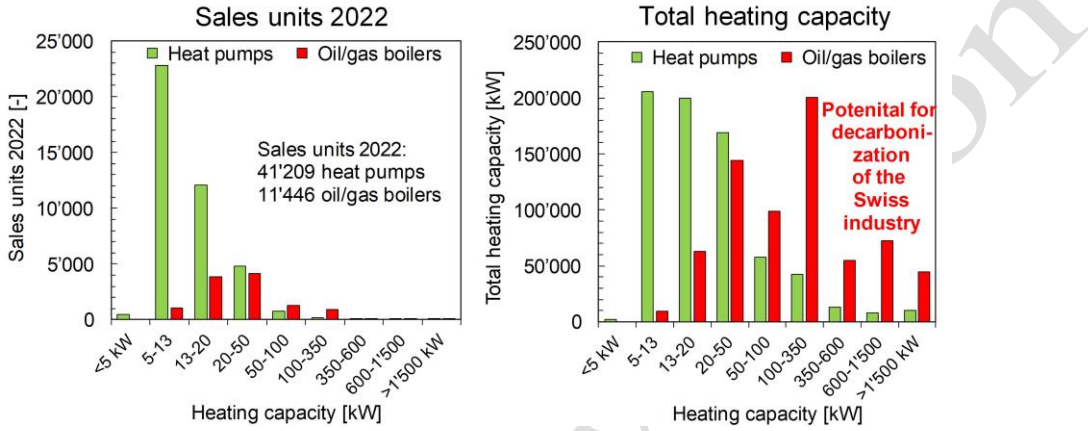

Figure 1. Sales statistics of heat pumps and oil/gas boilers in Switzerland. The distribution of the total heating capacity illustrates the potential for decarbonization of the Swiss industry (Data source: GKS, 2022).

Swiss industry accounts for about 19% (152.8 PJ) of the total final energy consumption (795 PJ) (BFE, 2022) (Figure 2). Besides space heating (9.5%, 14.5 PJ) and hot water (1.7%, 2.7 PJ), process heat (marked in red) is the largest share of energy consumption (53.8%, 82.2 PJ or 22.8 TWh) (BFE, 2022). Of this, around 48% is based on fossil fuels (i.e., gas, oil, coal).

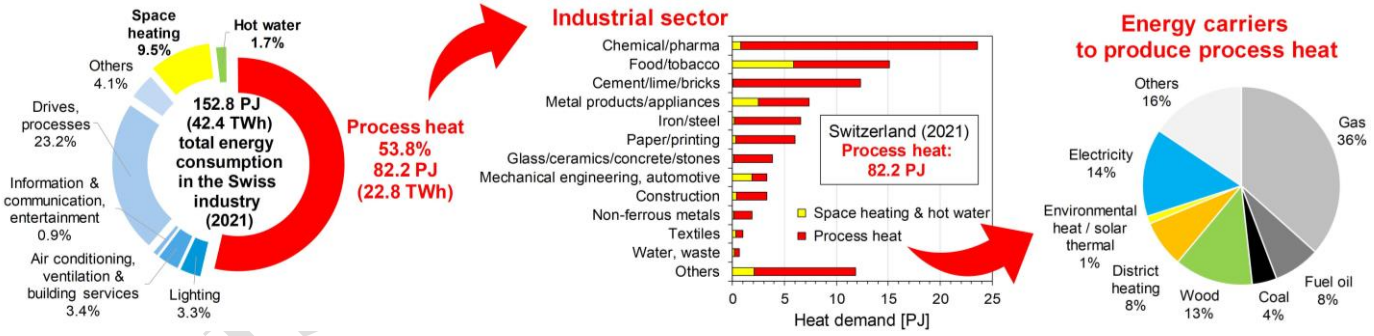

Figure 2. Process heat demand structured by intended use and industrial sector showing the potential for industrial heat pump integration. Today, 48% of process heat is produced by fossil fuels (Data source: BFE, 2022).

The greatest process heat demand is in the chemical/pharmaceutical, minerals, food and beverage, metals, and paper sectors. In comparison, the food/tobacco sector requires about 11% (9.3 PJ) of the total Swiss process heat consumption and about 40% for space heating and hot water. A breakdown of industrial process heat by temperature level states that 18% (15.1 PJ) is below 100 °C and 11% (9.3 PJ) between 100 °C and 200 °C (BFE, 2022), thus, in a temperature range reachable by industrial HTHP.

2.2. Electrification of process heat in the food industry by industrial heat pumps

Electrically-driven industrial HTHP powered by renewable electricity is one of the most promising technical solutions for decarbonizing the food and beverages sector, as elaborated in various studies in Germany (Dumont et al., 2023), Ireland (ESB, 2022), Australia (Jutsen et al., 2017), the United Kingdom (Cooper et al., 2019), or the United States (Zuberi et al., 2022).

For the Swiss food and beverage industry, Obrist et al. (2023) estimated an economic potential of 900 MW heating capacity for heat pumps by 2050. However, this significant exploiting potential requires high CO_2 prices of several hundred EUR/tCO_2 and additional policy measures to overcome investment barriers. As stated by Wallerand et al. (2020), the CO_2 reduction potential in the Swiss food and beverage sector through industrial heat pumps ranges from 24% in a conservative case to 41% in an optimistic case.

In particular, HTHP with supply temperatures above 100 °C is an efficient technology compared to electrode boilers to produce low-pressure steam by upgrading various waste heats. With a 2nd Law efficiency of about 45% to 50% (Arpagaus et al., 2018), COPs of 5.7 to 6.5 for a 30 K temperature lift or 2.2 to 2.8 for 70 K are achieved in practice. In addition, as reviewed by Arpagaus et al. (2023, 2022c), over 30 industrial HTHP products are now available on the market, mainly from European suppliers.

The greatest needs for developing industrial heat pumps is in the restricted temperature range, cost reduction (i.e., investment, maintenance and operation), efficiency improvement, and the provision of standardized heat pumps (Wolf et al., 2017). Ongoing research mainly focuses on natural and low-GWP refrigerants, optimal cycle designs reducing exergy losses, and components extending the temperature range (Arpagaus et al., 2018). As pointed out by the Swiss multinational food company Nestlé (2022), there is a particular market demand for HTHP with hydrocarbons as refrigerants that can generate steam at 200 °C to replace fossil fuels.

2.3. Applications examples of industrial heat pumps in the Swiss food industry

In Switzerland, the food and beverage industry is considered the most important sector for industrial heat pumps (Wolf et al., 2017) because of the wide range of applications and the relatively low-temperature process heat demand, typically between 80 °C to 200 °C (Arpagaus et al., 2022d; Cooper et al., 2019; Dumont et al., 2023). In addition, there is also a great need for cooling food in warehouses and production facilities to extend shelf life.

Concerning potential applications, the international IEA HPT Annex 48 project (Jakobs and Stadtländer, 2020) demonstrated that more than 25% of 342 documented industrial heat pumps installations were in the food and beverage industry, including beer breweries, fruit juice producers, wineries, dairies (e.g., for milk processing, drying of milk powder, ice cream), bakeries, slaughterhouses, manufacturers of cheese, chocolate, frozen foods, pasta, sugar, and others. Potential heat sources are waste heat from refrigeration plants, fermentation processes, wastewater, exhaust air from drying plants, or steam from cooking, evaporation, and distillation processes at about 30 °C to 70 °C.

For illustration, Figure 3 provides an overview of industrial processes suitable for integrating HTHP in the food and beverage industry. Overall, there is a large application potential in heating process water, cleaning-in-place (CIP) and washing systems, drying, pasteurization, sterilization, cooking, thickening, evaporation, and distillation processes. The temperature ranges are color-coded, indicating the available Technology Readiness Level (TRL) of heat pumps (Arpagaus, 2018).

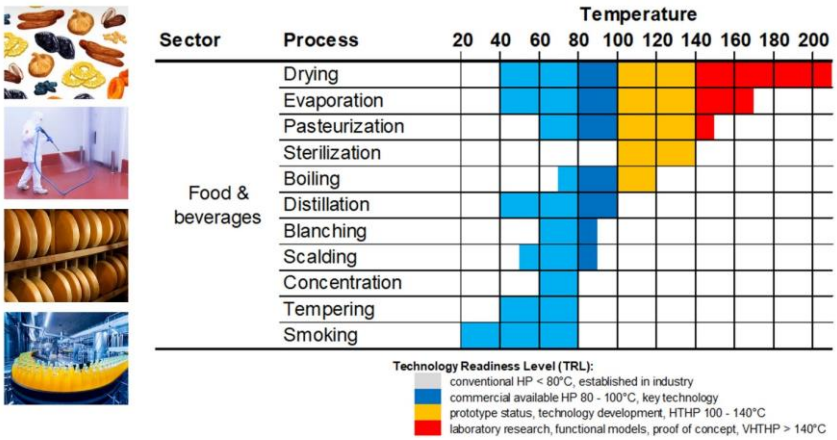

Figure 3. Temperature ranges of typical industrial processes in the food industry. The temperature ranges are color-coded according to the available Technology Readiness Level (TRL) of heat pumps (Arpagaus, 2018).

Moreover, the Pinch temperatures of food processes are often in a range that can be covered by standard heat pumps, such as for dairy products (60 °C), cheese (40 °C), sugar (70 °C), chocolate (25 °C), fresh bread (25 °C), beer (15 °C), tobacco (65 °C), and meat (25 °C) (Wallerand et al., 2020).

Table 1 summarizes some examples of industrial heat pump installations in the Swiss food and beverage industry, classified by company, application/process, heating capacity and temperature range. The installed heat pumps are mainly used to produce hot water, hot air, steam, and cooling.

Table 1. Examples of industrial heat pump installations in Switzerland in the food and beverage sector structured by company, process, capacity, and temperature range (References: (1) (Arpagaus and Bertsch, 2020a), (2) (Arpagaus and Bertsch, 2020b), (3) (Arpagaus, 2019a), (4) (Möhr and Bertsch, 2022), (5) (EnergieSchweiz, 2022a), (6) (Arpagaus, 2019b), (7) (Arpagaus, 2019c), (8) (EnergieSchweiz, 2021), (9) (EnergieSchweiz, 2022b), (10) (Arpagaus et al., 2023).

Company, location	Application, process	Heating capacity (kW)	Temperature range (°C)		ΔT_{Lift} (K)	Reference
Kably SA, Trubschachen	Hot water for biscuit production	471	20	65	45	(1), (2)
Kellermann AG, Ellikon an der Thur	Hot water for greenhouse heating	1000	6	65	59	(1), (2)
Hilcona AG, Schaan (LI)	Hot water for fresh convenience foods	507	31	67	36	(1), (2)
Nutrex, Busswil bei Büren	Vinegar fermentation and pasteurization	194	30	70	40	(1), (2)
Chocolate factory Maestrani, Flawil	Hot water, heating, cooling	276	17	70	53	(1), (2), (3)
Feldschlösschen, Rheinfelden	Hot water for beer pasteurization	400	16	73	57	(4), (5)
Slaughterhouse, Zurich	Hot water, cleaning water	800	20	90	70	(1), (2)
Cheese factory, Gais Appenzell	Hot water for cheese processes, heating	520	18	92	74	(6), (7)
GVS Weinkellerei, Schaffhausen	Hot water for cleaning, heating, cooling	63	37	95	58	(1), (2), (8)
New Roots AG, Oberdiessbach	Cold air and process water for cheese	n.a.	-8	105	113	(9)
Gustav Spiess AG, Berneck	Steam for sausage cooking	550	50	115	65	Potential (10)
Cremo SA, Villars sur Glâne	Hot air for drying process of milk products	940	38	120	82	Potential (10)
ELSA, Estavayer-le-Lac	Steam for CIP process in milk production	3150	50	148	98	Potential (10)

Application examples in the Swiss food and beverage sector include the production of cookies, vegetables, convenience foods, cheese, chocolate, beer, meat, sausages, milk products, and beverages. Traditionally, ammonia (NH_3) chillers provide most of the required cooling demand and heat recovery from the condensers is a suitable heat source for potential heat pump integrations applied in several examples. Overall, the case studies show the variety of applications.

Although industrial HTHP products with supply temperatures above 100 °C are available on the market, Table 1 shows that there are hardly any published installations in Switzerland so far. The market acceptance of industrial HTHP is hampered by a low degree of standardization, resulting in few practical application examples. Manufacturers and designers still lack a critical mass of customers to develop standardized solutions that could reduce costs and planning efforts. From the author's point of view, accelerating market introduction requires, in particular:

- the creation of guidelines and training of qualified personnel capable of optimally integrating industrial heat pumps,
- pilot projects to learn from experience, reduce implementation risks and multiply application potential,
- support for rapid implementation to avoid investments in less optimal energy solutions that block the introduction of industrial heat pumps in the future, and
- increase of CO_2 taxes and fossil fuel prices as external factors to push industries to decarbonize quickly.

3. APPROACH FOR HTHP INTEGRATION USING PINCH ANALYSIS

The selection of appropriate integration points for a heat pump in an industrial process is a challenging task due to the heterogeneity of heat sinks and possible waste heat sources. The selection depends on the characteristics of the heat source and the heat sink (i.e., capacity, medium, supply and return temperature) as well as the techno-economic conditions.

In many cases, potential integration points and heat recovery potentials can be determined directly by a Pinch Analysis and the resulting Grand Composite Curve (GCC). Once the integration points are determined, a rough design and dimensioning of the heat pump system can be made.

The major questions to be answered in a heat pump integration task are:

- What processes have a heating demand?
- What processes have a cooling demand?
- What is the required heat supply temperature?
- Are there suitable heat sources available?
- Is the heat source capacity approximately in the same order of magnitude as the heat demand?
- Is the heat source available at about the same time as the heat sink?
- What is the heat recovery potential?
- What is the operating profile of the heat pump (e.g., part load, fluctuations)?

Figure 4 shows a possible procedure for analyzing energy systems to implement electrification technologies (Power-to-Heat) and design options for heat pumps (integration across the Pinch temperature), electrode boilers, or electric heaters (Son et al., 2022). Electric heaters offer high availability and faster start-up times compared to heat pumps. On the other hand, heat pumps provide higher energy efficiency.

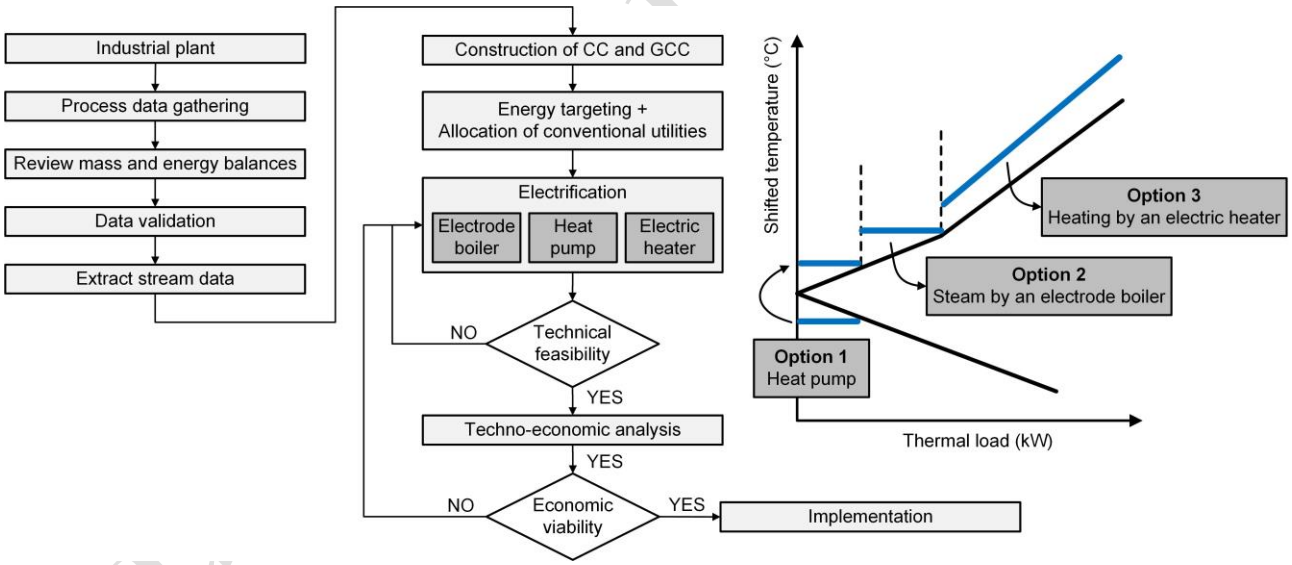

Figure 4. Procedure for analyzing energy systems with electrification and GCC with design options heat pump, electrode boiler, and electric heater (Adapted from Son et al., 2022).

4. CASE STUDIES WITH POTENTIAL HTHP INTEGRATION

Recently, (Arpagaus et al., 2023) presented potential HTHP integrations in the Swiss food companies ELSA (steam for a CIP process in milk production), Cremo SA (hot air for a drying process of milk permeate) and Gustav Spiess AG (steam for sausage cooking) (Table 1, marked as “potential”). This section focuses on two additional potential HTHP integrations in Swiss food companies with a spray drying process and a distillation process for schnapps, i.e., alcoholic beverages made from fruits.

4.1. Spray dryer case study

The first case study describes a multi-purpose spray dryer for drying various food products of a multinational Swiss company in a region where a carbon-neutral electricity supply is available. The spray dryer requires hot air of 200 °C. The ambient inlet air is dehumidified and heated before entering the spray dryer. Considering the temperatures and flow rates involved, the heat of the humid exhaust air (typically 80 °C) can be recovered with a recuperator. A HTHP integration is proposed to increase the thermal efficiency further. Another argument for a HTHP is the continuous spray drying process and heat demand offering high operating time.

Figure 5 (left) shows a schematic of the proposed heat recovery system. The heat from the exhaust air is partly recuperated through a heat exchanger and partially upgraded through a HTHP (black box). Intermediate water loops are utilized at the evaporator and condenser of the HTHP and for the recuperator. In addition, an electrical heater is included to raise the air temperature to the desired 200 °C for better control and fine-tuning. A steam boiler could work as a backup. Figure 5 (right) shows the general concept with the HTHP and recuperator.

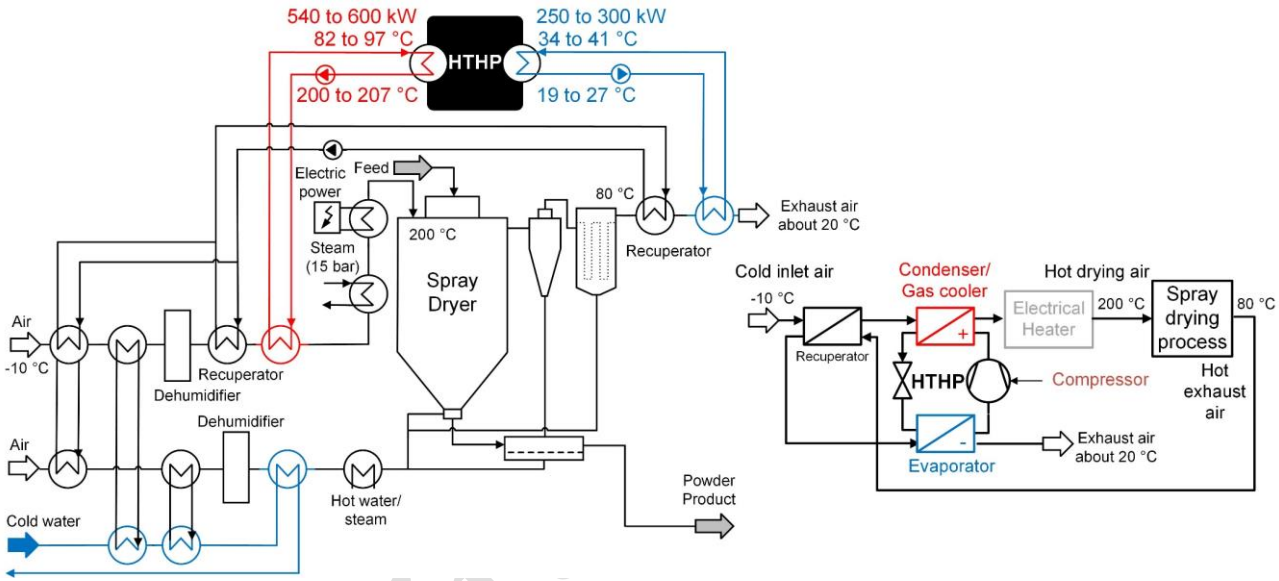

Figure 5. Spray drying process with integration concept of a HTHP with recuperator and electric heater.

As a first step towards the HTHP integration, a Pinch Analysis was performed using the available airflow data of the spray dryer system (i.e., temperatures, capacities, and flow rates). Figure 6 (left) shows the considered hot and cold composite curves (CC) of a winter case with an outdoor air temperature of -10 °C. Thus, the cold drying air stream (blue) starts at -10 °C and ends at 200 °C, while the hot exhaust air (red) begins at 80 °C and ends at about 23 °C. Consequently, the shifted pinch temperature is at 75 °C. To account for the additional temperature difference imposed by the intermediate water circuits, a pinch temperature of 10 °C was assumed in the heat exchangers.

In addition, the grand composite curve (GCC) shows a net heating demand of 1,126 kW and a net cooling demand of 385 kW after heat recuperation (694 kW). The shape of the GCC indicates that the spray drying process requires a large temperature gradient to produce the hot drying air. Possible HTHP technologies providing large temperature glides are a transcritical cycle with hydrocarbons, CO_2 or low-GWP HFOs (Arpagaus et al., 2020), a reversed Brayton cycle (Joule cycle with noble gases such as argon), an Osenbrück cycle (e.g., a hybrid heat pump with NH_3/H_2O), or vapor compression cycles with refrigerant mixtures (Arpagaus et al., 2022c, 2021).

In this spray dryer case study, a standard HTHP and a transcritical HTHP, each with a recuperator, were investigated. The Engineering Equation Solver (EES) software (Version V10.834-3D) was used for model simulation. In the case of the standard HTHP with recuperator, a simplified heat pump model was used to calculate the heating COP_H from the heat source and sink temperatures assuming 50% 2nd Law efficiency. The heat transfer rates and the electrical power (W_C) were calculated from the energy balance. A pinch temperature difference of 10 K was assumed in all heat exchangers.

The inlet air is heated from -10 °C to 70 °C in the recuperator by heat exchange with the hot exhaust air at 80 °C. The exhaust air leaves the recuperator at 26 °C and is used as a heat source ($\dot{Q}_L$, 259 kW) for the HTHP to heat the air ($\dot{Q}_H$, 597 kW) from 70 °C to 140 °C (max. assumed supply temperature for the refrigerant R245fa). Finally, the air is further heated from 140 °C to 200 °C by an electric heater ($\dot{Q}_{eh}$, 529 kW).

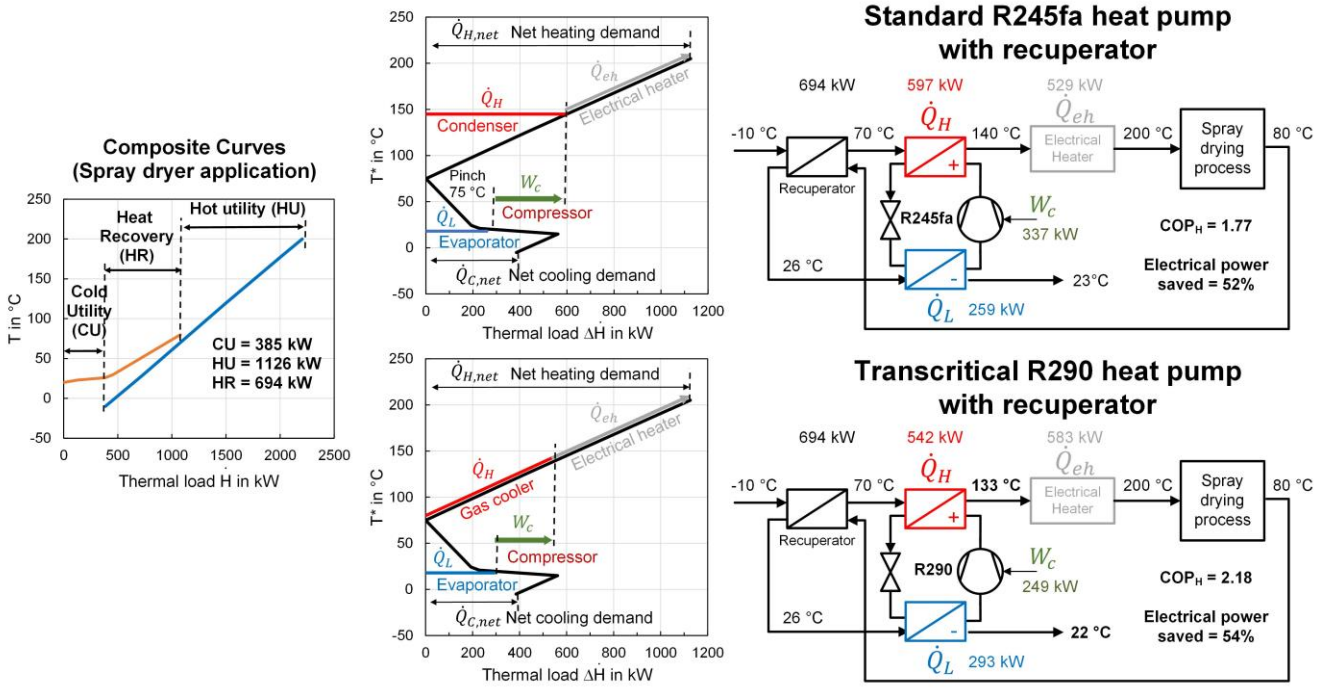

Figure 6. Composite curve (CC) and grand composite curve (GCC) of a food spray drying process with integration of a standard R245fa heat pump and a transcritical R290 (propane) heat pump, each with a recuperator.

Figure 6 (top) shows the corresponding GCC and integration scheme. Due to the large temperature lift of 117 K (from 23 °C $T_{source,in}$ to 140 °C $T_{sink,out}$), the COP_H is only 1.77. Overall, the net electrical power saved with the HTHP integration and recuperator is about 52% (compared to no integration = purely electric air heating). Since the air has a large temperature glide, there are exergy losses (not calculated in this paper) associated with the condenser of a standard HTHP.

Therefore, a transcritical HTHP was considered since the gas coolers can provide the required temperature glide. Different refrigerants were simulated, including R600 (n-butane), R600a (iso-butane), R290 (propane), R1234ze(E), R1224yd(Z), and R1233zd(E) (Figure 7). In addition, a pinch temperature of 10 K was assumed in the evaporator and gas cooler, 5 K superheat after the evaporator and an isentropic compressor efficiency of 0.7. Given the practical pressure and temperature limitations of commercially available compressors, gas cooler pressures in the range of 40 to 60 bar were considered for performance calculations.

As a result, it was found that the COP_H was about 2.1 for all refrigerants. Figure 7 shows the other relevant performance parameters graphically at 40 bar gas cooler pressur, i.e., heat sink outlet temperature ($T_{sink,out}$), volumetric heat capacity (VHC), and pressure ratio (p_{ratio}).

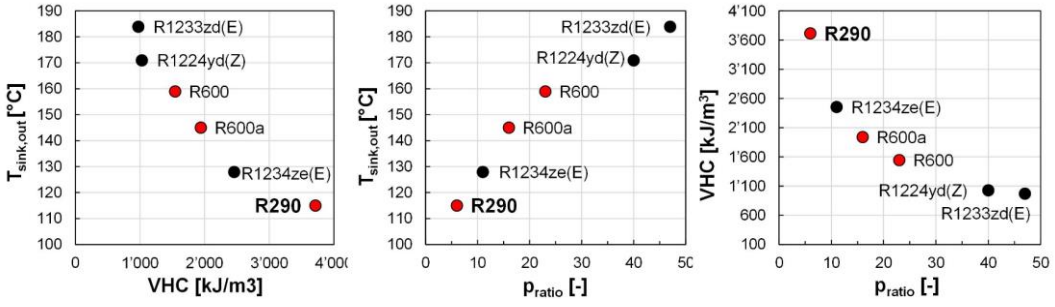

Figure 7: Comparison of the performance parameters ($T_{sink,out}$, VHC, p_{ratio}) in a transcritical HTHP cycle using different refrigerants ($T_{sink,in} = 84\ °C$, $T_{source,in} = 34\ °C$, $T_{source,out} = 19\ °C$, 40 bar gas cooler pressure).

R290 (propane) turned out to be the most suitable refrigerant for further investigation since it is cheap and the required compressor size is smaller compared to the other refrigerants thanks to the highest VHC, even though the $T_{sink,out}$ was limited to a maximum of about 160 °C (in the case of 40 bar, 115 °C, see Figure 7). In addition, the p_{ratio} was the smallest for R290.

Figure 6 (bottom) shows the integration of a R290 transcritical HTHP along with a recuperator in the spray drying process and its corresponding GCC. Using this concept, a $T_{sink,out}$ of 133 °C was reached and the COP_H was found to be 2.18 resulting in a net electrical power saving of 54%.

Overall, the spray dryer case study shows that from the energy efficiency point of view, a transcritical HTHP with a recuperator is a more efficient option than a standard HTHP. However, the investment and operating costs should be considered in the practical implementation of the heat recovery system. Another HTHP concept used in practice is two heat pumps connected in series using, e.g., R1234ze(E) and R1233zd(E), but this was not further considered in this study.

4.2. Schnapps distillation case study

The second case study considers a potential HTHP integration in a fruit schnapps distillery. Figure 8 shows a simplified schematic of the schnapps distillation process with a copper still, dephlegmator, and condenser. Before distillation begins, the fermented mash flows through an intermediate storage vessel into the still. Then, distillation occurs in the still with distinct pre-, middle- and post-distillation runs.

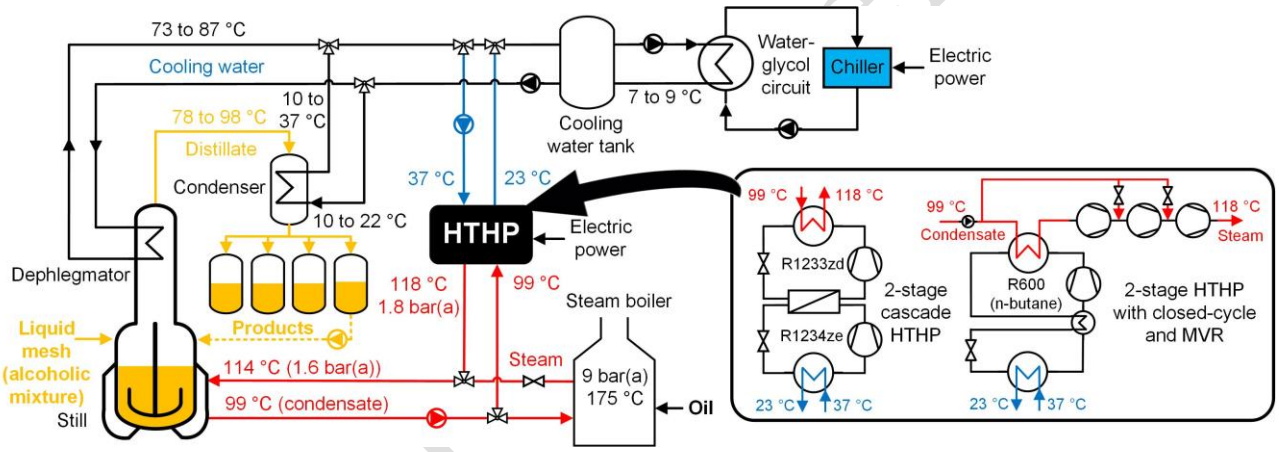

Figure 8. Schematic of a schnapps distillation process with integration of a steam-generating HTHP, either as a 2-stage cascade (R1234ze/RR1233zd(E) or as a combined cycle with mechanical vapor recompression (MVR).

In the beginning, the mash is heated for about 1 hour. Next, the ethanol-water mixture heats up to 92 °C and starts to evaporate. Then, the resulting vapor is cooled and condensed, reaching a temperature of 12 °C to 24 °C. The pre-distillate, with an alcohol content of 88 vol%, is toxic and must be separated from the usable schnapps and discarded. The middle-distillation run with an alcohol content of about 72 vol% corresponds to around 28% of the total distillate, and the process step takes about 1.5 hours.

The first part of the post-distillation lasts for about 70 minutes and contains, on average, 56 vol% alcohol and important aromas, such as propanol, butanol, and acetic acid. It is added to the mash for the next distillation batch, increasing the ethanol content and simplifying the distillation process. The second part of the post-distillation run (again 70 minutes) with an average of 31 vol% alcohol is distilled again. Overall, the multi-stage distillation process takes about 7 hours per batch, resulting in 2,550 operating hours per year.

An oil boiler is a classic heating technology for distilleries for steam generation. In this case study, the oil boiler produces 9 bar(a) (175 °C) steam that is reduced to 1.6 bar(a) (114 °C) to allow gentle distillation and prevent degradation of the product in the still. The steam condensate at 99 °C flows back to the boiler. The cooling water (10 to 22 °C) used in the dephlegmator and the distillate condenser are produced by a chiller with an intermediate water-glycol circuit.

The goal of the distillery is to decarbonize the steam supply and replace the oil boiler with electrification technology, e.g., a steam-generating HTHP or/and an electrode boiler. A small electrode boiler can serve as

an auxiliary heater for rapidly generating clean hot water (11 °C to 70 °C) for cleaning operation, steam for start-up, fine-tuning, and covering peak loads. Other common technologies in food distillation include an evaporator with mechanical vapor recompression (MVR), which is not considered in this study.

Figure 9 (left) shows the CC from a Pinch Analysis and the corresponding GCC (right) of the schnapps distillation process. As can be seen, the Pinch temperature is at 59 °C, and the hot utility (HU) is 186 kW.

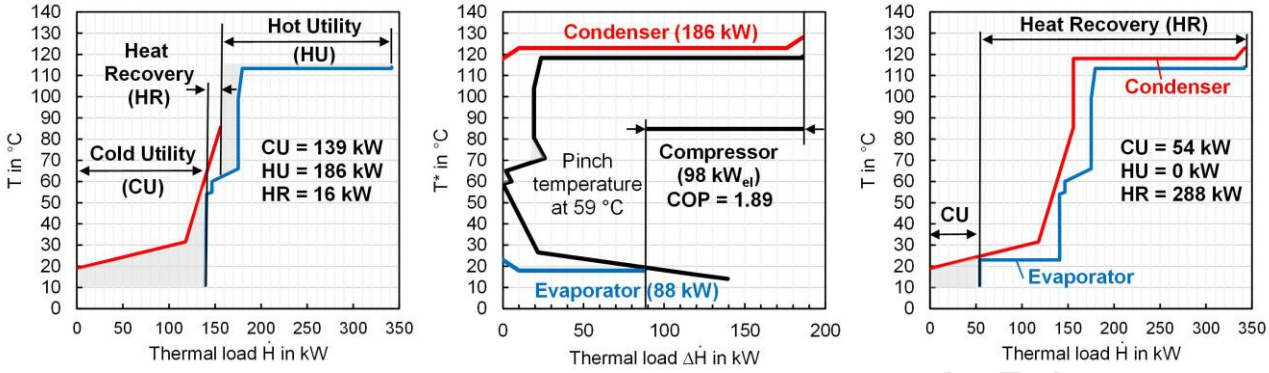

Figure 9: Composite curves (CC) and Grand Composite Curve (GCC) of a schnapps distillation process (alcoholic beverage) showing the potential for integrating a steam-generating HTHP providing low-pressure steam by using the cooling water as a heat source (pinch temperature at 59 °C, evaporation temperature at 18 °C, condensation temperature at 123 °C, COP of 1.89 based on fit-function $COP = 52.94 \cdot \Delta T_{lift}^{-0.716}$).

Figure 8 illustrates the proposed concept for integrating a steam-generating HTHP into the schnapps distillation process. Heat is recovered from the cooling water return as a heat source, and steam is generated by the HTHP for the distillation process. The HTHP design point considered was $T_{source,in} = 37\ °C$ (water), $T_{source,out} = 23\ °C$, $T_{sink,in} = 99\ °C$ (condensate), and $T_{sink,out} = 118\ °C$ (1.8 bar(a) steam).

The large temperature lift from the heat source to the heat sink requires a two-stage vapor compression system. Therefore, a two-stage cascade with R1234ze(E) in the lower stage and R1233zd(E) in the upper stage is proposed as a practical option (Figure 8). In addition, a steam accumulator would be integrated to control the steam pressure. A second efficient design for steam generation is a combined HTHP system with a closed-cycle heat pump in the lower stage using R600 (n-butane) and a MVR system with steam (R718) in the upper stage (Uhlmann et al., 2022).

As theoretical calculations with an EES simulation model show (Table 2), a COP of 2.34 with 62% Carnot efficiency (2nd Law efficiency) is theoretically possible with the two-stage cascade (R1234ze(E)/R1233zd(E)) without heat losses. An intermediate temperature of 70 °C in the cascade heat exchanger, 5 K pinch temperature, 10 K superheat, 3 K subcooling and 70% isentropic compressor efficiency were assumed.

Table 2. COP estimations for the HTHP integration in the schnapps distillation process.

Parameter	Theoretical model calculations with EES software		Calculations based on data from various HTHP manufacturers
HTHP concept	2-stage cascade with low-GWP HFO R1234ze(E)/R1233zd(E)	Combined cycle 2-stage with closed-cycle (R600) and 3-stage MVR (R718)	COP based on 32 datapoints (Arpagaus et al., 2022a, 2022b) $COP = 52.94 \cdot \Delta T_{lift}^{-0.716}$ *(R^2 = 0.8826)*
HTHP design point temperatures	$T_{source.in} = 37\ °C$ (water), $T_{source.out} = 23\ °C$ $T_{sink.in} = 99\ °C$ (condensate), $T_{sink.out} = 118\ °C$ (1.8 bar(a) steam) $T_{evap} = 18\ °C$, $T_{cond} = 123\ °C$, $COP_{Carnot} = 3.77$		
COP	2.34	2.48	**1.89**
Carnot efficiency (2nd Law)	62%	66%	50%
Condensation capacity	**186 kW** (according to Pinch Analysis and GCC, pinch temperature at 59 °C, Figure 9)		
Evaporation capacity	106 kW	114 kW	**88 kW**
Compressor power	80 kW	74 kW	**98 kW**

Even higher efficiencies can be achieved with the combined cycle (R600 bottom cycle) and 3-stage steam recompression with a pressure ratio of 1.58 per stage (3 centrifugal fans connected in series with 82.5% isentropic efficiency, 3.9 total pressure ratio). The calculation results in a COP of 2.48, i.e., an increase of 6% compared to the two-stage cascade. However, such a combined cycle has never been implemented in practice and is probably associated with higher investment costs and a higher maintenance effort.

Using a COP fit-curve $COP = 52.94 \cdot \Delta T_{lift}{}^{-0.716}$ based on 32 data points from different HTHP suppliers (Arpagaus et al., 2022a, 2022b), a COP of 1.89 is estimated, which is lower than the simulated values because it accounts for heat losses. Depending on which COP calculation is used (theoretical or based on manufacturer data) and the heat pump cycle design, the HTHP integration may take slightly different values.

Figure 9 (middle) considered the more conservative COP value of 1.89 from the COP-fit formula (Arpagaus et al., 2022a, 2022b). This way, integrating a steam-generating HTHP in the schnapps distillation process covers the total hot utility of 186 kW in the condenser. In addition, it results in an evaporator capacity of 88 kW and 98 kW of compressor work.

Additionally, integrating a HTHP would significantly reduce the carbon footprint of the schnaps distillation process, as it does not generate such emissions as an oil boiler. Compared with oil, which has a CO_2 emission factor of 0.265 kg CO_2 per kWh of useful heat (BAFU, 2022a), the electricity mix produced in Switzerland is relatively low in emissions, with about 57% hydropower (0.0296 kg CO_2/kWh) (FOEN, 2022). By contrast, the average consumer electricity mix emits 0.128 kg CO_2/kWh (FOEN, 2022) due to the more fuel-based imported electricity. Therefore, the CO_2 emission reduction by replacing a fuel-driven steam boiler with an electrically-driven HTHP can be calculated according to Eq. (1):

$$E_{CO2,reduction} = \dot{Q}_h \cdot t \cdot \left(\frac{f_{CO2,fuel}}{\eta_{fuel}} - \frac{f_{CO2,el}}{COP} \right) \quad \text{Eq. (1)}$$

where η_{fuel} is the efficiency of the fuel-fired steam boiler (0.9 is assumed), and $f_{CO2,fuel}$ and $f_{CO2,el}$ are the CO_2 emissions factors for fuel and electricity. The HTHP integration leads to an annual CO_2 emission reduction of 108 tCO_2 or 77%, resulting in an annual CO_2 tax refund of 12,900 CHF at a CO_2 levy of 120 CHF/tCO_2 imposed on fossil fuels (e.g. heating oil) (BAFU, 2022b).

In summary, integrating a steam-generating HTHP into the distillation process is an environmentally friendly alternative to an oil-fired boiler, as the oil consumption for steam generation can be replaced by renewable electricity. The COP varies depending on assumptions and calculations. At the same time, 61 % of the cold utility (cooling water) can be saved (reduction from 139 kW to 54 kW, see Figure 9).

5. CONCLUSIONS

Sales of heat pumps are on the rise in Switzerland (22.8% growth rate in 2022). The food and beverage industry offers great application potential for integrating heat pumps in numerous processes with supply temperatures that can be achieved with heat pumps. Although industrial HTHP with supply temperatures above 100 °C are available on the market, there are hardly any installed examples in Switzerland.

So far, only the innovators have the courage to invest in industrial heat pumps. The low number of case studies increases the perceived risk among industrial companies. Relevant barriers are a need for more awareness of the available options and a lack of specific know-how and planning tools for planners, heat pump designers, installers, and investors. Therefore, it is key to create planning certainty, expand professional training, and work on further demonstration projects to mitigate the risk for industrial customers.

Heat pump integration in industrial processes is a difficult task due to the heterogeneity of heat sinks and potential waste heat sources. The pinch analysis with the corresponding grand composite curve is a promising approach for analyzing a possible heat pump integration and allows the proper sizing of a heat pump with source and sink temperatures across the pinch temperature as a basic rule.

The two case studies presented with a spray drying process and a distillation process of liquor have shown the consideration steps for HTHP integration into a standardized approach. The spray dryer case study

showed that a transcritical heat pump using natural refrigerant R290 (propane) is an efficient design option that provides a large temperature glide to heat the drying (around 600 kW), extracting humid exhaust as a heat source. Compared to all-electric air heating, an energy savings of 54% is achieved. The concept includes a combination of HTHP and an electric heater for temperature fine-tuning. The schnapps distillation case study shows that a steam-generating HTHP is an environmentally friendly alternative to an oil-fired steam boiler, reducing CO_2 emissions by 77% (assuming an average Swiss electricity mix). At the same time, the cooling demand is reduced by 61% by using cooling water as a heat source.

As an outlook, the spatial distances between heat sources and sinks and safety and process engineering aspects have to be investigated. These factors affect the accuracy of sizing, potential and efficiency of heat pumps. Therefore, further research should focus on addressing these practical constraints and identifying retrofit options in the specific context of an application. Another step is to conduct an economic analysis of the case studies and expand to other potential case studies in the Swiss food and beverage industry in collaboration with Pinch Analyses and multipliable Grand Composite Curves.

ACKNOWLEDGEMENTS

The authors gratefully acknowledge the Swiss Federal Office of Energy (SFOE) for the financial support of the project Annex 58 HTHP-CH (Contract number SI/502336-01), IntSGHP (Contract number SI/502292), and the SWEET (SWiss Energy research for the Energy Transition) project DeCarbCH (DeCarbonisation of Cooling and Heating in Switzerland) (www.sweet-decarb.ch).

NOMENCLATURE

COP	Coefficient of performance (-)	CC	Composite Curve
$E_{CO2,reduction}$	CO_2 emissions reduction (tCO_2)	GCC	Grand Composite Curve
$f_{CO2,fuel}$	CO_2 emissions factors for fuel (kg CO_2/kWh)	ΔT_{Lift}	Temperature lift (K)
$f_{CO2,el}$	CO_2 emissions factors for electricity (kg CO_2/kWh)	p	Pressure (bar)
η_{fuel}	Efficiency of fuel-fired steam boiler (-)	T	Temperature (°C)
$\dot{Q}_h$	Heating capacity (kW)	sink	Heat sink
t	Annual operating time (h)	source	Heat source
TRL	Technology Readiness Level	$\dot{H}$	Thermal load (kW)

REFERENCES

Arpagaus, C., 2019a. Maestrani setzt auf Energieeffizienz. Alimenta Vol. 18 p. 24-26.

Arpagaus, C., 2019b. From Waste Heat to Cheese. HPT Mag. 37, 23–26.

Arpagaus, C., 2019c. High Temperature Heat Pump in a Swiss Cheese Factory, in: 2nd Conference on High Temperature Heat Pumps, September 9, 2019, Copenhagen.

Arpagaus, C., 2018. Hochtemperatur-Wärmepumpen: Marktübersicht, Stand der Technik und Anwendungspotenziale, 138 Seiten, ISBN 978-3-8007-4550-0 (Print), ISBN 978-3-8007-4551-7 (E-Book). VDE Verlag GmbH, Offenbach, Berlin.

Arpagaus, C., Bertsch, S.S., 2020a. Industrial Heat Pumps in Switzerland: Application Potentials and Case Studies, Final Report, 23 July 2020 [WWW Document]. URL https://www.aramis.admin.ch/Dokument.aspx?DocumentID=66033

Arpagaus, C., Bertsch, S.S., 2020b. Successful Application Examples of Industrial Heat Pumps in Switzerland, in: Rankine2020, Glasgow, 26-29 July, 2020. pp. 1–8. https://doi.org/10.18462/iir.rankine.2020.1183

Arpagaus, C., Bertsch, S.S., Bless, F., 2021. Industrial Heat Pumps - Research and Market, DeCarbCH Lunch Talk, November 9, 2021 [WWW Document]. DeCarbCH Lunch Talk, Novemb. 9, 2021. URL https://www.sweet-decarb.ch/events/event/lunch-talk-3

Arpagaus, C., Bertsch, S.S., Bless, F., Krummenacher, P., Flórez-Orrego, D.A., Pina, E.A., Maréchal, F., Calame Darbellay, N., Rognon, F., Vesin, S., Achermann, P., Jansen, C., 2023. Integration of High-Temperature Heat Pumps in Swiss Industrial Processes (HTHP-CH), in: 14th IEA Heat Pump Conference, 15-18 May 2023, Chicago, Illinois. pp. 1–12.

Arpagaus, C., Bless, F., Bertsch, S., 2022a. Techno-economic analysis of steam generating heat pumps for integration into distillation processes, in: 15th IIR-Gustav Lorentzen Conference on Natural Refrigerants, June 13-15, Trondheim, Norway. https://doi.org/http://dx.doi.org/10.18462/iir.gl2022.0029

Arpagaus, C., Bless, F., Bertsch, S.S., 2022b. Techno-Economic Analysis of Steam-Generating Heat Pumps in Distillation Processes, in: 3rd HTHP Symposium, 29-30 March, 2022, Copenhagen, Denmark.

Arpagaus, C., Bless, F., Bertsch, S.S., 2020. Theoretical Analysis of Transcritical HTHP Cycles with Low GWP HFO Refrigerants and Hydrocarbons for Process Heat up to 200 ° C. Rank. Glas. 26-29 July, 2020 2, 1–8. https://doi.org/10.18462/iir.rankine.2020.1168

Arpagaus, C., Bless, F., Uhlmann, M., Schiffmann, J., Bertsch, S.S., 2018. High temperature heat pumps: Market overview, state of the art, research status, refrigerants, and application potentials. Energy 152, 985–1010. https://doi.org/10.1016/j.energy.2018.03.166

Arpagaus, C., Brendel, L., Paranjape, S., Bless, F., Uhlmann, M., Bertsch, S., 2022c. High-Temperature Heat Pumps for Industrial Applications - New Developments and Products for Supply Temperatures above 100 °C, in: China Heat Pump Conference (CHPC2022), Hangzhou, Zhejiang Province, China, October 24-27, 2022.

Arpagaus, C., Payá, J., Hassan, A.H., Bertsch, S.S., 2022d. Potential Impact of Industrial HTHPs on the European Market, in: 3rd HTHP Symposium, 29-30 March, 2022, Copenhagen, Denmark. p. Poster.

BAFU, 2022a. CO2 -Emissionsfaktoren des Treibhausgasinventars der Schweiz, Faktenblatt, Januar 2022, Bundesamt für Umwelt BAFU [WWW Document]. URL https://www.bafu.admin.ch/dam/bafu/en/dokumente/klima/fachinfo-daten/CO2_Emissionsfaktoren_THG_Inventar.pdf.download.pdf/Faktenblatt_CO2-Emissionsfaktoren_01-2022_DE.pdf

BAFU, 2022b. CO2 levy [WWW Document]. URL https://www.bafu.admin.ch/bafu/en/home/topics/climate/info-specialists/reduction-measures/co2-levy.html

BFE, 2022. Analyse des schweizerischen Energieverbrauchs 2000 - 2021 nach Verwendungszwecken 101.

Cooper, S.J.G., Hammond, G.P., Hewitt, N., Norman, J.B., Tassou, S.A., Youssef, W., 2019. Energy saving potential of high temperature heat pumps in the UK Food and Drink sector. Energy Procedia 161, 142–149. https://doi.org/10.1016/j.egypro.2019.02.073

Dumont, M., Wang, R., Wenzke, D., Blok, K., Heijungs, R., 2023. The techno-economic integrability of high-temperature heat pumps for decarbonizing process heat in the food and beverages industry. Resour. Conserv. Recycl. 188, 106605. https://doi.org/10.1016/j.resconrec.2022.106605

EnergieSchweiz, 2022a. CO2-freundliche Produktion veganer Alternativen zu Käse [WWW Document]. URL https://www.energieschweiz.ch/stories/waermepumpe-lebensmittelherstellung/

EnergieSchweiz, 2022b. Wie Wärmepumpen zur Energieeffizienz der Bierproduktion beitragen [WWW Document]. URL https://www.energieschweiz.ch/stories/waermepumpe-getraenkeindustrie/

EnergieSchweiz, 2021. Getränkeabfüllanlage klimaneutral reinigen mit einer Wärmepumpe [WWW Document]. URL https://www.energieschweiz.ch/stories/waermepumpe-lebensmittelindustrie/

ESB, 2022. Decarbonising Ireland's Industrial Sector: The Role of Industrial Heat Pumps [WWW Document]. URL https://esb.ie/docs/default-source/leading-lights/industrial-heat-pumps-insights-paper.pdf

FOEN, 2022. Climate change: Questions and answers, 8. How climate-friendly is the Swiss energy supply? Federal Office for the Environment [WWW Document]. URL https://www.bafu.admin.ch/bafu/en/home/topics/climate/questions-answers.html

GKS, 2022. GebäudeKlima Schweiz: Statistik für Heizkessel, Brenner, Wärmepumpen, Solaranlagen, Energiespeicher, Wassererwärmer, Stand 17.1.2023 1–8.

Jutsen, J., Pears, A., Hutton, L., 2017. High Temperature Heat Pumps for the Australian food industry: Opportunities assessment, August 2017, Sydney, Australian Alliance for Energy Productivity (A2EP).

Möhr, E., Bertsch, S., 2022. Gross-Wärmepumpe für prozessintegrierten Einsatz. planer+installateur 7, 40–43.

Nestlé, 2022. Nestlé Needs High-Temperature Hydrocarbon Heat Pumps for Steam Generation, November 23, 2022 [WWW Document]. ATMO Eur. Summit, Brussels, Novemb. 15-16, 2022. URL https://hydrocarbons21.com/atmo-europe-nestle-needs-high-temperature-hydrocarbon-heat-pumps-for-steam-generation/

Obrist, M.D., Kannan, R., McKenna, R., Schmidt, T.J., Kober, T., 2023. High-temperature heat pumps in climate pathways for selected industry sectors in Switzerland. Energy Policy 173, 113383. https://doi.org/10.1016/j.enpol.2022.113383

Son, H., Kim, M., Kim, J.-K., 2022. Sustainable process integration of electrification technologies with industrial energy systems. Energy 239, 122060. https://doi.org/10.1016/j.energy.2021.122060

Uhlmann, M., Olmedo, L.E., Arpagaus, C., Bless, F., Schiffmann, J., Bertsch, S., 2022. Efficient steam generation in industry - Combined heat pump cycle with mechanical vapor recompression, in: 15th IIR-Gustav Lorentzen Conference on Natural Refrigerants, June 13-15, Trondheim, Norway. pp. 1–11. https://doi.org/http://dx.doi.org/10.18462/iir.gl2022.0049

Wallerand, A.S., Kantor, I., Maréchal, F., 2020. Integrated industrial heat pump systems: Background, software development & Swiss potentials, Final Report 30/07/2020 [WWW Document]. URL https://www.aramis.admin.ch/Dokument.aspx?DocumentID=66431

Wolf, S., Flatau, R., Radgen, P., Blesl, M., 2017. Systematische Anwendung von Großwärmepumpen in der Schweizer Industrie, Endbericht, 10. Mai 2017.

Zuberi, M.J.S., Hasanbeigi, A., Morrow, W., 2022. Bottom-up assessment of industrial heat pump applications in U.S. Food manufacturing. Energy Convers. Manag. 272, 116349. https://doi.org/10.1016/j.enconman.2022.116349

DOI: 10.18462/iir.gl2022.0029

Techno-economic analysis of steam generating heat pumps for integration into distillation processes

Cordin ARPAGAUS*, Frédéric BLESS, Stefan BERTSCH

Eastern Switzerland University of Applied Science, Institute for Energy Systems IES,
CH-9471 Buchs, Switzerland
*Corresponding author: cordin.arpagaus@ost.ch

ABSTRACT

To decarbonize process heat in industry, there is an urgent need to promote more energy-efficient and environmentally friendly technologies. In this context, electrically driven steam generating heat pumps (SGHPs) attract great attention for upgrading waste heat to low-pressure steam with high efficiency. This study analyses different integration concepts of SGHPs into distillation processes with heat source temperatures ranging from 20 to 45 °C providing low-pressure steam at about 110 to 120 °C and about 0.5 to 2.5 MW heating capacity. The technical and economic feasibility of the integration is investigated based on case studies in the Swiss chemical industry. Furthermore, a heat pump and cost model was developed based on fit curves to evaluate the economic feasibility considering the investment, operating, maintenance costs, potential subsidies, and CO_2 taxes. The analysis shows that the integration of SGHPs is technically feasible and economical. Furthermore, payback periods of 3 to 5 years are reached.

Keywords: Steam Generating Heat Pumps, High-Temperature Heat Pumps, Process Integration, Steam Compressors, Distillation

1. INTRODUCTION

Today, the chemical sector is responsible for about one-third of the total energy consumption and associated CO2 emissions in the industrial sector (Kiss & Smith, 2020). In particular, process heat generation in distillation processes dominates and consumes about 40 % of energy in the chemical industry (Kiss, 2019). In Switzerland, the final energy consumption of the chemical and pharmaceutical industry was around 24.7 PJ in 2020, which corresponded to 22% of total industrial consumption (BFE, 2021). Of this, thermal energy from the combustion of fossil fuels, mainly natural gas, accounted for around 63 %.

Although the overall energy consumption in the Swiss chemical industry has been slightly decreasing in recent years, there is still room for improving energy use by increasing heat recovery through process heat integration and upgrading low-grade heat through electrically-driven heat pumps (Zuberi et al., 2018, 2020). High-temperature heat pumps (HTHP) (Arpagaus et al., 2018) and especially steam-generating heat pumps (SGHP) (Bless et al., 2020) are an advanced technology for the supply of process heat and are expected to become more widespread in the coming years, helping reduce primary energy consumption and greenhouse effect gas emission. Furthermore, experimental research on SGHP has intensified worldwide in recent years, and new products on the market enable new integration concepts for heat pump-assisted distillation processes and efficient electrification of the industrial sector.

However, the number of heat pumps in industry is still low, mainly due to skepticism about the economic benefits and few realized case studies. For investment decisions, cost-effectiveness is of utmost importance. In this context, the number of studies evaluating the techno-economic feasibility of integrating industrial heat pumps has increased in recent years, including (Arnitz et al., 2018; Brückner et al., 2015; Cox et al., 2022; Hansen, 2019; Jesper et al., 2021; Kim et al., 2022; Kosmadakis et al., 2020; Meyers et al., 2018; Ommen et al., 2015; Schlosser et al., 2020; Schlosser et al., 2020; Vieren et al., 2021; Wang & Zhang, 2019; Wolf, 2017; Zuberi et al., 2018; 2021), which are worthwhile reading.

This study aims to investigate the integration of SGHP in distillation processes based on case studies from Switzerland and the literature. It is intended to provide a simple way of checking whether using an SGHP is technically feasible and economically viable at an early planning stage. The focus is on electrically driven SGHPs delivering low-pressure steam at about 110 to 120 °C, which is interesting for the chemical sector due to the already existing steam pipe infrastructure and heat exchangers. The investment and operating costs of SGHPs are analyzed for these case studies using a simple cost model with different energy prices and economic input parameters. The payback periods are calculated to compare the economic feasibility of SGHP integration. Finally, the avoided CO_2 emissions and energy savings are evaluated, and the main factors affecting the results are discussed.

2. CASE STUDIES

Three case studies were selected for this analysis based on hypothetical situations of distillation applications in Switzerland and literature. Figure 1 shows the principle flow diagrams of the distillation processes with the SGHP integration concepts for heat recovery.

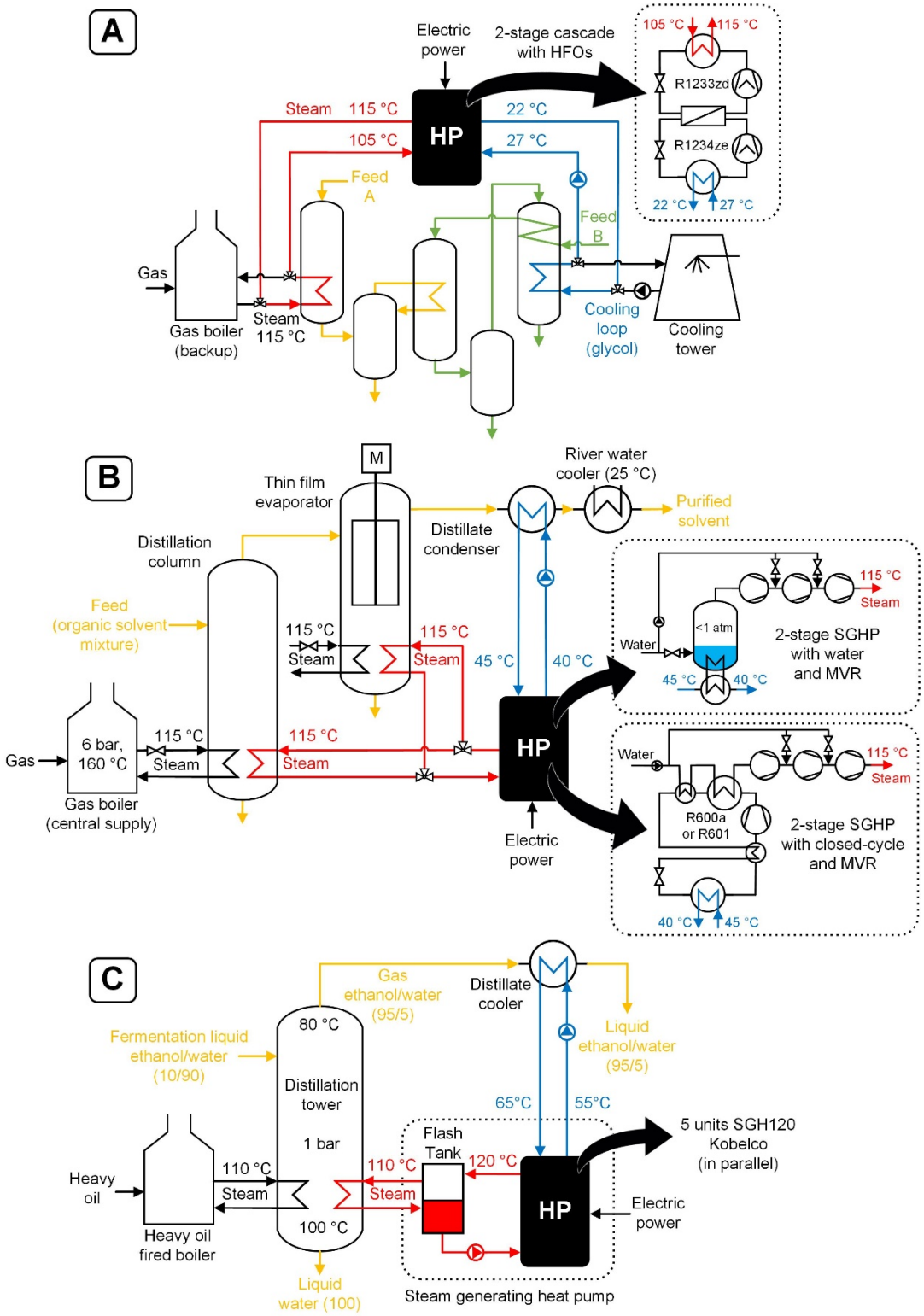

Figure 1: Principle flow diagrams of the case studies with the SGHP integration concepts. (A) Distillation process for an organic solvent of a Swiss biopharma company (SGHP proposal: 2-stage cascade with R1234ze/R1233zd), (B) Distillation process of an organic solvent in a Swiss chemical company producing vitamins (2-stage SGHP with water as refrigerant or closed-cycle heat pump with MVR), (C) Distillation process for bioethanol production at the Japanese manufacturer (Hokkaido Bioethanol Co., 2015) using 5 SGH120 units, adapted from (Kaida, 2019).

Case study A is a distillation process for a pharmaceutical product in a Swiss biopharmaceutical company (Figure 1, A). The company requires saturated steam at 110 °C (1.58 bar) for two parallel distillation process lines, each with 462 kW heating capacity running continuously over 24 hours (7'200 h/a). The goal is to replace the gas boiler with SGHPs. The cooling is currently met by a cooling tower using an ethylene glycol loop (27 °C/22 °C). Thus, two 462 kW heat pumps or one large 924 kW SGHP are needed. An attractive solution envisages a 2-stage cascade water-steam HTHP with screw compressors and synthetic low-GWP HFO refrigerants R1234ze(E) and R1233zd(E) from Ochsner (AT). A combined heat pump cycle with open mechanical vapor recompression (MVR) would be another option under investigation. Energy prices are 0.057 EUR/kWh for gas and 0.1 EUR/kWh for electricity. A high CO_2 levy of 92.5 EUR per ton of CO_2 has been in force in Switzerland since 2018 and will further increase to 115 EUR per ton of CO_2 from 2022.

Case study B is a chemical process for evaporating and regenerating an organic solvent for vitamin production. Figure 1 (B) shows the simplified process diagram. A gas boiler in the energy center produces slightly superheated steam of 6 bar, which is expanded in the distillation plant to the operating pressure of 1.8 bar (115 °C) for heating the distillation column and a downstream thin-film evaporator for evaporation of the residual solvent. The heating capacity is about 2'500 kW. The condensers and coolers are operated with river water of about 25 °C. A large-scale SGHP is being considered for heat recovery, using the heat of solvent condensation as a heat source (45 °C) and generating 115 °C (1.74 bar) steam on the hot side for evaporation (temperature lift 70 K). One proposed solution is a 2-stage heat pump using water as a refrigerant with an intermediate pressure vessel and downstream MVR. A challenge is the low suction pressure of approx. 96 mbar at 45 °C and correspondingly high volume flow (approx. 46'000 m3/h, 3'000 kg/h). Roots blowers in two stages and MVR technology are being considered. Possible manufacturers are Piller (DE) or EPCON (NO). An alternative concept envisages a 2-stage heat pump with a natural hydrocarbon refrigerant (e.g., iso-butane R600a, n-butane R600, or n-pentane R601) followed by a multistage MVR Mitsubishi MHPS (DE) or Turboden (IT) can offer.

Case study C is based on Kaida (2019) and describes the integration of SGHPs into the process of the bioethanol producer Hokkaido Bioethanol Co. (2015) in Japan. Figure 1 (C) illustrates the distillation process and SGHP integration. During distillation, steam is used to separate the aqueous ethanol solution. The evaporated ethanol is cooled and liquefied in a distillate cooler. In the conventional plant, a heavy oil-fired boiler supplies 120 °C steam. In the new heat pump system, the waste heat from the distillation process is recovered in the distillate cooler as a heat source for 5 units of SGH120 from Kobelco (JP) and converted from 65 °C to saturated steam at 120 °C (temperature lift 55 K). The SGHPs simultaneously provide cooling for the condenser and heating for the reboiler at the bottom of the distillation tower. The installed heating capacity is about 1'850 kW, and the operating pressure in the distillation tower is at atmosphere.

Table 1 summarizes the characteristics of the three case studies, including temperature conditions at the heat sources/sinks, heating capacities, energy prices, CO_2 tax, CO_2 emissions, and CO_2 emission factors. Electricity and fuel prices depend on location and energy supplier. The electricity prices of case studies A and B are close to the average price for large consumers in Switzerland of 0.11 EUR/kWh (Statista, 2022). The gas price of Case study A is equal to the average gas price of large industrial companies (Type X) in Switzerland of 0.057 EUR/kWh, including CO_2 tax (WBF, 2022). In Case study B, the gas price is lower than the average due to special contracts with the gas supplier. This results in an electricity-to-gas price ratio of 1.75 and 2.55, respectively. The Japanese prices in Case study C have been converted to Euro and are higher than the Swiss. In addition, the CO_2 emissions factor for electricity (0.681 $kgCO_2/kWh$) (Hokkaido Bioethanol Co., 2015) is substantially higher. Case studies A and B buy high shares of renewable electricity.

Table 1. Conditions and input parameters of the case studies

			Case study A	**Case study B**	**Case study C**
			Swiss Biopharma company	**Swiss Chemical company**	**Japanese Bioethanol manufacturer**
Heat pump conditions	*Symbol*	Unit	**Distillation of organic solvent**	**Distillation of organic solvent**	**Distillation of bioethanol**
Heat sink outlet temperature	$T_{h,out}$	°C	115 (steam)	115 (steam)	120 (2 bar) (steam)
Heat source inlet temperature	$T_{c,in}$	°C	27 (water)	45 (water)	65 (water loop)
Temperature lift	ΔT_{lift}	K	88	70	55
Heating capacity	$\dot{Q}_h$	kW	950 (2 lines)	2'500	1'850 (5 SGHP120 units)
Fuel prices, CO_2 tax, CO_2 emissions					
Fuel (gas, oil) price	c_{fuel}	EUR/kWh	0.057	0.042	0.071
Electricity price	c_{el}	EUR/kWh	0.100	0.107	0.131
CO_2 tax	$c_{CO2\,tax}$	EUR/tCO_2	92.5	92.5	3.0
CO_2 emissions factor electricity	$f_{CO2\,el}$	$kgCO_2/kWh$	0.0157	0.031	0.681
CO_2 emissions factor fuel	$f_{CO2\,fuel}$	$kgCO_2/kWh$	0.201	0.201	0.250
CO_2 emissions ratio el/fuel	$e_{CO2,el/fuel}$	-	0.08	0.15	2.73
Electricity-to-fuel price ratio	$p_{el/fuel}$	-	1.75	2.55	1.85

3. HEAT PUMP MODEL BASED ON COP FIT CURVES

The COP is the main parameter to describe the efficiency of a vapor compression heat pump. The Carnot COP ideally defines it by dividing the temperature of the heat sink (process heat demand) ($T_{h,out}$) by the temperature lift between the sink and the source ($\Delta T_{lift} = T_{h,out} - T_{c,in}$). A first COP estimate is obtained by multiplying the COP_{Carnot} by the 2nd Law efficiency (η_{2nd}). A 2nd Law efficiency of 0.45 is reasonable for several industrial HTHPs, as shown by (Arpagaus, 2018, 2020; Arpagaus et al., 2018) (Eq. 1), resulting in COPs between 2 and 6 depending on ΔT_{lift}. Eq. (2) describes the corresponding power function of the COP fit with an R^2 value of 0.78.

Based on regression analysis of literature data, Schlosser et al. (2020a) and Jesper et al. (2021) developed a more advanced fitting formula for water/water VHTHPs using HCFO, HFC, or HFO refrigerants as a function of $T_{h,out}$ and ΔT_{lift} (Eq. 3). Moreover, Schlosser et al. (2020 & 2020) presented a COP correlation explicitly for water/steam VHTHPs (Eq. 4).

$$COP = \eta_{2nd} \cdot COP_{Carnot} = 0.45 \cdot \left(T_{h,out} + 273.15\right)/\Delta T_{lift} \text{ with } \Delta T_{lift} = \left(T_{h,out} - T_{c,in}\right) \quad \text{Eq. (1)}$$

$$COP = a \cdot {\Delta T_{lift}}^{b} = 68.455 \cdot {\Delta T_{lift}}^{-0.76} \text{ with } R^2 = 0.78 \quad \text{Eq. (2)}$$

$$COP = a \cdot \left(\Delta T_{lift} + 2 \cdot b\right)^{c} \cdot \left(T_{h,out} + b\right)^{d} = 1.9118 \cdot \left(\Delta T_{lift} + 2 \cdot 0.044189\right)^{-0.89094} \cdot \left(T_{h,out} + 0.044189\right)^{0.67895}$$

valid between $80\ °C \leq T_{h,out} \leq 160\ °C$ and $25\ K \leq \Delta T_{lift} \leq 95\ K$ with $R^2 = 0.95$ Eq. (3)

$$COP = a \cdot \left(\Delta T_{lift} + 2 \cdot b\right)^{c} \cdot \left(T_{h,out} + b\right)^{d} = 8.898 \cdot \left(\Delta T_{lift} + 2 \cdot 0.042214\right)^{-0.52137} \cdot \left(T_{h,out} + 0.042214\right)^{0.16395}$$

valid between $110\ °C \leq T_{h,out} \leq 160\ °C$ and $25\ K \leq \Delta T_{lift} \leq 70\ K$ with $R^2 = 0.77$ Eq. (4)

Figure 2 shows the variation of COP with temperature lift (ΔT_{lift}) using the COP fit curves (Eqs. 2, 3, and 4). In addition, 32 data points from industrial SGHPs are plotted based on quotes from European heat pump suppliers and data from the Japanese Kobelco SGH120 and SGH165 models (Kaida, 2021, 2019). The power function $COP = 52.94 \cdot {\Delta T_{lift}}^{-0.716}$ (black line) (Eq. 5) represents the 32 data points and COP correlations well ($R^2 = 0.8826$). The COP decreases from about 3.8 to 2.0 with an increase in temperature lift from 40 to 100 K. In this study, this power function (Eq. 5) is used for the COP calculation of the case studies. Overall, a temperature lift of up to about 100 K seems technically feasible.

$$COP = 52.94 \cdot {\Delta T_{lift}}^{-0.716} \text{ with } R^2 = 0.8826 \quad \text{Eq. (5)}$$

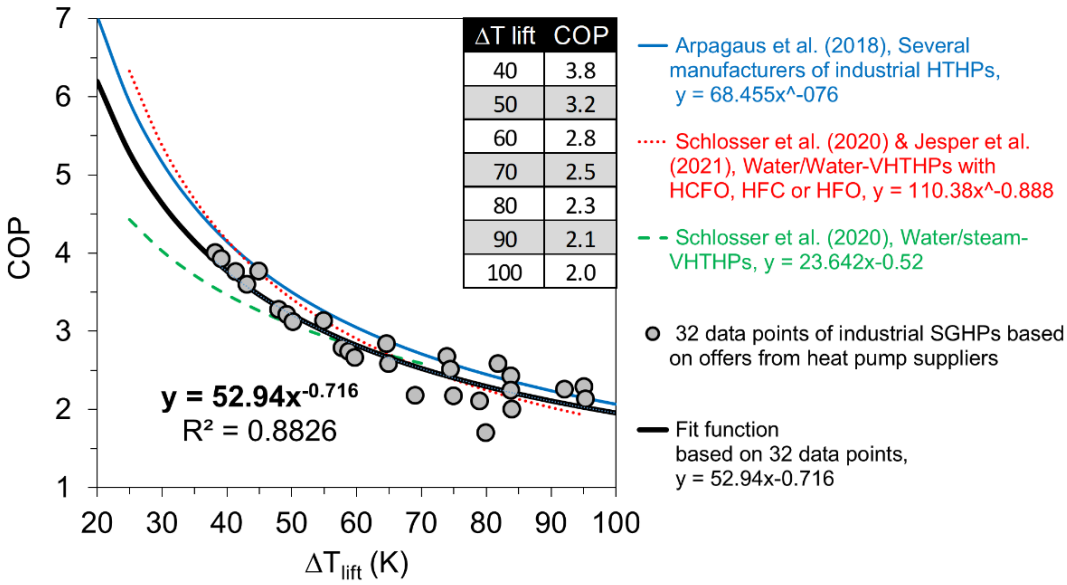

Figure 2: COP fit curves for industrial HTHPs from literature and SGHPs from 32 data points

A more detailed thermodynamic heat pump model could consider the influence of refrigerant (e.g., HFOs, NH_3, CO_2, R600), compressor efficiency (e.g., screw, piston, turbo compressors), cycle optimizations (e.g., multistage, economizer, MVR combination), temperature glide, capacity, etc. However, this is outside the scope of this study but could eventually lead to a more integrated techno-economic calculation tool.

While the efficiency of the heat pumps depends on the application (i.e., heat sink and source temperatures), a fixed efficiency of 90% (η_{fuel}) is assumed for fuel-fired (gas/oil) boilers (see average value in Table 2).

4. COST MODEL

A simple cost model was developed for the economic evaluation of the SGHP integration in the case studies. It is assumed that the gas(oil) boilers are already in operation today and that the investment is depreciated. The gas boilers remain for production reliability, redundancy, start-up operation, and cover peak loads. First, the investment costs of the industrial SGHPs are evaluated. Then, the operating costs are calculated considering efficiency and energy prices (gas, oil, electricity) and possible refunds of CO_2 taxes. Next, a maintenance factor is used to estimate the additional maintenance costs of the SGHPs. After that, the payback period of the heat pump investment is evaluated for decision. Finally, the discount rates are considered to calculate the discounted payback period.

4.1. Investment costs

The investment cost of an industrial SGHP is calculated by the specific investment cost and nominal heating capacity. Local installers or heat pump suppliers are possible information sources on investment costs. Other good sources of cost data are peer-reviewed publications, like Wolf (2017), Alstone et al. (2021), and (Grosse et al., 2017), who published cost functions presented in Eq. (6) to (8) with the capacity ranges.

$$c_{inv,HP} = 1'521 \cdot \dot{Q}_h^{-0.363}$$ *up to 200 kW (residential sector)* (Wolf, 2017) Eq. (6)

$$c_{inv,HP} = 1'658 \cdot \dot{Q}_h^{-0.174}$$ *up to 10 MW* (Alstone et al., 2021) Eq. (7)

$$c_{inv,HP} = 352 \cdot \dot{Q}_h^{-0.122}$$ *for 1 to 10 MW, $\dot{Q}_h$ in MW* (Grosse et al., 2017) Eq. (8)

According to Wolf (2017), the specific investment costs for industrial heat pumps with a heating capacity above 500 kW range from 250 to 700 EUR/kW. Fleckl et al. (2015) evaluated similar investment costs of about 300 to 800 Eur/kW in industrial heat recovery processes. 250 to 900 EUR/kW was also estimated by Vieren et al. (2021) for heat pumps larger than 500 kW. Meyers et al. (2018) reported 300 to 900 EUR/kW for industrial heat pumps larger than 100 kW. Schlosser, Jesper, et al. (2020) and Jesper et al. (2021) used 420 EUR/kW for a 300 kW heat pump.

Figure 3 illustrates the cost functions (Eq. 6 to 8) and shows that the specific investment costs decrease with increasing heating capacity (system size). Additionally, 17 data points for industrial SGHPs are shown, based on pricing information from heat pump suppliers. These prices are indicative and depend on the sales distribution channels. The power function (black line) (Eq. 9) represents the 17 data points and estimates the investment costs in this study.

$$c_{inv,HP} = 3'157 \cdot \dot{Q}_h^{-0.322}$$ 100 to 2'500 kW, R^2=0.4129 (this study) Eq. (9)

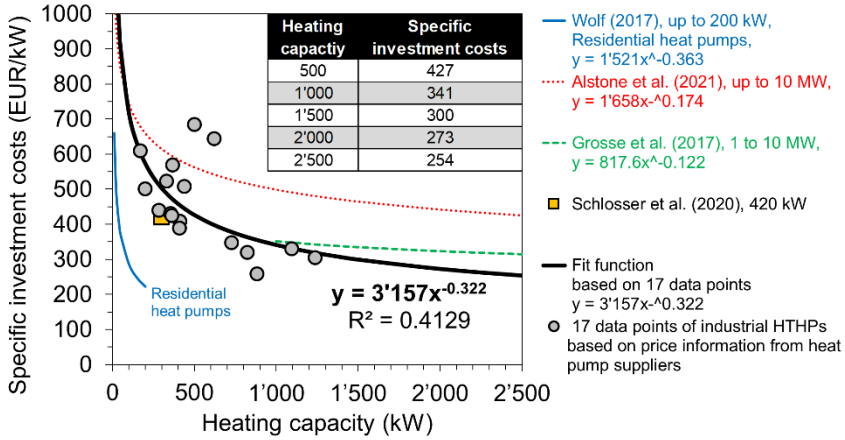

Figure 3: Specific investment cost for industrial HTHPs and SGHPs (excluding planning and integration)

The specific investment costs include the capital costs of the heat pump itself but not the costs associated with planning, integration, and labor. Therefore, a cost multiplication factor ($f_{inv,hp}$) is usually applied to account for planning and integration. A factor of 2.0 is applied in Case Study A according to Wolf (2017) and a factor of 3.0 in Case Study C because of an additional flash tank and better fit to about 3.5 years payback reported by (Kaida, 2019). In Case Study B, a factor of 4.0 is used to account for all project costs in a rather complex installation environment (Kosmadakis et al., 2020). Finally, the investment cost for the SGHP (C_{inv}) follows from Eq. (10) and considers the multiplication factor ($f_{inv,hp}$).

$$C_{inv,HP} = c_{inv,HP} \cdot \dot{Q}_h \cdot f_{inv,hp}$$ Eq. (10)

In comparison, industrial natural gas boilers have specific investment costs of about 60 to 80 EUR/kW (500 to 3'600 kW range) (BMVBS, 2012; Grosse et al., 2017; The UK 2050 Calculator, 2010), which is about 4 to 6 times lower than SGHPs.

4.2. Operating cost and net annual cost savings

The operating costs for the SGHP include the electricity cost for running the heat pump calculated by the electricity consumption and the electricity price and a fixed annual maintenance factor based on the capital cost. The energy prices (electricity, gas, oil) vary depending on the case study location and are provided in Table 1. For simplicity, energy price growth rates are neglected, and constant operating conditions are assumed at the nominal heating capacity.

Eq. (11) is used to calculate the annual fuel cost savings (C_{fuel}), Eq. (12) calculates the annual electricity cost (C_{el}) to operate the HTHP, Eq. (13) calculates the annual additional maintenance cost for the HTHP ($C_{maintain}$), and Eq. (14) determines the carbon tax refund (C_{CO2}) due to the reduction of CO_2 emissions.

$$C_{fuel} = \left(\dot{Q}_h \cdot t \cdot c_{fuel}\right)/\eta_{fuel} \quad \text{Eq. (11)}$$

$$C_{el} = \left(\dot{Q}_h \cdot t \cdot c_{el}\right)/COP \quad \text{Eq. (12)}$$

$$C_{maintain} = f_{maintain} \cdot C_{inv,hp} \quad \text{Eq. (13)}$$

$$C_{CO2} = \dot{m}_{CO2,savings} \cdot c_{CO2\,tax} \quad \text{Eq. (14)}$$

where $\dot{Q}_h$ is the heating capacity, t the annual operating time of the HTHP and boiler, c_{fuel} the fuel (gas, oil) price, c_{el} the electricity price, η_{fuel} the efficiency of the gas(oil)-fired boiler, COP the efficiency of the HTHP, $f_{maintain}$ the maintenance factor, $c_{CO2\,tax}$ the carbon tax, and $\dot{m}_{CO2,savings}$ the annual CO2 emissions savings by replacing fuel energy with electrical energy. Finally, Eq. (15) describes the net annual cost savings ($C_{savings}$) (in EUR/year) by use of the HTHP replacing the fuel-driven boiler.

$$C_{savings} = C_{fuel} - C_{el} - C_{maintain} + C_{CO2} \quad \text{Eq. (15)}$$

Table 2 also shows the typical lifetime for heat pumps and different interest rates (discount rates) for investment decisions. A lifetime of 20 years seems most reasonable. Interest rates range from 5% to 15%, depending on the investor's risk tolerance (see the discussion in Section 4.3 on the payback period). Typical annual operating times are between 4'000 to 8'400 hours for heat pumps, which agrees with various techno-economic studies presented in the literature review (Table 2). Distillation processes are typically operated continuously with a readily available heat source and sink with 6'000 and more operating hours per year (Case study A: 7'200 h, B: 8'400 h, C: 8'400 h). The annual maintenance cost for the SGHP was fixed to 4% of the investment cost as an average value compared to various literature (Table 2). The CO_2 tax also depends on the location, region, and country (The World Bank, 2022). A heat pump may even be exempted from the CO_2 tax as using electricity often does not require paying a tax on the CO_2 emission of the electricity mix consumed.

Table 2. Literature values as input parameters for payback calculation

Reference	Gas boiler efficiency (η_{fuel})	Interest rate (discount rate) (i)	Operating hours (t)	System lifetime (T)	Maintenance factor (% of capital cost) ($f_{maintain}$)
	[%]	[%]	[h]	[years]	[%]
Schlosser, Wiebe, et al. (2020)	87	12	6'000	20	2.5
Schlosser, Jesper, et al. (2020)	96	7	6'000	20	1.5
Jesper et al. (2021)	96	7	3'500	20	1.5
Kosmadakis et al. (2020)	90	5	7'000	20	4
Meyers et al. (2018)	n.a.	6.4	2000	20	2.5
Wang and Zhang (2019)	n.a.	10	7'000	15	6
Arnitz et al. (2018)	90	n.a.	3'500	n.a.	n.a.
Wolf (2017)	n.a.	15	4'000	20	2.5
Vieren et al. (2021)	n.a.	8.4	n.a.	15	n.a.
Brückner et al. (2015)	n.a.	10	4'000	25	n.a.
Cox et al. (2022)	80	15	7'300	20	5
Zuberi et al. (2018)	n.a.	10.5	n.a.	15	n.a.
Range	**80 to 96**	**5 to 15**	**2'000 to 7'300**	**15 to 25**	**1.5 to 6**
Average values	**90**	**10**	**5'410**	**20**	**3.2**

4.3. Payback period

Payback calculations are commonly used in practice for financial investment decisions. For example, the simple (static) payback period (PP) calculated according to Eq. (16) assesses the trade-off between the investment costs versus the expected annual cost savings resulting from the heat pump investment. The Discounted payback period (DPP) is simply the period after which the cumulative discounted cash inflows cover the initial investment (Bhandari, 2009). DPP can therefore be interpreted as a period beyond which a project generates economic profit, whereas PP gives a period beyond which a project generates accounting profit. The shorter the payback period, the more economical the project. If the annual net savings are assumed constant each year, the DPP is calculated by Eq. (17) (Bhandari, 2009; Kosmadakis et al., 2020) using a risk-adjusted discount rate (i).

$$Payback\ period\ (PP) = {C_{inv}}/{C_{savings}} \quad \text{Eq. (16)}$$

$$Discounted\ payback\ period\ (DPP) = {-ln\left(1 - \left(C_{inv} \cdot i / C_{savings}\right)\right)}/{ln(1+i)} \quad \text{Eq. (17)}$$

A discount rate of 10% was chosen in Case study A to reflect the risk and uncertainty associated with the new SGHP technology. In Case study B, a discount rate of 15% was selected because it is a high-risk project where a new SGHP is directly integrated into the distillation process with a high heating capacity of 2'500 kW. In Case study C, 5% was chosen because SGH120 heat pumps from Kobelco (JP) have been commercially available in Japan since 2011, and there are some reference cases with practical experience with the same technology (Hokkaido Bioethanol Co., 2015).

Payback periods demanded by the industry are typically in the range of 2 to 5 years (De Boer et al., 2020). For payback periods over 5 years, there is a discussion about how high the residual risk is for the product or the impact on the process.

4.4. CO_2 emissions reduction and energy savings

Compared with natural gas, which has an emission factor of 0.201 kg CO_2 per kWh of useful heat (BAFU, 2022), the electricity mix produced in Switzerland is relatively low in emissions, with about 57% hydropower (0.0296 kg CO_2/kWh) (FOEN, 2022). By contrast, the average consumer electricity mix is more emission-intensive with 0.128 kg CO_2/kWh (FOEN, 2022) due to the more fuel-based imported electricity. For case studies A and B, the CO_2 emission factors for electricity are only 0.0157 and 0.031 kgCO_2/kWh, respectively, because a renewable electricity mix is purchased.

In contrast, Case study C in Japan has a CO_2 emissions factor for electricity of 0.681 kgCO_2/kWh and 0.250 kgCO_2/kWh for heavy oil, resulting in a ratio of 2.73 compared to only 0.08 and 0.15 in the Swiss case studies. The CO_2 emission reduction by replacing a fuel-driven boiler with an industrial SGHP is calculated according to Eq. (18):

$$E_{CO2,reduction} = \dot{Q}_h \cdot t \cdot \left(\frac{f_{CO2,fuel}}{\eta_{fuel}} - \frac{f_{CO2,el}}{COP}\right) \quad \text{Eq. (18)}$$

where η_{fuel} is the efficiency of the fuel-fired boiler, and $f_{CO2,fuel}$ and $f_{CO2,el}$ are the CO_2 emissions factor for fuel and electricity. For the fuel-fired boilers, an efficiency of 0.9 is assumed, the average value of compared literature values (Table 2).

A further reduction in CO_2 emissions is controlled by a CO_2 tax on fossil fuels, which currently accounts for 92.5 EUR/tCO_2 in Switzerland and only around 3 EUR/tCO_2 in Japan. The CO_2 tax creates incentives for economical energy consumption and the increased use of low-CO_2 energy sources. Together with a more favorable electricity to fuel price ratio ($p_{el/fuel}$) (Case studies A and B Switzerland: about 1.75 to 2.55, Case study C Japan: 1.8) this can significantly increase the applicability (market attractiveness) of industrial SGHPs.

5. RESULTS AND DISCUSSION

5.1. Payback period, energy savings, and CO_2 emissions reduction

Table 3 shows the results of the economic analyses for all case studies. The calculations lead to payback periods (PP) of 2.9, 6.4, and 3.2 years, which means that Case Study A and C would be cost-effective under the current assumptions (payback periods < 3 to 5 years). However, it is observed that the financial evaluation is highly dependent on the case study input parameters. End users are exposed to uncertainties in the boundary conditions like energy and CO_2 prices that determine the business case for an industrial SGHP.

Table 3. Case study results: Payback period, energy savings, and CO_2 emissions reduction

	Symbol	Unit	Case A	Case B	Case C		Ref
Fit curves							
COP from Eq. (5)	COP		2.15	2.53	3.00		2.53
Specific investment costs from Eq. (9)	$c_{inv,hp}$	EUR/kW	347	254	280		341
Other input parameters							
Annual operating time	t	h/a	7'200	8'400	8'400		7'200
Efficiency of fuel boiler	η_{fuel}	-	0.90	0.90	0.90		0.90
Maintenance factor (on capital costs)	$f_{maintain}$	-	0.04	0.04	0.04		0.04
Cost multiplication factor for planning & integration	$f_{inv,hp}$	-	2.0	4.0	3.0		2.0
CO_2 emissions reduction and energy savings							
Annual CO_2 emissions reduction	$E_{CO2,reduction}$	tCO_2/a	1'478	4'432	785		1'243
Annual CO_2 emissions reduction	-	-	**97%**	**95%**	**18%**		**77%**
Annual energy savings	$E_{savings}$	MWh/a	4'412	15'025	12'093		5'151
Annual energy savings	-	-	**58%**	**64%**	**70%**		**64%**
Economic calculations							
Investment costs	$C_{inv,hp}$	kEUR	659	2'542	1'554		683
Annual fuel cost savings	C_{fuel}	kEUR/a	433	980	1'226		456
Annual electricity costs	C_{el}	kEUR/a	319	889	678		285
Annual heat pump maintenance costs	$C_{maintain}$	kEUR/a	26	102	62		27
Annual CO_2 tax compensation	C_{CO2}	kEUR/a	137	410	2		115
Annual cost savings	$C_{savings}$	kEUR/a	225	399	488		259
Payback							
Discount rate	i	-	0.10	0.15	0.05		0.10
Payback period	PP	years	**2.9**	**6.4**	**3.2**		**2.6**
Discounted payback period	DPP	years	**3.6**	**22.2**	**3.6**		**3.2**

Case Study C shows a PP of 3.2 years, made possible in part by government subsidies (Kaida, 2019) and set accordingly in this study with a cost multiplication factor for planning and integration of 3.0. The high DPP of 22.2 years in Case study B is significantly worse than in Case Studies A and C, although the COP is higher than in Case Study A. This situation is due to the high planning and integration costs (multiplication factor of 4.0), the low gas price of 0.042 EUR/kWh, and the high discount rate of 15%, making the integration of an industrial SGHP unfavorable. Therefore, Case Study B may be classified as a non-profitable high-risk project with a DPP even longer than the expected average SGHP lifetime of 20 years (Table 2). However, an investment of about 1 million Euros per MW of heating capacity seems a plausible first estimate for a large-scale industrial SGHP.

The economics of an industrial SGHP is highly influenced by the temperature lift, which determines the COP and electricity consumption and thus the operating costs of the heat pump, as well as the avoided fuel consumption. The COP varies between 2.15 and 3.0 obtained by the fit function (Eq. 5). Case study A has the highest temperature lift of 88 K and consequently the lowest COP of 2.15. This outcome is reflected in lower annual energy savings comparatively. The other two Case Studies B and C achieve significant annual energy savings of 64% and 70%, respectively.

Replacing gas and oil boilers with electrically driven industrial SGHPs leads to significant CO_2 reduction and fossil fuel savings. The application examples show that annual CO_2 emissions can be drastically reduced by 97% and 95% in the Swiss Case Studies A and B, respectively, using renewable electricity. In comparison, the reduction is only 18% in Case Study C because the CO_2 emission factor of electricity in Japan is comparatively high because of the long-term shutdown of nuclear power plants after the Great Tohoku earthquake and subsequent tsunami in Eastern Japan in 2011.

5.2. Sensitivity analysis of payback time for a reference case (Ref) at 45 °C/115 °C (heat source/sink)

A sensitivity analysis was performed to investigate the uncertainty of the model result (payback period) when input parameters change. This study serves primarily as a stress test for the modeled assumptions and leads to value-added insights. For this purpose, an economic reference case (Ref) with a 45 °C heat source and 115 °C heat sink (lift of 70 K, COP of 2.53), 1'000 kW heating capacity, PP of 2.6 years, and DPP of 3.2 years were used. The other input parameters are the same as in Case Study A (see column Ref in Table 3 and Figure 4), except for the CO2 emission factor, the average Swiss consumer electricity mix of 0.128 $kgCO_2$/kWh (FOEN, 2022) was applied. All input factors of the model were individually varied starting from the (Ref) conditions in a range from -50% to +50% (or variation factor 0.5 to 1.5), while the other parameters were kept constant. Figure 4 shows the sensitivity analysis results for the payback period in years. The results are intuitive, but one can now identify the most important influencing parameters.

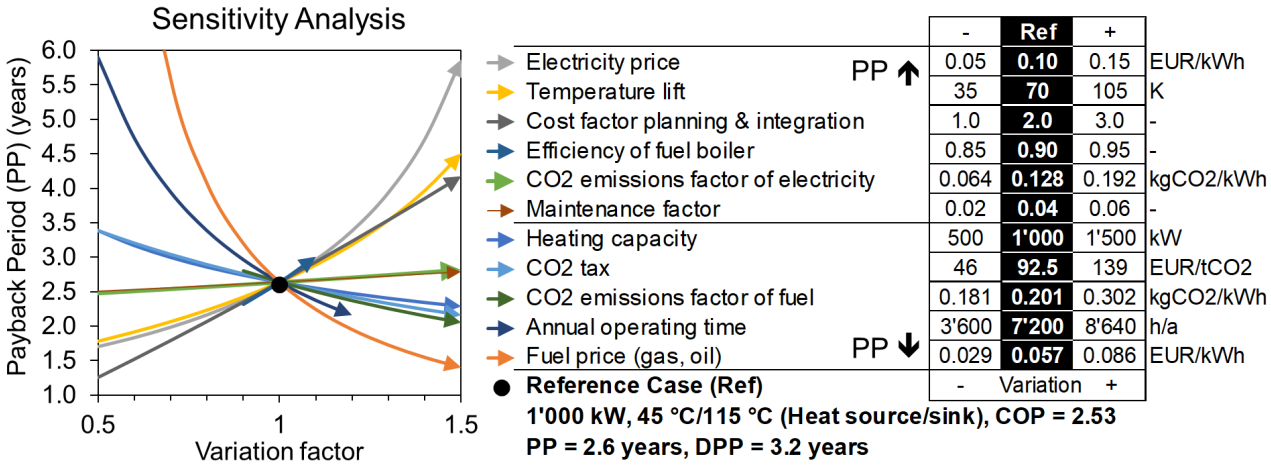

	-	Ref	+	
Electricity price (PP ↑)	0.05	**0.10**	0.15	EUR/kWh
Temperature lift	35	**70**	105	K
Cost factor planning & integration	1.0	**2.0**	3.0	-
Efficiency of fuel boiler	0.85	**0.90**	0.95	-
CO2 emissions factor of electricity	0.064	**0.128**	0.192	kgCO2/kWh
Maintenance factor	0.02	**0.04**	0.06	-
Heating capacity	500	**1'000**	1'500	kW
CO2 tax	46	**92.5**	139	EUR/tCO2
CO2 emissions factor of fuel	0.181	**0.201**	0.302	kgCO2/kWh
Annual operating time	3'600	**7'200**	8'640	h/a
Fuel price (gas, oil) (PP ↓)	0.029	**0.057**	0.086	EUR/kWh
	-	Variation	+	

Figure 4: Sensitivity analysis of the payback period for a reference case (Ref) at 45 °C/115 °C heat source/sink and 1'000 kW heating capacity (CO_2 emission electricity 0.128 $kgCO_2$/kWh, other input factors like in Case Study A)

The sensitivity analysis indicates that the payback period is strongly responsive to a change in electricity and fuel prices. The payback time (PP ↓) is reduced mainly by higher fuel prices, annual operating time, CO_2 emissions factor of fuel, CO_2 tax, and heating capacity (economy of scale). Low gas prices and high electricity prices lead to unfavorable conditions for electrically driven heat pumps and are a significant barrier to the investment of industrial SGHPs. The case studies have electricity-to-fuel price ratios of 1.75, 2.55, and 1.81, respectively (Table 1). In European countries, electricity to fuel price ratios range from 1 to 5 (De Boer et al., 2020). An increasing CO_2 tax and the possible CO_2 compensation through the emission trading system in Europe increase the financial incentives for industrial SGHPs than investing in a gas boiler.

On the other hand, the payback period (PP ↑) increases with higher electricity prices, temperature lift, cost factor for planning and integration, and fuel boiler efficiency. More minor increase effects have the CO_2 emission factor of electricity and the maintenance factor. The greatest uncertainty for quantifying the payback period results from the planning and implementation multiplication factor, which depends on the complexity of the project and possible financially supporting subsidies.

For a better evaluation of the cost-effectiveness of industrial SGHP, the discounted payback period (DPP) is used as an indicator. Figure 5 shows the DPP as a function of the discount rate (i) and the temperature lift (ΔT_{lift}), which represents the application view of the heat source and sink. Under the assumptions of the reference case (Ref) (DPP of 3.2 at a 10% discount rate), cost-effective solutions are achieved for temperature lifts below 70 K (reddish colored conditions). Even with a discount rate of 15%, a temperature lift of 50 K is profitable.

Discounted Payback Period (DPP)

Temperature lift (K) \ Discount rate (-)	3.2	0.05	0.06	0.07	0.08	0.09	**0.10**	0.11	0.12	0.13	0.14	0.15
30		1.8	1.8	1.9	1.9	1.9	1.9	2.0	2.0	2.0	2.1	2.1
40		2.0	2.0	2.1	2.1	2.1	2.2	2.2	2.3	2.3	2.3	2.4
50		2.3	2.3	2.3	2.4	2.4	2.5	2.5	2.5	2.6	2.6	2.7
60		2.5	2.6	2.6	2.7	2.7	2.8	2.8	2.9	3.0	3.0	3.1
70		2.9	3.0	3.0	3.1	3.1	**3.2**	3.3	3.4	3.4	3.5	3.6
80		3.3	3.4	3.5	3.6	3.7	3.8	3.9	4.0	4.1	4.2	4.3
90		3.9	4.0	4.1	4.2	4.4	4.5	4.6	4.8	4.9	5.1	5.3
100		4.7	4.9	5.0	5.2	5.4	5.6	5.8	6.0	6.3	6.5	6.9

Figure 5: Discounted Payback Period (DPP) as a function of discount rate and temperature lift for the (Ref) Case

5.3. Technical feasibility of SGHP case studies

Furthermore, the technical feasibility of the SGHP case studies is evaluated. There is a limited number of SGHP manufacturers, mainly from Japan and Europe. Table 4 shows a non-exhaustive list of industrial SGHPs currently on the market, proving heat supply temperatures over 100 °C. The list is structured by maximum supply temperatures, manufacturer, product, refrigerant, cycle type, and heating capacity (updated from Arpagaus et al., 2018). The cycles are subcritical, transcritical, or subcritical combined with MVR. Heating capacities range from about 100 kW to the MW range. SGHP case studies can look at the products listed and contact the manufacturers for decision-making, as integration is primarily tailor-made and customer-specific. The main evaluation criteria for SGHP integration are the achievable heating capacity and heat source and sink temperatures, the choice of refrigerant (natural or synthetic), and open/closed cycle/combined concepts (see examples in Figure 1).

Suitable vapor compressors are needed to integrate SGHPs with an open cycle and water or as a combined two-stage cycle with MVR (Figure 1, B). Table 5 provides a non-exhaustive list of possible vapor compressors from several suppliers (updated from Bless et al., 2022). For use in SGHPs, the vapor compressors must preferably provide high volume flows at low suction pressure, high pressure ratios to reduce the number of compression stages, temperature resistance (e.g., need for water injection), and long-term corrosion resistance. For example, Piller's VapoFans operate down to a minimum suction pressure of 200 mbar, which corresponds to a potential heat source of 60 °C. Therefore, it is technically possible to compress from 60 °C to 110 °C in 5 stages with a 10 K lift per stage. Overall, the availability of SGHPs and vapor compressor products (Tables 4 and 5) and technical clarifications with the suppliers show that all three case studies are technically feasible with the integration concepts provided in Figure 1.

Table 4. Industrial SGHPs providing heat supply temperatures > 100 °C, updated from Arpagaus et al. (2018)

Manufacturer (Country)	Product	Refrigerant	Cycle type	Heating capacity	T_supply (before MVR)
Kobelco (JP)	SGH 165	R245fa + R134a + R718	Subcritical + MVR	Up to 624 kW	175 °C (120 °C)
Mitsubishi MHPS (DE)	D-GWP	R600a + R718 (Iso-Butane + Water)	Subcritical + MVR	4.3 MW	174 °C (130 °C)
Heaten (NO)	HeatBooster	HFOs, e.g. R1336mzz(Z)	Subcritical	1 to 6 MW	165 °C
SPH Process Heat (DE)	ThermBooster	HFOs, e.g. R1336mzz(Z), or hydrocarbons	Subcritical	400 kW to 1 MW	160 °C
Siemens Energy (DE)	Large-scale	HFOs, e.g. R1233zd(E)	Subcritical	4 to 70 MW	150 °C
MAN Energy (CH)	ETES	R744 (CO2)	Transcritical	5 to 50 MW	150 °C
ECOP (AT)	Rotational heat pump	Nobel gas (Argon, Krypton)	Joule cycle	700 kW	150 °C
Friotherm (CH)	Tailor-made steam HP	HFOs, e.g. R1233zd(E)	Subcritical	Up to 25 MW	137 °C
Ochsner (AT)	IWWDSS R2R3b	Öko (R245fa) or R1233zd(E)	Subcritical	60 to 750 kW	130 °C
Ochsner (AT)	IWWHS ER3b TWIN	HFOs, e.g. R1233zd(E)	Subcritical	TWIN 2.4 MW	130 °C
MHI Thermal Systems (JP)	ETW-S	R134a	Transcritical	627 kW	130 °C
Combitherm (DE)	HWW	R245fa or R1233zd(E)	Subcritical	60 to 750 kW	120 °C
Kobelco (JP)	SGH 120	R245fa or HFOs, e.g. R1224yd(Z)	Subcritical	370 kW	120 °C
Mayekawa (JP)	Eco Sirocco	R744 (CO2)	Transcritical	110 kW	120 °C
Fuji Electric (JP)	Fuji HP	R245fa	Subcritical	30 kW	120 °C
Turboden(IT)	LHP30, LHP150	R601 + R718 (n-Pentane + Water)	Subcritical	2.7 MW, 14.4 MW	115 °C
Engie (DE)	Thermeco2 HHR	R744 (CO2)	Transcritical	45 kW to 1.2 MW	110 °C
Oilon (FI)	ChillHeat P60 to P450	R134a or R1234ze(E)	Subcritical	30 kW to 1 MW	100 °C

Table 5. Vapor compressors for potential use in SGHPs with MVR application, updated from Bless et al. (2022)

Manufacturer (country)	Type	Remarks	Capacity, suction pressure	Temperature	Mass/volume Flow
Piller (DE)	Multi-stage MVR blowers, VapoFan 2-stage	Water injection, efficiency up to 86%	Up to 5 MW_el, VapoFan 90 kW_el, minimum suction 200 mbar, temperature lift 10 K per stage	up to 140 to 150 °C	up to 400'000 kg/h, 200 to 5'000 kg/h (VapoFan)
EPCON (NO)	MVR-HP, IHP-MVR-4S-66, MVR fans in series, MVR roots blowers	Open and closed cycles, distillation processes	0.65 to 4.5 MW_th, 50 to 1'250 kW_el, minimum suction 200 mbar	98, 112 to 150 °C	up to 6'600 kg/h
AERZEN (CH)	Rotary blowers, GM 240S, DeltaBlower	Several 2-stage blowers in series	Minimum suction 300 mbar, discharge 2 bar	up to 120 °C	3'600 kg/h 15'000 m3/h
Continental Industrie (DE)	Multistage centrifugal blowers, Type 600	96 to 500 mbar feasible with turbo blowers	Suction 150 to 540 mbar, pressure increase 0.2 to 1.4 bar	up to 120 °C	13'000 to 45'000 m3/h
Hoffman & Lamson (by Gardner Denver) (USA)	Multistage centrifugal blowers	-	Minimum suction 500 mbar	-	3'400 to 70'100 m3/h air and other gases
Howden (CZ)	Roots blowers, Turbo blowers	Vapor compressor, MVR	2080 RGS-J (750 kW) 2022 RGS-J (653 kW)	up to 243 °C	13'000 to 46'000 m3/h 3'000 to 3'900 kg/h
Spilling (DE)	Pistons	30 to 100% control range	Suction 2 to 20 bar, discharge 35 to 65 bar	up to 280 °C	3'000 to 15'000 kg/h
Kaeser Kompressoren (CH)	Vapor recompression blowers OMEGA 83PB	Water injection, No multistage	Minimum suction 500 mbar, discharge 2 bar	up to 120 °C	5'580 to 10'000 m3/h
Atlas Copco (DE)	Screw compressors Series ZA6	Oil-free, air or water cooled	Customized solutions	-	up to 7'200 m3/h
Johnson Controls (EDF) (FR)	2-state radial compressor (PACO Prototyp TRL 6)	Water injection, parallel arrangement possible	110 kWel, 600 kW_th, minimum suction 600 mbar	up to 130 °C	about 2'500 m3/h
DBS (UK)	TurboClaw MVR	Protoype status	Capacity 500 kW, pressure ratio up to 1.8, temperature lift 15 to 25 K per stage	-	100 to 800 m3/h
ToCircle (NO)	Two phase rotary vane compressor with water injection	Protoype status	500 kW to 5 MW, pressure ratio up to 5.5, temperature lift 50 K per stage	-	1'000 to 8'000 m3/h

6. CONCLUSIONS

In this study, a cost model was developed to evaluate the cost-effectiveness of integrating steam-generating heat pumps (SGHP) into distillation processes. Three case studies from Switzerland and Japan were analyzed, and the integration concepts were designed along with the SGHP cycle, including an open cycle with water, a combined two-stage cycle with MVR, a two-stage cascade, and SGHP with a flash tank.

A COP-fit function was derived based on 32 data points from European and Japanese heat pump manufacturers to estimate the efficiency of the industrial SGHP. The correlation calculates a COP from about 3.8 to 2.0 when the temperature lift increases from 40 to 100 K.

The economic model calculates the payback period based on several case-specific input parameters, including energy prices (electricity, gas, oil), heat source and heat sink temperatures, heating capacity, operating time, maintenance factor, planning and integration cost factor, fuel boiler efficiency, CO_2 emission factors for electricity and fuel, CO_2 tax, and discount rate. The model's outputs are the investment cost and annual cost savings calculated from the annual fuel cost savings, electricity cost, maintenance cost, and CO_2 tax compensation. The application examples show significant annual energy savings of 58%, 64%, and 70%, and CO_2 emissions can be drastically reduced by 97% and 95% using renewable electricity and 18% in the case study in Japan.

The economic calculations lead to payback periods of 2.9, 6.4, and 3.2 years, which means two case studies would be cost-effective under the current assumptions (payback periods < 3 to 5 years). As a rule of thumb, the investment cost for industrial SGHPs, including planning and integration, is on the order of 1 million EUR per MW of heating capacity.

However, it should be noted that the financial evaluation is highly dependent on the individual case. A sensitivity analysis showed that the payback period is shortened mainly by higher fuel prices, annual operating time, fuel CO_2 emission factor, CO_2 tax, and heating capacity (economies of scale). A low ratio of electricity to gas prices is beneficial for SGHP integration. In addition, SGHP integration becomes more economical with higher CO_2 compensation and subsidies. Temperature lifts below 70 K appear to be profitable. Economic challenges arise at high temperature lifts above 70 K, low gas prices, and high discount rates.

Technical feasibility was positive for all three case studies, as commercial SGHP technologies and vapor compressors are available on the market. An overview of a non-exhaustive list of manufacturers is provided. A major challenge is the availability of steam compressors that offer high displacement at low suction pressure (corresponding to suitable temperatures of heat sources for heat recovery by SGHPs).

As a next step, more detailed discussions with manufacturers are necessary to clarify end-user-specific integration conditions. Future work could include integrating an advanced thermodynamic heat pump model that considers the influence of refrigerant, compressor efficiency, and cycle design. In addition, the techno-economic analysis can be applied to other case studies to obtain an initial feasibility check and cost estimate.

ACKNOWLEDGEMENTS

This work was performed in the research project DeCarbCH (DeCarbonisation of Cooling and Heating in Switzerland, www.sweet-decarb.ch) sponsored by the Swiss Federal Office of Energy's SWEET program (Call 1-2020) (SWiss Energy research for the Energy Transition).

REFERENCES

Alstone, A. P., Mills, E., Carman, J., & Cervantes, A. (2021). *Toward Carbon-Free Hot Water and Industrial Heat with Efficient and Flexible Heat Pumps*. Schatz Energy Research Center. http://schatzcenter.org/pubs/2021-heatpumps-R1.pdf

Arnitz, A., Rieberer, R., & Wilk, V. (2018). An analysis of heat pumps for industrial applications. *ISEC International Sustainability Energy Conference 2018, 3-5 October, 2018, Graz, Austria*, 520–527.

Arpagaus, C. (2018). *Hochtemperatur-Wärmepumpen: Marktübersicht, Stand der Technik und Anwendungspotenziale, 138 Seiten, ISBN 978-3-8007-4550-0 (Print), ISBN 978-3-8007-4551-7 (E-Book)*. VDE Verlag GmbH. https://www.vde-verlag.de/buecher/494550/hochtemperatur-waermepumpen.html.

Arpagaus, C. (2020). Industrial Heat Pumps - Supplier update, suitable refrigerants and application examples in food & steam generation. *A2EP Briefing: Advances in Industrial Heat Pumps, 3 September 2020*.

Arpagaus, C., Bless, F., Uhlmann, M., Schiffmann, J., & Bertsch, S. S. (2018). High temperature heat pumps: Market overview, state of the art, research status, refrigerants, and application potentials. *Energy*, *152*, 985–1010. https://doi.org/10.1016/j.energy.2018.03.166

BAFU. (2022). *CO2 -Emissionsfaktoren des Treibhausgasinventars der Schweiz, Faktenblatt, Januar 2022, Bundesamt für Umwelt BAFU*. https://www.bafu.admin.ch/dam/bafu/en/dokumente/klima/fachinfo-daten/CO2_Emissionsfaktoren_THG_Inventar.pdf.download.pdf/Faktenblatt_CO2-Emissionsfaktoren_01-2022_DE.pdf

BFE. (2021). *Energieverbrauch in der Industrie und im Dienstleistungssektor, Resultate 2020, July 2021, Bundesamt für Energie*.

Bhandari, S. B. (2009). Discounted Payback Period - Some Extensions. *Proceedings of ASBBS Annual Conference, Las Vegas, February 2009*, *16*(1), 1–10.

Bless, F., Arpagaus, C., & Bertsch, S. (2020). Theoretical investigation of high-temperature heat pump cycles for steam generation. *13th IEA Heat Pump Conference, May 11-14, 2020, Jeju, Korea, Postponed to 26-29 April 2021*, 1–9.

Bless, F., Arpagaus, C., Speich, M., & Bertsch, S. (2022). Electrification of Heat Generation in Industry: State of Technologies, Integration Examples, and Integration Barriers. *Young Energy Researchers Conference 2022 Electrification, 5. April 2022, Wels, Austria*, 1–14.

BMVBS. (2012). *Ermittlung von spezifischen Kosten energiesparender Bauteil-, Beleuchtungs-, Heizungs- und Klimatechnikausführungen bei Nichtwohngebäuden für die Wirtschaftlichkeitsuntersuchungen zur EnEV 2012, BMVBS-Online-Publikation, Nr. 08/2012*. https://www.bbsr.bund.de/BBSR/DE/veroeffentlichungen/ministerien/bmvbs/bmvbs-online/2012/ON082012.html

Brückner, S., Liu, S., Miró, L., Radspieler, M., Cabeza, L. F., & Lävemann, E. (2015). Industrial waste heat recovery technologies: An economic analysis of heat transformation technologies. *Applied Energy*, *151*, 157–167. https://doi.org/10.1016/j.apenergy.2015.01.147

Cox, J., Belding, S., & Lowder, T. (2022). Application of a novel heat pump model for estimating economic viability and barriers of heat pumps in dairy applications in the United States. *Applied Energy*, *310*(December 2021), 118499. https://doi.org/10.1016/j.apenergy.2021.118499

De Boer, R., Marina, A., Zühlsdorf, B., Arpagaus, C., Bantle, M., Wilk, V., Elmegaard, B., Corberan, J., & Benson, J. (2020). *Strengthening Industrial Heat Pump Innovation, Decarbonizing Industrial Heat, White Paper*.

Fleckl, T., Wilk, V., & Hartl, M. (2015). Effiziente Abwärmenutzung durch Hochtemperaturwärmepumpen in der Industrie. *Energietag 2015, Temperaturdifferenzen Als Energiequellen, Arbeitskreis Energie Der Österreichischen Physikalischen Gesellschaft, 31. August 2015, Wien*, 1–31. www.ak-energie.at/e20150831_review.shtml

FOEN. (2022). *Climate change: Questions and answers, 8. How climate-friendly is the Swiss energy supply? Federal Office for the Environment*. https://www.bafu.admin.ch/bafu/en/home/topics/climate/questions-answers.html

Grosse, R., Christopher, B., Stefan, W., Geyer, R., & Robbi, S. (2017). Long term (2050) projections of techno-economic performance of large-scale heating and cooling in the EU. In *Publications Office of the European Union* (Vol. EUR28859, Issue EUR28859). https://doi.org/https://doi.org/10.2760/24422

Hansen, K. (2019). Decision-making based on energy costs: Comparing levelized cost of energy and energy system costs. *Energy Strategy Reviews*, *24*(June 2018), 68–82. https://doi.org/10.1016/j.esr.2019.02.003

Hokkaido Bioethanol Co., L. (2015). *Introduction of high efficiency steam supply heat pump innovates energy saving in the distillation process, Tokachi Shimizu Factory*. https://www.hptcj.or.jp/Portals/0/english/Learning/HOKKAIDO.pdf

Jesper, M., Schlosser, F., Pag, F., Walmsley, T. G., Schmitt, B., & Vajen, K. (2021). Large-scale heat pumps: Uptake and performance modelling of market-available devices. *Renewable and Sustainable Energy Reviews*, *137*(November 2020), 110646. https://doi.org/10.1016/j.rser.2020.110646

Kaida, T. (2021). A Steam Supply Heat Pump System - Technology overview, energy performance and operating characteristics. *IEA HPT Annex 58, Deep Dive about Steam Generation and MVR, 30 August, 2021*.

Kaida, T. (2019). High-temperature heat pumps in Japan - Potential, development trends and case studies. *2nd Conference on High Temperature Heat Pumps, September 9, 2019, Copenhagen*, 92–107.

Kim, J., Son, H., & Yun, S. (2022). Heat integration of power-to-heat technologies: Case studies on heat recovery systems subject to electrified heating. *Journal of Cleaner Production*, *331*(July 2021), 130002. https://doi.org/10.1016/j.jclepro.2021.130002

Kiss, A. A. (2019). Rethinking energy use for a sustainable chemical industry. *Chemical Engineering Transactions*, *76*, 13–18. https://doi.org/https://doi.org/10.3303/CET1976003

Kiss, A. A., & Smith, R. (2020). Rethinking energy use in distillation processes for a more sustainable chemical industry. *Energy*, *203*, 117788. https://doi.org/10.1016/j.energy.2020.117788

Kosmadakis, G., Arpagaus, C., Neofytou, P., & Bertsch, S. (2020). Techno-economic analysis of high-temperature heat pumps with low-global warming potential refrigerants for upgrading waste heat up to 150 °C. *Energy Conversion and Management*, *226*. https://doi.org/10.1016/j.enconman.2020.113488

Meyers, S., Schmitt, B., & Vajen, K. (2018). The future of low carbon industrial process heat: A comparison between solar thermal and heat pumps. *Solar Energy*, *173*(October), 893–904. https://doi.org/10.1016/j.solener.2018.08.011

Ommen, T., Jensen, J. K., Markussen, W. B., Reinholdt, L., & Elmegaard, B. (2015). Technical and economic working domains of industrial heat pumps: Part 1 – Single stage vapour compression heat pumps. *International Journal of Refrigeration*, *55*, 168–182. https://doi.org/10.1016/j.ijrefrig.2015.02.012

Schlosser, F., Jesper, M., Vogelsang, J., Walmsley, T. G., Arpagaus, C., & Hesselbach, J. (2020). Large-scale heat pumps: Applications, performance, economic feasibility and industrial integration. *Renewable and Sustainable Energy Reviews*, *133*, 110219. https://doi.org/10.1016/j.rser.2020.110219

Schlosser, F., Wiebe, H., Walmsley, T. G., Atkins, M. J., Walmsley, M. R. W., & Hesselbach, J. (2020). Heat Pump Bridge Analysis Using the Modified Energy Transfer Diagram. *Energies*, *14*(1), 137. https://doi.org/10.3390/en14010137

Statista. (2022). *Industriestrompreise in der Schweiz nach Verbrauchertyp von 2013 bis 2020*. https://de.statista.com/statistik/daten/studie/330392/umfrage/industriestrompreis-in-der-schweiz/

The UK 2050 Calculator. (2010). *Gas Boiler Cost Data*. NERA & AEA GAS BOILER INDUSTRIAL (LARGE) 2009. http://2050-calculator-tool-wiki.decc.gov.uk/cost_categories/82

The World Bank. (2022). *Carbon Pricing Dashboard*. https://carbonpricingdashboard.worldbank.org/map_data

Vieren, E., Couvreur, K., De Paepe, M., & Lecompte, S. (2021). Techno-Economic Analysis of High Temperature Heat Pumps: A Case Study. *Proceedings of the 15th International Conference on Heat Transfer, Fluid Mechanics and Thermodynamics (HEFAT2021)*, 2109–2114. http://hdl.handle.net/1854/LU-8718588

Wang, G., & Zhang, X. (2019). Thermoeconomic analysis of optimization potential for CO 2 vapor compression cycle: From transcritical to supercritical operation for waste heat recovery from the steam condenser. *International Journal of Energy Research*, *43*(1), 297–312. https://doi.org/10.1002/er.4263

WBF. (2022). *Preisüberwachung: Gaspreise in der Schweiz, Typ X*. http://gaspreise.preisueberwacher.ch

Wolf, S. (2017). *Integration von Wärmepumpen in industrielle Produktionssysteme - Potenziale und Instrumente zur Potenzialerschliessung, Dissertation Universität Stuttgart*.

Zuberi, M. J. S., Bhadbhade, N., Patel, M. K., Wallerand, A. S., Maréchal, F., Arpagaus, C., Bertsch, S., & Wellig, B. (2020). Decarbonizing Swiss industrial sectors by process integration, electrification, and traditional energy efficiency measures. *Eceee Industrial Summer Study Proceedings, Industrial Efficiency 2020 Decarbonise Industry! 14–17 September 2020 Online Event*, 307–318. https://www.eceee.org/library/conference_proceedings/eceee_Industrial_Summer_Study/2020/4-technology-products-and-systems/decarbonizing-swiss-industrial-sectors-by-process-integration-electrification-and-traditional-energy-efficiency-measures/

Zuberi, M. J. S., Bless, F., Chambers, J., Arpagaus, C., Bertsch, S. S., & Patel, M. K. (2018). Excess heat recovery: An invisible energy resource for the Swiss industry sector. *Applied Energy*, *228*, 390–408. https://doi.org/10.1016/j.apenergy.2018.06.070

Zuberi, M. J. S., Chambers, J., & Patel, M. K. (2021). Techno-economic comparison of technology options for deep decarbonization and electrification of residential heating. *Energy Efficiency*, *14*(7), 75. https://doi.org/10.1007/s12053-021-09984-7